ลักษณะสมบัติเชิงหน้าที่ของสารกันแดดธรรมชาติไมโคสปอรีน-2-ไกลซีนจากไซยาโนแบคทีเรียเอกซ์ทรีโมไฟล์ *Halothece* sp. PCC 7418 ในเซลล์ไลน์แมโครฝาจและไซยาโนแบคทีเรียน้ำจืด

นายศุภเมธ ธาราสันติสุข

วิทยานิพนธ์นี้เป็นส่วนหนึ่งของการศึกษาตามหลักสูตรปริญญาวิทยาศาสตรมหาบัณฑิต
สาขาวิชาจุลชีววิทยาและเทคโนโลยีจุลินทรีย์ ภาควิชาจุลชีววิทยา
คณะวิทยาศาสตร์ จุฬาลงกรณ์มหาวิทยาลัย
ปีการศึกษา 2560

FUNCTIONAL CHARACTERIZATION OF NATURAL SUNSCREEN COMPOUND MYCOSPORINE-2-GLYCINE FROM EXTREMOPHILIC CYANOBACTERIUM *Halothece* sp. PCC 7418 IN MACROPHAGE CELL LINE AND FRESH WATER CYANOBACTERIUM

Mr. Supamate Tarasuntisuk

A Thesis Submitted in Partial Fulfillment of the Requirements
for the Degree of Master of Science Program in Microbiology and Microbial Technology
Department of Microbiology
Faculty of Science
Chulalongkorn University
Academic Year 2017

Thesis Title	FUNCTIONAL CHARACTERIZATION OF NATURAL SUNSCREEN COMPOUND MYCOSPORINE-2-GLYCINE FROM EXTREMOPHILIC CYANOBACTERIUM *Halothece* sp. PCC 7418 IN MACROPHAGE CELL LINE AND FRESH WATER CYANOBACTERIUM
By	Mr. Supamate Tarasuntisuk
Field of Study	Microbiology and Microbial Technology
Thesis Advisor	Associate Professor Rungaroon Waditee-Sirisattha, Ph.D.

Accepted by the Faculty of Science, Chulalongkorn University in Partial Fulfillment of the Requirements for the Master's Degree

.....Dean of the Faculty of Science

(Associate Professor Polkit Sangvanich, Ph.D.)

THESIS COMMITTEE

.....Chairman

(Associate Professor Suchada Chanprateep Napathorn, Ph.D.)

.....Thesis Advisor

(Associate Professor Rungaroon Waditee-Sirisattha, Ph.D.)

.....Examiner

(Associate Professor Tanapat Palaga, Ph.D.)

.....External Examiner

(Assistant Professor Chaiyavat Chaiyasut, Ph.D.)

ศุภเมธ ธาราสันติสุข : ลักษณะสมบัติเชิงหน้าที่ของสารกันแดดธรรมชาติไมโคสปอรีน-2-ไกลซีนจากไซยาโนแบคทีเรียเอกซ์ทรีโมไฟล์ *Halothece* sp. PCC 7418 ในเซลล์ไลน์แมโครฝาจและไซยาโนแบคทีเรียน้ำจืด (FUNCTIONAL CHARACTERIZATION OF NATURAL SUNSCREEN COMPOUND MYCOSPORINE-2-GLYCINE FROM EXTREMOPHILIC CYANOBACTERIUM *Halothece* sp. PCC 7418 IN MACROPHAGE CELL LINE AND FRESH WATER CYANOBACTERIUM) อ.ที่ปรึกษาวิทยานิพนธ์หลัก: รศ. ดร. รุ่งอรุณ วาดิถี สิริศรัทธา, หน้า.

ไมโคสปอรีน-2-ไกลซีนเป็นหนึ่งในสารคัดกรองรังสี UV ที่หายากของกลุ่มไมโคสปอรีน-ไลก์ อะมิโน แอซิด โดยพบในไซยาโนแบคทีเรียเอกซ์ทรีโมไฟล์เพียงสองชนิด คือ *Euhalothece* sp. LK-1 และ *Aphanothece halophytica* (*Halothece* sp. PCC 7418) โครงสร้างของไมโคสปอรีน-2-ไกลซีนประกอบด้วยแกนหลัก 4-ดีออกซีแกดูซอล ที่มีไกลซีน 2 โมเลกุลทำพันธะกับคาร์บอนอะตอมตำแหน่งที่ 1 และ 3 ของแกน สารประกอบชนิดนี้มีค่าการดูดกลืนแสงสูงสุดที่ความยาวคลื่น 331 นาโนเมตร มีฤทธิ์ต้านอนุมูลอิสระได้ดีกว่าสารชนิดอื่นในกลุ่มเดียวกัน ดังนั้น ไมโคสปอรีน-2-ไกลซีนจึงน่าสนใจในการศึกษาฤทธิ์อื่น ๆ เพื่อการประยุกต์ใช้ทางอุตสาหกรรมความงามและเภสัชกรรม ในการศึกษานี้ได้ประสบความสำเร็จในการสกัดและทำบริสุทธิ์สารไมโคสปอรีน-2-ไกลซีนจากไซยาโนแบคทีเรียเอกซ์ทรีโมไฟล์ *Halothece* sp. PCC 7418 โดยใช้ strong cation exchange chromatography และ reverse phase chromatography ตามลำดับ ได้สารประกอบที่มีความบริสุทธิ์สูง และมีปริมาณเอนโดท็อกซินปนเปื้อนต่ำมาก (0.004 EU/mL) จากการทดสอบฤทธิ์ต้านอนุมูลอิสระในช่วง pH ที่ 5-9 ด้วยวิธี DPPH พบว่ามีฤทธิ์ต้านอนุมูลอิสระที่ดีที่สุดที่ pH 6 การศึกษานี้ยังได้ทดสอบฤทธิ์ต้านการอักเสบของไมโคสปอรีน-2-ไกลซีนกับเซลล์ไลน์แมโครฝาจ RAW 264.7 ในระดับการถอดรหัสของยีนภายใต้การกระตุ้นการอักเสบด้วยไลโพโพลีแซคคาไรด์ พบว่าสามารถกดการแสดงออกของยีน *iNOS* ซึ่งกำหนดรหัสของเอนไซม์ inducible nitric oxide synthase ได้เป็นอย่างดี (75±2 %) ซึ่งสอดคล้องกับระดับไนตริก ออกไซด์ ที่ลดลง และกดการถอดรหัสของยีน *COX-2* ได้ดีที่ความเข้มข้นต่ำกว่า 10 ไมโครโมลาร์ ในส่วนการตรวจสอบฤทธิ์ต้านออกซิเดชั่นในระดับการถอดรหัสยีนพบว่าไมโคสปอรีน-2-ไกลซีนที่ความเข้มข้น 5 ไมโครโมลาร์ กดการแสดงออกของยีน *sod1* ซึ่งกำหนดรหัสเอนไซม์ Cu/Zn SOD ที่ทำหน้าที่กำจัดอนุมูลอิสระ และส่งเสริมการแสดงออกของยีน *cat, Hmox1,* และ *Nrf2* ภายใต้ภาวะเครียดออกซิเดชั่นจากไฮโดรเจน เปอร์ออกไซด์ได้เป็นอย่างดี นอกจากนี้ จาก heterologous expression ในไซยาโนแบคทีเรียน้ำจืด *Synechococcus elongatus* PCC 7942 ของยีนชีวสังเคราะห์ไมโคสปอรีน-2-ไกลซีน (*Ap3858-Ap3855*) เป็นผลให้เซลล์แสดงออกต้านต่อภาวะเครียดออกซิเดชั่นได้ดีกว่าเซลล์ชุดควบคุม โดยมีค่า IC_{50} ต่อไฮโดรเจน เปอร์ออกไซด์เป็น 2.293±0.06 และ 1.523±0.05 ตามลำดับ และการตรวจสอบระดับการถอดรหัสของยีนที่เกี่ยวข้องกับภาวะเครียดออกซิเดชั่นในเซลล์แสดงออกพบว่ายีน *cat*, *sodB*, และ *tpxA* มีการแสดงออกมากขึ้น 4.5±0.4, 2±0.2 และ 5±0.2 เท่าตามลำดับ ภายใต้ภาวะเครียดออกซิเดชั่นจากไฮโดรเจน เปอร์ออกไซด์

ภาควิชา จุลชีววิทยา ลายมือชื่อนิสิต .....

สาขาวิชา จุลชีววิทยาและเทคโนโลยีจุลินทรีย์ ลายมือชื่อ อ.ที่ปรึกษาหลัก .....

ปีการศึกษา 2560

5972066523 : MAJOR MICROBIOLOGY AND MICROBIAL TECHNOLOGY
KEYWORDS: MYCOSPORINE-2-GLYCINE / ANTI-INFLAMMATION / ANTIOXIDATION / HETEROLOGOUS EXPRESSION

SUPAMATE TARASUNTISUK: FUNCTIONAL CHARACTERIZATION OF NATURAL SUNSCREEN COMPOUND MYCOSPORINE-2-GLYCINE FROM EXTREMOPHILIC CYANOBACTERIUM *Halothece* sp. PCC 7418 IN MACROPHAGE CELL LINE AND FRESH WATER CYANOBACTERIUM. ADVISOR: ASSOC. PROF. RUNGAROON WADITEE-SIRISATTHA, Ph.D., pp.

Mycosporine-2-glycine (M2G) is a rare UV-screening compound in a group of mycosporine-like amino acids (MAAs). This molecule is found in only two cyanobacteria; *Euhalothece* sp. LK-1 and *Aphanothece halophytica* (*Halothece* sp. PCC 7418). The structure of M2G composed of 4-deoxygadusol as a core structure, attached by 2 molecules of glycine at C_1 and C_3 positions. M2G has a maximal adsorption at 331 nm and a better antioxidative activity than other MAAs. Thus, it is interesting in determination of other activities for further cosmeceutical and pharmaceutical applications. In this study, a high purity M2G was successfully extracted and purified from *Halothece* sp. PCC 7418 by using strong cation exchange chromatography, and reverse phase chromatography, respectively. The obtained M2G has a very low concentration of endotoxin (0.004 EU/mL). 2,2-diphenyl-1-picrylhydrazyl (DPPH) assay found that M2G exhibited the highest radical scavenging activity at pH 6. In this study, anti-inflammatory activity of M2G in RAW 264.7 murine macrophage cell line at the transcriptional level under lipopolysaccharide inflammatory-induction was also examined. It revealed that *iNOS*, encoding inducible nitric oxide synthase enzyme, was highly suppressed by M2G (75±2 %). This is consistent with a decrease in nitric oxide level. *COX-2* expression was also suppressed at < 10 µM M2G treatment. Anti-oxidative capability of M2G was inspected in transcriptional level under oxidative stress induced by H_2O_2. It was found that 5 µM of M2G suppressed *sod1*, which encodes the radical scavenging enzyme Cu/Zn SOD. Other antioxidant-related genes; *cat*, *Hmox1*, and *Nrf2*, were upregulated by the supportive of M2G as well. Heterologous expression of M2G biosynthetic gene cluster (*Ap3858-Ap3855*) in a fresh water cyanobacterium *Synechococcus elongatus* PCC 7942 revealed a higher H_2O_2-induced oxidative stress tolerance than that of the control cells. IC_{50} of H_2O_2 in the transformant cells harboring M2G genes and the control cells were 2.293±0.06 and 1.523±0.05, respectively. Transcriptional level of antioxidant genes in expressing cells revealed that *cat*, *sodB*, and *tpxA*, were 4.5±0.4, 2±0.2 and 5±0.2 times upregulated, respectively, under H_2O_2 oxidative stress.

Department:	Microbiology	Student's Signature	.....
Field of Study:	Microbiology and Microbial Technology	Advisor's Signature	.....
Academic Year:	2017		

ACKNOWLEDGEMENTS

I would first like to express my sincere gratitude and deep appreciation to my advisor, Associate Professor Dr. Rungaroon Waditee-Sirisattha for her exquisite instruction, guidance, encouragement, and support throughout the course of my research. I would also like to acknowledge Associate Professor Dr. Tanapat Palaga and Associate Professor Dr. Hakuto Kageyama as the excellent consultants for my successfully experiments.

My gratitude is expressed to my thesis committee, Associate Professor Dr. Suchada Chanpratheep Napathorn and Assistant Professor Dr. Chaiyavat Chaiyasut, for their valuable comments and suggestions in this thesis. My sincere appreciation also goes to Professor Dr. Teruhiro Takabe for his kindly help during my stay in Nagoya, Japan.

Special thanks for all my lovely friends and members of 1904/17 and 2015 laboratory rooms for encouragement, nice friendships, and suggestions. My thanks would also express to all my friends in Science Student Government of Faculty of Science, Chulalongkorn University, academic year 2015 for their given delight and encouragement along my master student time.

Finally, I would like to express my very thanks to my parents for their warmest love, care, encouragement, understanding, support, and attention throughout my life.

CONTENTS

Page

Page

Page

Page

Page

LIST OF TABLE

page

LIST OF FIGURE

page

page

page

CHAPTER I
INTRODUCTION

Mycosporine-like amino acids (MAAs) are a group of secondary metabolites which naturally biosynthesized from various microorganisms, such as fungi, micro- and macroalgae, and cyanobacteria. These molecules are colorless, water-soluble, and can absorb energy from the wavelength in range of ultraviolet A and B (309-362 nm). MAAs are composed of cyclohexinimine or cyclohexanone as a core structure, attaching with amino acid (s) at the third (and the first) carbon atoms (Singh *et al.*, 2008; Wada *et al.*, 2013; Pope *et al.*, 2015). The variation of bonded amino groups results in the variety of MAAs (Wada *et al.*, 2015). To date, there are more than 25 MAAs discovered. The MAAs molecules can be intracellular modified by terrestrial and desiccated cyanobacteria via glycosylation, yielded glycosylated-MAAs (Matsui *et al.*, 2011; Ishihara *et al.*, 2017; Shang *et al.*, 2018).

MAAs are known as multifunctional compounds by their direct and indirect properties. The direct property involved in photoprotection as being a sunscreen (UV-screening) compound. Unlike other organic sunscreen compound, these molecules can absorb the energy from the wavelength and release it in form of heat without producing reactive oxygen species (ROS) (Wada *et al.*, 2013). The indirect properties of MAAs are widely described to date, especially in antioxidant, anti-inflammation and anti-aging cosmeceutical properties for applications. For instance, majority of the compounds exhibited an antioxidation ability by radical quenching and scavenging mechanisms. Three commonly found MAAs (shinorine, porphyra-334, and mycosporine-glycine) were found to promote wound healing via focal adhesion kinase (FAK) and mitogen-activated protein kinase (MAPK) pathways induction in human keratinocyte (HaCaT). These MAAs were also found as having anti-aging capability by enhancing procollagen I enhancer and elastin genes transcription (Oyamada *et al.*, 2008; Ryu *et al.*, 2014). Anti-inflammation activity was discovered in mycosporine-glycine by decreasing expression of *COX-2* (Suh *et al.*, 2014). According to these

functions, MAAs become the interesting biocompounds for cosmeceutical and pharmaceutical approaches, nowadays.

Inflammation is an important cellular mechanism to get rid of pathogens and injured cells. An inflammation pathway is initiated by induction of various stimuli, such as bacterial lipopolysaccharide, molecular patterns released from damaged cells, UV radiation, and ROS. The stimulation consequences of an activation of transcription nuclear factor-kappa B (NF-κB) (Napetschnig & Wu, 2013). This action leads to the transcription of various proinflammatory genes. There are two genes remarked as key regulators for an inflammation; *iNOS* and *COX-2*, which encode two mediators, inducible nitric oxide synthase and cyclooxygenase-2, respectively. To promote an inflammation, these two enzymes generates nitric oxide, the chemical inflammation inducer, and prostaglandin E2, an essential proinflammatory cytokine, respectively (Wendum *et al.*, 2003; Alexander & Supp, 2014). Thus, these genes regulation capability is of interest property for pharmaceutical application to prevent skin inflammation.

Oxidative stress is found to be one of the effective stimulators in inflammation pathway. In general, cells generate oxidants from their routine mechanisms, whether aerobic metabolism, immune functions, or cells division. The produced oxidants are controlled by the equilibrium of oxidants and antioxidants in cells. Keap1/Nrf2/ARE signaling pathway is the major mechanism to produce enzymatic antioxidants for the equilibrium maintenance. This pathway is directly activated by an induction of oxidants, leads to the synthesis of antioxidant enzymes, such as catalase, superoxide dismutases, and glutathione peroxidase (Ahmed *et al.*, 2017). Overproduction or excessive exposure; however; disrupts this equilibrium, leads to damaging of macromolecules (*i.e.* DNA, proteins, and phospholipids) (Watt *et al.*, 2004).

Mycosporine-2-glycine (M2G) is a rare MAA, which is naturally produced as a major MAA compound in only two cyanobacteria; *Euhalothece* sp. and *Aphanothece halophytica* (*Halothece* sp. PCC 7418) (Kedar *et al.*, 2002; Waditee-Sirisattha *et al.*, 2014). This sunscreen molecule is composed of a core structure 4-deoxygadusol (4-DG), attached with two glycine molecules at C_3 and C_1 positions, respectively. M2G can absorb the wavelength in a range of UV radiation with a maximal adsorption at 331 nm. M2G was found in having a stronger antioxidant capability than the commonly

found MAAs. This molecule exhibited an activity as an oxidative protectant against cell-death induction and DNA damaging in A375 human melanoma (Cheewinthamrongrod *et al.*, 2016).

Although the described abilities of M2G indicate a potent feasibility in being an effective multifunctional sunscreen compound. Other indirect functions; however, were uncharacterized to date. This study aimed to examine other capability of M2G. The interested functional properties are (1) oxidative scavenging activity under a wide range of pHs, (2) anti-inflammation and antioxidation activities in macrophage cell line, and (3) heterologous expression of M2G biosynthetic genes in a fresh water cyanobacterium.

The objective of this research:

1. To extract and purify the natural sunscreen compound mycosporine-2-glycine
2. To functionally characterize the natural sunscreen compound mycosporine-2-glycine
3. To examine the functions of mycosporine-2-glycine in macrophage cell line under oxidative stress and lipopolysaccharide (LPS)-induced inflammation
4. To evaluate the contribution of mycosporine-2-glycine in heterologous expression system

The hypotheses in this research are:

1. A natural sunscreen compound M2G from *Halothece* sp. PCC 7418 possesses antioxidative and anti-inflammatory activities in cell line.
2. Heterologous expression of M2G biosynthetic genes contributes the oxidative stress response in fresh water cyanobacterium *Synechococcus elongatus* PCC 7942.

CHAPTER II
LITERATURE REVIEW

2.1 Mycosporine-like amino acids

2.1.1 Basic features

Mycosporine-like amino acids (MAAs) are a group of secondary metabolites found in various microorganisms. These compounds are colorless, water soluble, and low molecular weight (≤1050 Da). The structures are composed of a cyclohexanone or a cyclohexinimine as a core, attaching by one or two amino acid (s) at the third (and the first) carbon position of the core structure (Singh *et al.*, 2008; Pope *et al.*, 2015). The differences of attached amino acids generate a variety of MAA species (Wada *et al.*, 2015). For instance, the addition of glycine to the third carbon position produces mycosporine-glycine, while further attachment of another amino acid serine to the first carbon position yields shinorine. To date, there are more than 25 MAAs discovered in fungi, corals, micro- and macroalgae, and cyanobacteria (Rastogi *et al.*, 2015). MAA molecules can be further modified by glycosylation. This modification is specific in terrestrial and desiccated cyanobacteria, such as *Nostoc commune*, *N. sphaericum*, *N. flagelliforme*, and *Scytonema* cf. *cripsum* (Matsui *et al.*, 2011; Nazifi *et al.*, 2013; D'Agostino *et al.*, 2016; Ishihara *et al.*, 2017; Shang *et al.*, 2018).

2.1.2 Biosynthesis of MAAs

Biosynthesis of MAAs occurred from the systematized activity of at least three enzyme groups; dimethyl-4-deoxygadusol synthase (DDGS), *O*-Methyltransferase (*O*-MT) and ATP grasp family. The biosynthetic pathway was extensively studied in cyanobacteria. This pathway commonly begins with the first step reaction of DDGS, which converts sedoheptulose-7-phosphate (SH7P), an intermediate from Pentose Phosphate Pathway, to dimethyl-4-deoxygadusol (DDG). Then, DDG is methylated by *O*-MT, resulting in 4-deoxygadusol (4-DG). The biosynthesis of 4-DG was reported in relevant to Shikimate pathway by the methylation of *O*-MT to an intermediate of the

pathway, 3-dehydroquinate (3-DHQ) in the cyanobacterium *Anabaena variabilis* ATCC 29413 (Figure 1) (Pope *et al.*, 2015). After that, an amino acid is attached to the 4-DG core at C_3 position by an ATP grasp family, causing one-amino group MAAs, such as mycosporine-glycine and mycosporine-taurine. In addition to ATP grasp, the second addition of an amino acid can be occurred by non-ribosomal peptide-like synthase. The second amino acid is added into the structure at C_1 position, leading to two-amino groups MAAs, such as shinorine (C_1 = serine and C_3 = glycine), porphyra-334 (C_1 = threonine and C_3 = glycine), and mycosporine-2-glycine (C_1 = glycine and C_3 = glycine) (Carreto & Carignan, 2011; Rosic & Dove, 2011; Waditee-Sirisattha *et al.*, 2014).

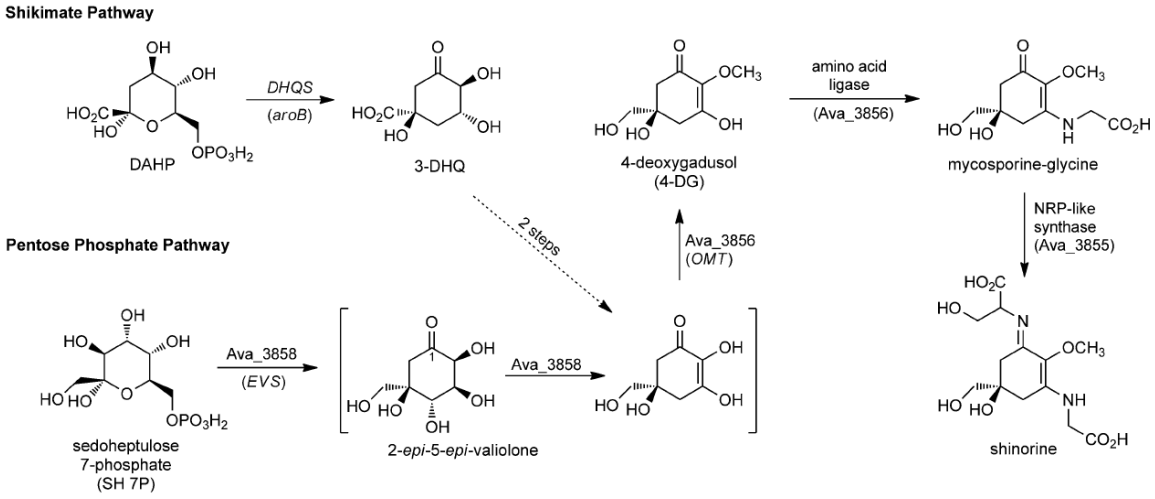

Figure 1: Biosynthetic pathway of a commonly found MAA, shinorine, in the filamentous cyanobacterium *A. variabilis* ATCC 29413. The relevance between shikimate pathway and pentose phosphate pathway by the reaction of O-MT is demonstrated (from: Pope *et al*., 2015)

2.1.3 Direct function of MAAs

MAAs are well recognized as bio-sunscreen compounds by their direct photoprotective function against UV radiation. These molecules can absorb UV in range of 309-362 nm, which are specific for UVA and UVB (Shang *et al.*, 2018). The maxima absorption is varied by the uniqueness of the molecules. Early evidence also revealed that MAA prevents 3 out of 10 photons from striking cytoplasmic targets in cyanobacteria (Garcia-Pichel *et al.*, 1993). Unlike other organic UV-screening compounds, MAAs can absorb an energy from the electromagnetic waves and dissipate it as a heat without any reactive oxygen species (ROS) production. This proficiency is believed in protonation to an amino group by the acid-base reaction, resulting in a zwitterionic property of the molecule. The protonation initiates the delocalization of electrons on a nitrogen atom through the chromophore ring. Thus, this leads to the resonance stabilization of electrons at the carbon atoms number 3 to 1, causing the loss of energy during electron transition in form of heat (Figure 2) (Wada *et al.*, 2013). A study in two common MAAs, shinorine and mycosporine-glycine, revealed that the availability of H^+ in environment affected on their zwitterionic properties (Matsuyama *et al.*, 2015).

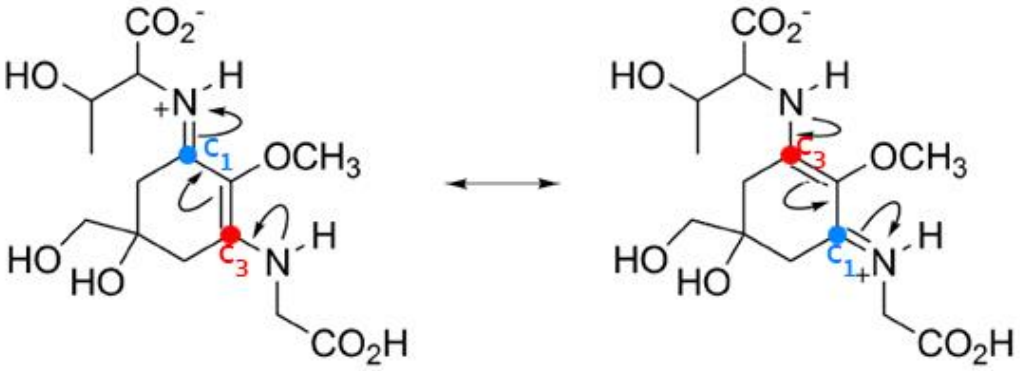

Figure 2: Electron resonance stabilization of porphyra-334. The lone pair electrons shift from a nitrogen atom of an amino acid to another nitrogen atom through carbon atoms of the core structure. This movement caused an energy loss during an excitation and relaxation of electrons in form of heat (modified from: Wada *et al*., 2013).

2.1.4 Indirect functions of MAAs

Apart from direct property as a sunscreen (UV-screening) compounds, MAAs are widely described in having indirect functions. Various examples were reported in both native producers and *in vitro* experiments, especially in terms of medical and pharmaceutical applications. Three common MAAs (*i.e.* shinorine, porphyra-334, and mycosporine-glycine) were found to stimulate the growth of human skin fibroblast (TIG-114) and promote wound healing via focal adhesion kinase (FAK) and mitogen-activated protein kinase (MAPK) pathways in human keratinocyte (HaCaT) (Oyamada *et al.*, 2008; Choi *et al.*, 2015). These MAA compounds were also reported as anti-aging substances by enhancing of procollagen I enhancer and elastin genes transcription in HaCaT cell line (Suh *et al.*, 2014) as well as in human skin fibroblast for porphyra-334 (Ryu *et al.*, 2014). Anti-inflammation property was found in mycosporine-glycine by the decreasing of cyclooxygenase-2 (*COX*-2) after the cell treatment (Suh *et al.*, 2014). Furthermore, majority of MAAs exhibited an effective antioxidative capability by radical quenching and scavenging (Wada *et al.*, 2015; Cheewinthamrongrod *et al.*, 2016).

According to these indirect functions, MAAs are becoming an interest in application whether medical and pharmaceutical approaches.

2.2 Inflammation

Inflammation is an important cellular mechanism to eliminate pathogens or damaged cells, initiate tissue wound healing and decide cells death (Newton & Dixit, 2012). This mechanism can be stimulated by damage associated molecular patterns (DAMPs) from damaged cells, pathogen associated molecular patterns (PAMPs) from pathogens, irradiations, and oxidative stresses. These stimuli induce cells inflammation in various manners. For example, DAMPs and PAMPs trigger cells by binding to toll-like receptors (TLRs), the pattern recognition receptors which are specific to each molecular pattern. UV radiation promotes a trigger protein elF2α by induce the expression of *GCN/PERK2* (Mitchell *et al.*, 2016). On the other hands, oxidative stress can induce directly to the classical (canonical) pathway (Siomek, 2012).

Although cells stimulation mechanisms are different, all the signals are aimed for nuclear factor-Kappa B (NF-κB) pathway activation (Siomek, 2012). In general, NF-κB protein is inactivated by complementation of the inhibitor κB (IκB), forming complemented protein NF-κB-IκB. The activation of NF-κB pathway is occurred when the protein complex inhibitor κB kinase (IκK) is activated via proinflammatory signals. Then, NF-κB-IκB complex is phosphorylated by an activated IκK, leads to a detachment and degradation by ubiquitination of an inhibitor protein IκB from the complex. Thereafter, the liberated NF-κB protein is transported into nucleus and acts as a transcription factor by binding with the inflammatory genes promotor. Consequently, several proinflammatory genes are transcribed (Napetschnig & Wu, 2013).

Two proinflammatory genes are remarked as key regulators for an inflammation among the cascade. These are *inducible nitric oxide synthase* (*iNOS*) and *COX-2*, which encode two proinflammatory enzymes iNOS and COX-2, respectively. Mechanism of

action of iNOS is to generate nitric oxide, an inflammation chemical inducer. The reaction catalyzing by iNOS is occurred between *L*-arginine and oxygen (Alexander & Supp, 2014). In case of COX-2, this enzyme has an importance by cooperating with PLA2 in conversion of phospholipids to an essential cytokine prostaglandin-E2 (PGE2) (Wendum *et al.*, 2003) (Figure 3).

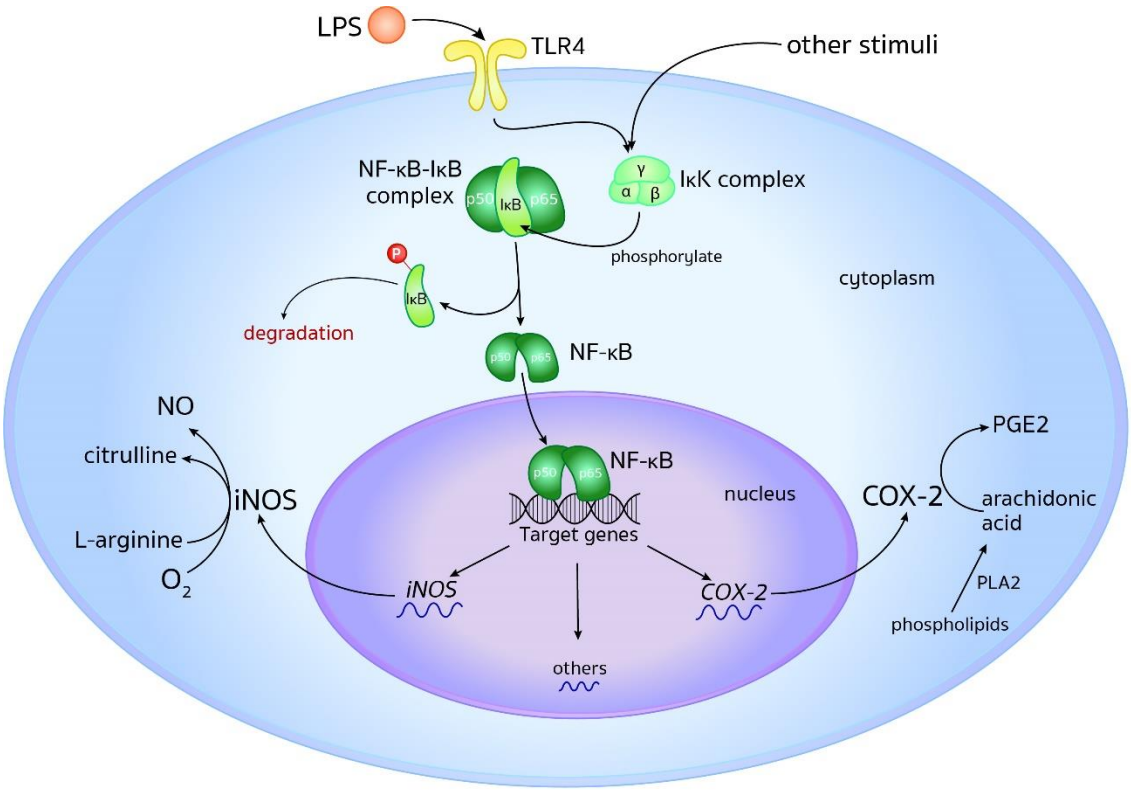

Figure 3: NF-κB pathway and the mechanism of action of two key regulator enzymes iNOS and COX-2 (modified from: Infantino *et al*., 2011)

COX-2: cyclooxygenase-2

iNOS: inducible nitric oxide synthase

IκB: inhibitor kappa B

IκK: inhibitor kappa B kinase

LPS: lipopolysaccharide

NO: nitric oxide

NF-κB: nuclear factor-kappa B

PLA2: phospholipase A2

PGE2: prostaglandin E2

TLR4: toll-like receptor 4

2.3 Cellular oxidative responses

In normal condition, oxidants are generated in cells in a disciplined manner. The produced oxidants serve as cell signaling molecules to trigger cells processing, such as cell division, inflammation, immune functions, and stress responses (Ma, 2013). These mechanisms are controlled by the equilibrium of oxidants/antioxidants. Overproduction or excessive exposure of oxidants; however, causes the equilibrium disturbance, leading to the oxidative stress in cells. Furthermore, enormous oxidants can cause damages to organic matters and organelles in cells through lipid peroxidation and oxidative modifications (Watt *et al.*, 2004), as well as to cells survival by trigger cells inflammation and programmed cell death mechanisms (Zhang *et al.*, 2015). Thus, the elimination of overabundant oxidants is essential for cells to maintain their oxidants/antioxidants equilibrium and to survive upon the stress conditions.

Kelch-like ECH-associated protein 1/nuclear factor erythroid 2-related factor 2/antioxidant response element (Keap1/Nrf2/ARE) signaling pathway is the major mechanism to alleviate the oxidative stress in human cells via regulation of antioxidant and detoxification enzymes (Ma, 2013). Generally, the transcription factor Nrf2 is attached with Keap1 inhibitor protein, forming Keap1/Nrf2 complex. This inactivated protein is detained in cytosol by the binding of Keap1 and actin or myosin. The activation of Keap1/Nrf2/ARE pathway is occurred after the detachment of Keap1 and Nrf2 via thiol modification at Keap1 cysteine residues. This step is induced by oxidative species and electrophiles. The activated Nrf2 is then localizes into nucleus and binds to the basic leucine zipper-musculoaponeurotic fibrosarcoma (bZip-Maf) protein at ARE region. Finally, the interaction between heterodimers and ARE promotor region initiates antioxidative genes transcription (Figure 4) (Zhang *et al.*, 2015; Ahmed *et al.*, 2017; Krajka-Kuzniak *et al.*, 2017).

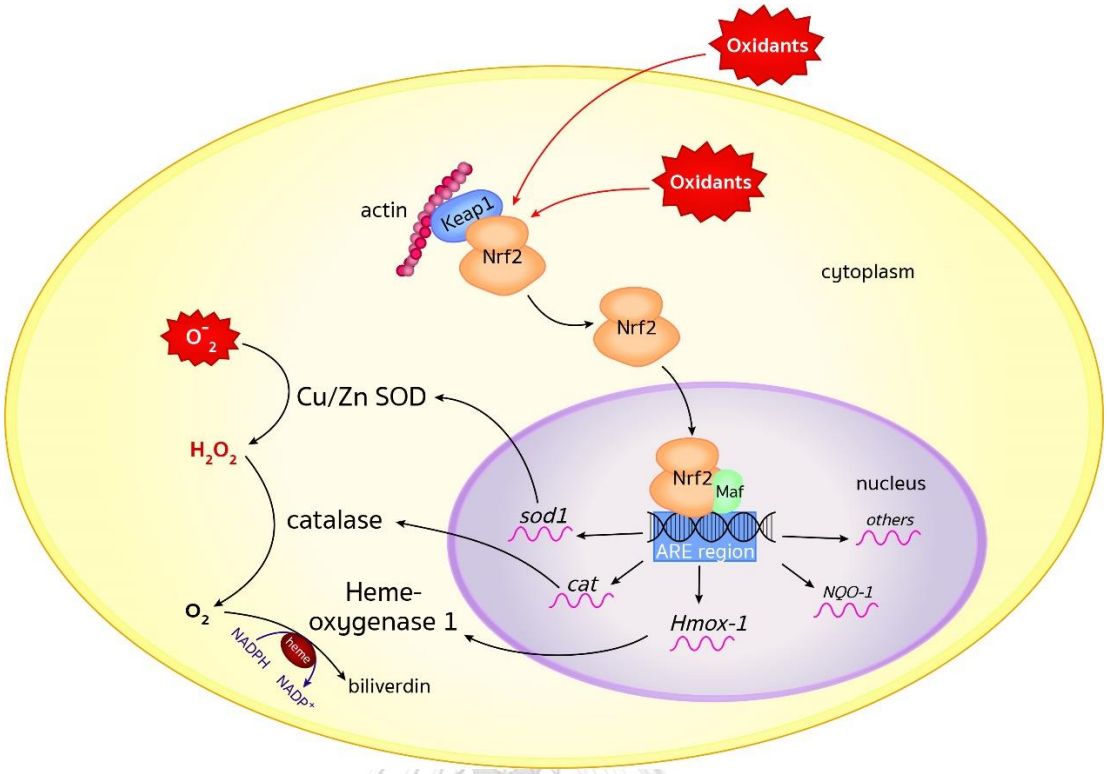

Figure 4: Keap1/Nrf2/ARE pathway and the mechanism of enzymes to eliminate excessive oxidants in mammalian cells (modified from: Krajka-Kuzniak *et al*., 2017).

ARE: antioxidant response element

Cu/Zn SOD: Cu/Zn superoxide dismutase

Keap1: Kelch-like ECH-associated protein 1

Maf: musculoaponeurotic fibrosarcoma

Nrf2: nuclear factor erythroid 2-related factor 2

2.4 MAA from extremophilic cyanobacterium *Halothece* sp. PCC 7418

Mycosporine-2-glycine (M2G) is a rare natural sunscreen compound in a group of MAAs. To date, M2G was found in some marine microorganisms; sea anemone *Anthopleura elegantissima* (Stochaj *et al.*, 1994; Shick *et al.*, 2002), and dinoflagellate *Maristentor dinoferus* (Sommaruga *et al.*, 2006), and two halophilic cyanobacteria *Euhalothece* sp. LK-1 (Kedar et al., 2002) and *Aphanothece halophytica* (*Halothece* sp. PCC 7418) (Waditee-Sirisattha et al., 2014). The discovered M2G in *A. elegantissima* was; however, predicated as accumulated from its food, while M2G was detected at an extremely low amount in *M. dinoferus*. Thus, these can be concluded that M2G is naturally produced as a major MAA by only two cyanobacteria nowadays.

2.4.1 Features of M2G and its biosynthesis

The structure of M2G is composed of a 4-deoxygadusol as a core, attached by two molecules of glycine at C_3 and C_1 positions, respectively (Figure 5 (A)). M2G can absorb the UV with the maxima absorbance at 331 nm, which is a unique characteristic of the compound.

In 2014, Waditee-Sirisattha *et al*. discovered and clarified M2G biosynthetic pathway in the halophilic cyanobacterium *Halothece* sp. PCC 7418. The M2G gene cluster composed of *Ap3858*, *Ap3857*, *Ap3856*, and *Ap3855*, encoding for DDGS, OMT, C-N ligase, and *D*-ala *D*-ala ligase, respectively. The amino acid sequences of Ap3857 to Ap3856 were highly homologous to MAAs biosynthetic enzyme models Ava_3857 to Ava_3856 from *Anabaena variabilis* ATCC 29413 (63% and 61%, respectively) and NpR5599 to NpR5598 from *Nostoc punctiforme* ATCC 29133 (61% and 60%, respectively), while Ap3858 was found in only 38% and 39% homolog of Ap_3858 and Nrp5600, respectively, and Ap3855 was 38% identity to NpR5596, respectively. Gene organization for M2G biosynthesis comprised of two regions, the first cluster composed of *Ap3857-56-55*, and the second *Ap3858* which is in a far distant. This organization was peculiar comparing to those two MAAs biosynthetic gene organization reporting in *A. variabilis* and *N. punctiforme*, which all genes are in a cluster (Figure 5 (B)).

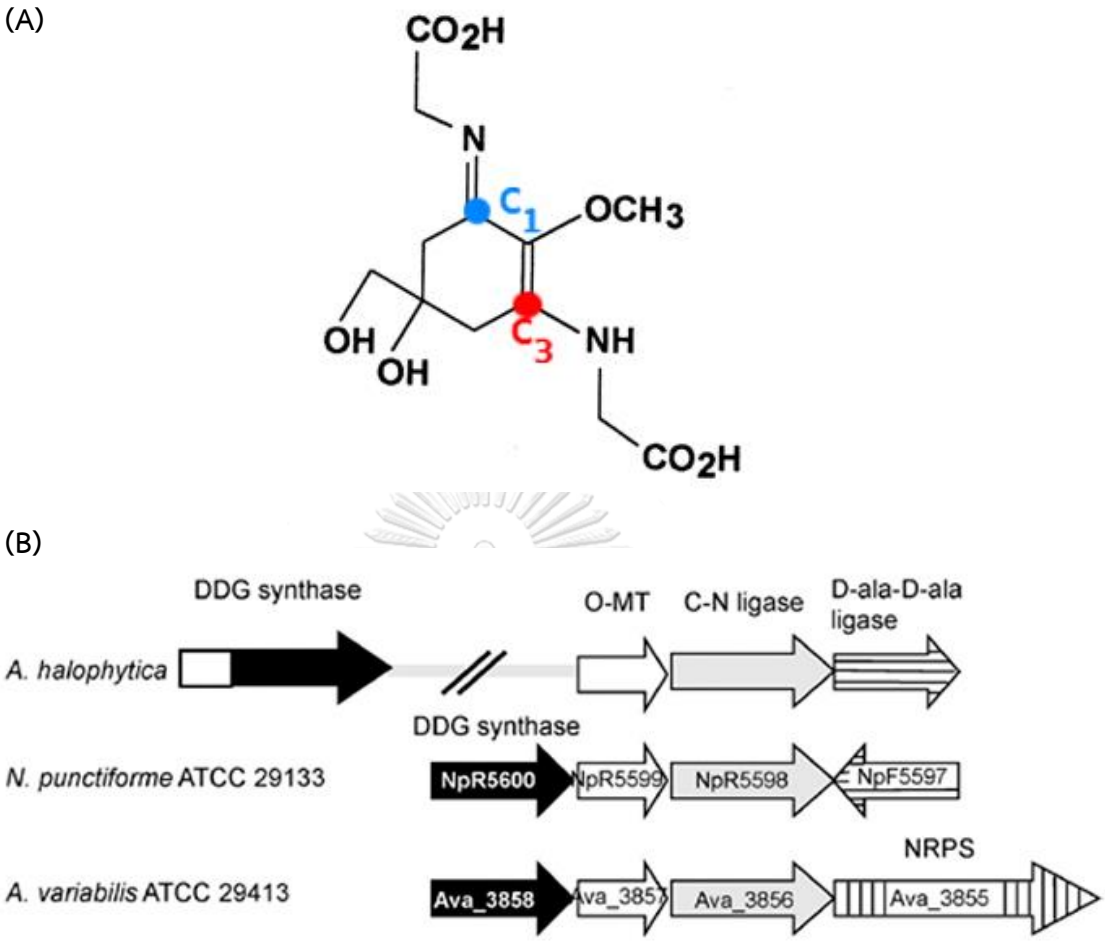

Figure 5: Chemical structure of M2G. Two molecules of glycine are attached to the 4-DG core at C_3 and C_1 positions **(A)**. Gene organization of M2G biosynthesis in *Halothece* sp. PCC 7418 compared to two MAAs biosynthetic gene organization models from *N. punctiforme* ATCC 29133 and *A. variabilis* ATCC 29413. Ap3858, encoded DDG synthase, was far separated from a cluster of other genes **(B)**.

2.4.2 Biological activity and function of M2G

M2G exhibits its indirect activities in both a native producer and *in vitro* approaches. In a halotolerant cyanobacterium *Halothece* sp. PCC 7418, the native M2G bio-synthesizer, accumulation of M2G was significantly upregulated by exposure to salt stress condition (Waditee-Sirisattha *et al.*, 2014). Thus, M2G functions as an osmoprotectant.

Cheewinthamrongrod *et al*. (2016) reported a strong antioxidant property of M2G by the *in vitro* experiments. Its oxidant scavenging activity was determined in high capability with SC_{50} at 22 ± 1.4 μM. This was two times greater than mycosporine-glycine (43 ± 1.3 μM). In this study also revealed an oxidative protection ability of M2G to human cell line. Proper concentrations of M2G could completely protect normal human skin fibroblast (NHSF) and A375 melanoma cell line against cell-death induction and DNA damaging triggered by hydrogen peroxide.

Although UV absorption and other indirect properties of M2G indicate a strong possibility as being a good multifunctional sunscreen compound; however, other indirect properties remain elusive. This study aimed to extract and purify M2G from *Halothece* sp. PCC 7418 and examine its functional characteristics. The interested functional properties are (1) oxidative scavenging activity under a wide range of pHs, (2) anti-inflammation and antioxidation activities using a macrophage cell line, and (3) heterologous expression of M2G biosynthetic genes in a fresh water cyanobacterium *S. elongatus* PCC 7942.

Thus, the study for these approaches would provide a deep information and support an acclamation of M2G as a high efficacy multifunctional sunscreen compound for further applications, such as in cosmeceutical and pharmaceutical industries.

The objective of this research:

1. To extract and purify the natural sunscreen compound M2G
2. To functionally characterize the natural sunscreen compound M2G
3. To examine the functions of M2G in a macrophage cell line under oxidative stress and lipopolysaccharide (LPS)-induced inflammation
4. To evaluate the contribution of M2G in a heterologous expression system

CHAPTER III

MATERIALS AND METHODS

3.1 Instruments

Autoclave: Model SS-325 and ES-215, TOMY Digital Biology, Japan

Autopipette: Eppendorf Research plus, Eppendorf, Germany

Bench-top centrifuge: MSC-6000, Biosan, Malaysia

Biological safety cabinet: Model MCV-131S, Sanyo, Japan

CO_2 incubator: Model 311: Thermo Electron Corporation, USA

Cuvette: Spectronic 401, Milton Roy, USA

DSC-SCX-SPE® cartridge, Sigma Aldrich, USA

DSC18 SPE® cartridge: Sigma Aldrich, USA

Gel imaging: Model Gel Doc EZ™, Bio-Rad Laboratories, USA

Gel electrophoresis: Model MJ-105, Major Science, USA

Hemacytometer: Bright-Line™, Sigma, USA

High Performance Liquid Chromatography (HPLC): Shimadzu, Japan

Hot air oven: Model UE600, Mammert, Germany

Incubator shaker: Model innova 4330, New Brunswick Scientific, USA

Laboratory glassware: Pyrex, USA

Laminar flow: Model H1, Microtech, Thailand

Magnetic stirrer: Model MMS-3000, Biosan, Latvia

Microplate reader: Multiskan™ FC Microplate Photometer, Thermo Scientific, USA

Microscope: Olympus, Japan

Nanodrop 200 UV-Vis Spectrophotometer: Thermo Scientific, USA

Orbital shaker: Model TT-20: Hercuvan Lab Systems, Malaysia

pH meter: SevenEasy™, Mettler Toledo, USA

Refrigerated centrifuge: Model Allegra 25R, Backman, Germany

Refrigerated microcentrifuge: Model 5418 R, Eppendorf, Germany

Thermal cycler: Model T100™ and C1000 Touch™, Bio-Rad Laboratories, USA

Transformer: PowerPac™ HC, Bio-Rad Laboratories, USA

UV-Vis Spectrophotometer: UV-240, Shimadzu, Japan

Vortex mixer: Model K-550-GE: Scientific Industries, USA

Water bath: Mammert, Germany

3.2 Chemicals and media

Acetic acid: Merck, Germany

Agar powder: Himedia, India

Agarose gel: Bio-Rad Laboratories, USA

Bacto® tryptone: Merck, Germany

Boric acid: Merck, Germany

Calcium chloride: Merck, Germany

Chloroform: RCI Labscan Limited, Thailand

Citric acid: Merck, Germany

Cobalt(II) nitrate: Ajax Finechem Pty Limited, Australia

Copper(II) sulfate: Ajax Finechem Pty Limited, Australia

DEPC (Diethylpyrocarbonate), Amresco, USA

Dimethyl sulfoxide: Amresco, USA

Dipotassium phosphate: Ajax Finechem Pty Limited, Australia

Disodium hydrogen phosphate: Carlo Erba, Italy

Disodium phosphate: Ajax Finechem Pty Limited, Australia

DPPH (2,2-diphenyl-1-picrylhydrazyl): Sigma, USA

Dulbecco's modified Eagle's medium/high glucose: HyClone, USA

EDTA (Ethylenediaminetetraacetic acid): Amresco, USA

Endotoxin-free purified water: E-Toxate™ water, Sigma, USA

Ethanol: Merck, Germany

Ferric ammonium nitrate: Merck, Germany

Fetal bovine serum: Gibco®, Life Technologies, USA

Glycerol: Merck, Germany

HEPES (4-(2-hydroxyethyl)-1-piperazineethanesulfonic acid): HyClone, USA

Hydrochloric acid: Merck, Germany

Hydrogen peroxide: Merck, Germany

Isopropanol: Merck, Germany

L-ascorbic acid: Sigma, USA

Magnesium chloride: Merck, Germany

Magnesium sulfate: Merck, Germany

Manganese(II) chloride: Ajax Finechem Pty Limited, Australia

MES sodium salt (Sodium 2-(*N*-morpholino)ethanesulfonic acid): Sigma, USA

Methanol: Merck, Germany

Monosodium phosphate: Ajax Finechem Pty Limited, Australia

MTT (3-(4,5-Dimethylthiazol-2-yl)-2,5-Diphenyltetrazolium Bromide): Sigma, USA

NED (*N*-1-napthylethylenediamine dihydrochlorides): Merck, USA

Penicillin-streptomycin solution: HyClone, UK

Phosphoric acid: Merck, USA

Potassium hydroxide: Merck, Germany

Sodium carbonate: Merck, Germany

Sodium chloride: Ajax Finechem Pty Limited, Australia

Sodium dihydrogen phosphate dihydrate: Merck, Germany

Sodium molybdate: Carlo Erba, Italy

Sodium nitrate: Merck, Germany

Sodium pyruvate solution: HyClone, UK

Streptomycin: Sigma, USA

Sulfanilamide: Merck, USA

SYBR® safe DNA gel strain: Invitrogen, USA

Trizma (2-amino-2-(hydroxymethyl)-1,3-propanediol): Sigma, USA

TRIzol® reagent: Invitrogen, USA

Yeast extract powder: Himedia, India

Zinc sulfate: Ajax Finechem Pty Limited, Australia

3.3 Membrane

YM-3 membrane Ultracel®-3K, Millipore, USA

3.4 Kits

HiYield™ Plasmid Mini Kit, RBC Bioscience, Taiwan

SuperScript™ III First Strand Synthesis system, Invitrogen, USA

3.5 Enzymes

BamHI: New England Biolabs, USA

Taq DNA polymerase: Invitrogen, USA

XhoI: New England Biolabs, USA

3.6 Plasmids and bacterial strains

Table 1: Plasmids and bacterial strains used this study.

Strains and plasmids	Descriptions	Sources/References
Ap3858-3855/pUC303	2.76 kb *Ap3858* (native promotor and coding region of *Ap3858*) together with 3.63 kb *Ap3857-3855* (native promotor and coding region of *Ap3857-3855)* cloned into pUC303	Waditee-Sirisattha *et al*., 2014
E. coli DH5α	Φ80lacZΔM15 Δ(lacZYA-argF) U169 recA1 endA1 hsdR17 (rK^-, mK^+) phoA supE44 λ– thi-1 gyrA96 relA1	Invitrogen, USA
Halothece sp. PCC 7418	Halotolerant cyanobacterium	This study
S. elongatus PCC 7942	Freshwater cyanobacterium	Research Institute of Meijo University, Japan

Table 2: Primers used in this study.

Primers	Sequences (5′ ⟶ 3′)	Base pairs
Ap3855_Forward	TTATCCGAGAAACTCTCC	18
Ap3855_Reverse	AGGTCATACTTATCCTGAG	19
Ap3856_Forward	GGATCCAATGCTTCTATTTGTCCGAGG	27
Ap3856_Reverse	ATAGTAACTAGAAACGGGAC	20
Ap3857_Forward	GGATCCAATGACGATCACTAACGATAAAC	29
Ap3857_Reverse	ATGCAGAATAGCCCGTAAAC	20
Ap3858_Forward	GGATCCAATGACGAAAACAACCTCTG	27
Ap3858_Reverse	TGAGGATCGGTTTCCACAAG	20
beta-actin_Forward	ATGGTGGGAATGGGTC	16
beta-actin_Reverse	CATACAGGGACAGCAC	16
Catalase_Forward	GGGATTCCCGATGGT	15
Catalase_Reverse	GCCAAACCTTGGTCAG	16
Cox-2_Forward	ACAGATTGCTGGCCG	15
Cox-2_Reverse	TGGTGCTCCAAGCTC	15
HemeOx1_Forward	CTGGGTGACCTCTCAG	16
HemeOx1_Reverse	GACGAAGTGACGCCA	15
iNos_Forward	AGATCGAGCCCTGGA	15
iNos_Reverse	GTGCTTGTCACCACC	15
Nrf2_Forward	GCCCAGAACTGTAGGA	16
Nrf2_Reverse	CATCCTCCCGAACCT	15
Sod1_Forward	GGAACCATCCACTTCG	16
Sod1_Reverse	TACGGCCAATGATGGA	16
7942Catalase_Forward	CTACCGAATTGCCGA	15
7942Catalase_Reverse	GGGATTGGTGCTTGG	15
7942sodB_Forward	ACCAAGGAAACGCTG	15
7942sodB_Reverse	CGGCTTGTTTGAACTC	16
7942ThioPerox_Forward	CCGTAAAGAAGGTGGT	16
7942ThioPerox_Reverse	CTTAACAGGGTCGGG	15

Primers	Sequences (5′ ⟶ 3′)	Base pairs
7942rnpB_Forward	GAGGAAAGTCCGGGCTCCC	19
7942rnpB_Reverse	TAAGCCGGGTTCTGTTCTC	19

3.7 Extraction and purification of M2G

3.7.1 Culture condition

Halothece sp. PCC 7418 was cultured in blue green-11 (BG-11) plus Turks island salts solution (Appendix 1) containing 2.5 M NaCl under continuous light condition at 30ºC (Waditee-Sirisattha *et al.*, 2014). The cyanobacterial growth was monitored via spectrophotometry at 730 nm until the absorbance reached four, approximately. The cells were harvested by centrifugation at 8,000 rpm for 10 minutes at 25ºC.

3.7.2 Extraction of M2G

Harvesting cells were weighed to gain appropriate fresh weights. HPLC-grade methanol was added in volume (mL) of five times per gram fresh weight. Then, the suspended cells were disrupted by sonication. The cell debris was precipitated by centrifugation at 8,000 rpm for 10 minutes at 25ºC. Resulting supernatants were collected in the new tubes. This extraction step was repeated twice. The combined supernatants were dried up using rotary evaporator at 45ºC. The dried samples were resuspended in one milliliter of distilled water. Thereafter, suspension was precipitated insoluble materials and high molecular weight compounds by YM-3 membrane column (Millipore, USA), yielding the methanolic extracted M2G.

3.7.3 Purification of M2G

3.7.3.1 Solid phase chromatography

The extracted M2G was purified by using strong cation chromatography (DSC-SCX-SPE® cartridge (Sigma, USA)). This column was washed with distilled water, then the YM-3-treated sample from step 3.7.2 was subjected to the cartridge. After that, distilled water was loaded onto the cartridge to elute M2G. The absorption of each

fraction was analyzed, and the fractions with high absorption at 330 nm were subjected to the reverse phase cartridge.

3.7.3.2 Reverse phase chromatography

The reverse phase cartridge (DSC18-SPE® (Sigma, USA)) was equilibrated with acetic acid (1%). Then, the obtained fractions were adjusted the concentration of acetic acid to 1% and subjected to the cartridge. Thereafter, acetic acid (1%) was loaded into the cartridge to elute M2G. The absorption of each collected fraction was analyzed. The fractions with high absorption at 330 nm were dried up by rotary evaporator. The dried sample was dissolved in 0.1 M ammonium acetate (1 mL). Another DSC18-SPE® cartridge was equilibrated with 0.1 M ammonium acetate. Then, the sample was subjected to the cartridge. The ammonium acetate was loaded into the cartridge to elute M2G, the absorption of each fraction was analyzed. Fractions with high absorption at 330 nm were dried up and stored at -40°C for further experiments. Concentration of M2G was determined using the authentic compound MAA.

3.7.4 Endotoxin assay

The purified M2G obtaining from step 3.7.3.2 was dissolved in an endotoxin-free ultrapure water (E-Toxate™ water, Sigma, USA). The M2G solution was diluted to be a concentration of 10 μM by the ultrapure water. Ten micromolar of M2G solution was examined its biological toxicity via Limulus Amoebocyte Lysate (LAL) bacterial endotoxin assay. The experiment was performed by an authority at Nephrology department, King Chulalongkorn Memorial Hospital. The endotoxin amount was reported as endotoxin unit per milliliter (EU/mL).

3.8 Determination of antioxidant activity of M2G under various pHs

The M2G solution was diluted to the desired concentration in pH-adjusted buffers at pH 5.0, 6.0, 7.0, 8.0, and 9.0, respectively. DPPH solution was prepared by dissolving DPPH in the ethanol:water (1:1) solution for scavenging activity assay. Then, 200 μL of pH-adjusted M2G was added into 800 μL of DPPH solution. After 30 minutes of incubation in the dark, the absorbance of the solution was measured at 517 nm. The

obtained values were calculated to the percentage of scavenging activity using the following formula as described previously (Cheewinthamrongrod *et al.*, 2016).

$$\% \text{ scavenging activity} = [(A_{control} - A_{sample}) / A_{control}] \times 100$$

when A = absorbance at 517 nm

control = non-treated reaction

sample = treated reaction

3.9 Determination of anti-inflammatory and antioxidative activities in cell line

3.9.1 Anti-inflammatory activity in LPS-stimulated RAW 264.7 macrophage

3.9.1.1 Culture condition for RAW 264.7 macrophage

RAW 264.7 (ATCC TIB-71) macrophage was cultured in non-treated and treated plates with completed Dulbecco's modified Eagle's medium (DMEM). The medium contained 4 mM L-glutamine and 4.5 g/L of glucose and supplemented with fetal bovine serum (10%), sodium pyruvate (1%), HEPES (1%), 100 U/mL of penicillin, and 100 ng/mL of streptomycin. The cells were incubated at 37°C under 5% CO_2 in the humidified incubator (Thermo Electron Corporation, USA). The medium was renewed every 2-3 day during experiments.

3.9.1.2 Biocompatibility assay

The cells were seeded at 2×10^4 cells/well in 96-well cell culture plate with a total volume of 100 µL/well and incubated for overnight. Then, the medium was replaced by 100 µL/well of fresh completed DMEM containing M2G (final concentrations 0.1, 1, 5, and 10 µM, respectively). The treated cells were incubated for 20 hours. As for the cell viability assay, 0.5 mg/mL of 3-(4,5-dimethylthiazol-2-yl)-2,5-diphenyltetrazolium bromide (MTT) reagent was added into each well to be a substrate for the formazan crystals formation. The reaction occurred by the mechanism of action of the reduction enzyme, namely mitochondrial reductase. In this step, a yellow soluble reagent was reduced by mitochondrial reductase to be a non-soluble purple crystalline. After 4 hours of incubation, 200 µL of DMSO was added into each

well for dissolving the formazan crystal. The formazan solutions were determined using microplate reader at 540 nm (Thermo Scientific, USA).

3.9.1.3 Measurement of nitric oxide

RAW 264.7 cells were seeded at 2×10^5 cells/well in 96-well plate. The total volume was 200 µL/well. After overnight incubation, the seeded cells were pretreated for an hour by replacing medium with 50 µL of completed DMEM containing the tested concentrations of M2G. Then, an inflammatory stimulator, *Salmonella enterica* serovar Minnesota's lipopolysaccharide (LPS), was added into the pretreated wells by mixing in the M2G supplemented medium. The final volume of the medium in each well was 100 µL with 100 ng of LPS. The treated cells were incubated for 24 hours. After that, the supernatants were transferred into a round bottom 96-well plate. Fifty microliters of sulfanilamide solution, composed of sulfanilamide (1%) in phosphoric acid (5%), was subjected into the wells and incubated in the dark for 15 minutes, followed by an equal volume of NED solution (1% of *N*-1-napthylethylenediamine dihydrochlorides). The solutions were incubated again in the dark for 15 minutes and determined the absorbance at 540 nm using microplate reader.

3.9.1.4 Semiquantitative reverse transcription polymerase chain reaction (RT-PCR) analysis

3.9.1.4.1 Cell preparation

RAW 264.7 cells were seeded in 24-well cell culture plate at 3×10^5 cells/well with a volume of 500 µL/well and incubated for overnight. Then, the cells were pre-treated with 250 µL of completed DMEM with M2G concentrations as described in step 3.9.1.2 for an hour. The pre-treated cells were treated with *Salmonella enterica* serovar Minnesota's LPS, yielding the final volume of 500 µL.

3.9.1.4.2 RNA extraction and cDNA conversion

Total RNA was extracted after inflammatory stimulation for 0, 3, and 6 hours, respectively. This step was performed by removing all the medium and adding 500 µL of cold TRIzol® reagent (Invitrogen, USA). Suspensions were incubated for 5

minutes, mixing homogenously, and collecting in an RNAse-free microcentrifuge tube. Two hundred microliters of cold chloroform were added to the harvested solution. The suspension was mixed gently by inversion for 15 seconds. After 3 minutes of incubation at room temperature, the mixture was separated into 3 phases; (1) supernatant, (2) fats and proteins, and (3) phenolic phase by centrifugation at 12,000×g, 4°C for 10 minutes. The supernatant was collected in a new microcentrifuge tube. After that, 250 µL of cold isopropanol was added into the collected sample and further incubated for 10 minutes. Finally, this suspension was centrifuged at 12,000×g, 4°C for 10 minutes. The supernatant was discarded carefully to get a gel-like pellet. One milliliter of 75% ethanol was added and pipetted gently to wash the pellet, followed by centrifugation at 7,500×g, 4°C for 5 minutes. The supernatant was removed and the pellet was air dried by overturned the cap-opened microcentrifuge tube. The RNA pellet was dissolved in 30 µL of DEPC-treated water and incubated at 60°C for 15 minutes. RNA concentration and its quality were determined using Nanodrop 200 (Thermo Scientific, USA) and gel electrophoresis, respectively. High quality total RNA was kept at -80°C prior analysis. For the cDNA conversion, final concentration of total RNA was 1,680 ng. The reaction was performed using SuperScript®III First-Stranded synthesis kit (Invitrogen, USA) as per the manufacturer's instruction. The cDNAs were kept at -20°C for further experiments.

3.9.4.1.3 Proinflammatory gene expression analysis

Two proinflammatory genes; *iNOS* and *COX-2* were amplified by PCR, using specific primer pairs (Table 2 and Appendix 3). Gel electrophoresis was carried out using 1.2% agarose gel precasting with 0.1 µL/mL of SYBR® safe DNA gel stain (Invitrogen, USA). Band intensities were analyzed by ImageJ (https://imagej.nih.gov/ij/). The housekeeping gene *β-actin* was used as an internal control gene.

3.9.2 Antioxidative property in RAW 264.7 macrophage

3.9.2.1 Cell viability assay

3.9.2.1.1 H_2O_2 toxicity

The macrophage cells were seeded at 2×10^4 cells/well in 96-well cell culture plate, the total volume was 100 µL/well, and incubated for overnight. Then, the medium was replaced by equal volume of completed DMEM containing various concentrations of H_2O_2. The cell viability determination was performed using the protocol described in 3.9.1.2. Inhibition concentration (IC_{50}) was calculated by GraphPad Prism 7 (https://www.graphpad.com/scientific-software/prism/).

3.9.2.1.2 Antioxidative property of M2G by co-treatment

The cells were seeded at 2×10^4 cells/well in 96-well cell culture plate with total volume of 100 µL/well and incubated for overnight. Then, the medium was replaced by 100 µL/well of DMEM containing the IC_{50} or $2\times IC_{50}$ concentrations of H_2O_2 (obtaining from step 3.9.2.1.1) together with M2G. Determination of cell viability was performed using the same protocol described in 3.9.1.2.

3.9.2.1.3 Antioxidative property of M2G by pre-treatment

RAW 264.7 cells were seeded at 2×10^4 cells/well in 96-well cell culture plate with total volume of 100 µL/well and incubated for overnight. Then, the medium was replaced by 50 µL/well of DMEM with the concentrations of M2G and incubated for an hour to pretreat the cells. After that, 50 µL of DMEM contained M2G and $2\times IC_{50}$ or $4\times IC_{50}$ concentrations of H_2O_2 was added into each well. The final concentration of H_2O_2 was IC_{50} or $2\times IC_{50}$, respectively. Determination of cell viability was performed using the same protocol as described in 3.9.1.2.

3.9.2.2 Semiquantitative RT-PCR analysis

3.9.2.2.1 Determination of time for H_2O_2 treatment

3.9.2.2.1.1 Cell preparation

RAW 264.7 cells were seeded in 24-well cell culture plate at 3×10^5 cells/well with 500 µL/well of total volume and incubated for overnight. Then, the cells were treated with equal volume of completed DMEM containing IC_{50} of H_2O_2.

3.9.2.1.1.2 RNA extraction and cDNA conversion

RNA extraction was performed at 0, 1, 3, and 6 hours after stress followed the protocol described in 3.9.1.4.2. High quality total RNA solutions were kept at -80°C prior analysis. For the cDNA conversion, final concentration of total RNA was 1,680 ng. The reaction was performed using SuperScript®III First-Stranded synthesis kit followed the manufacturer's instruction. The cDNAs were kept at -20°C for further experiments.

3.9.2.1.1.3 Antioxidant gene expression analysis

Four genes; *Nrf2, sod1, cat,* and *Hmox1* were amplified by PCR using specific primer pairs (Table 2 and Appendix 3). Gel electrophoresis was carried out using 1.2% agarose gel precasting with 0.1 µL/mL of SYBR® safe DNA gel strain. Band intensities were analyzed by ImageJ. The housekeeping gene *β-actin* was used as an internal control gene.

3.9.2.2.2 Determination of antioxidative property of M2G

3.9.2.2.2.1 Cells preparation

RAW 264.7 cells were seeded in 24-well cell culture plate at 3×10^5 cells/well with 500 µL/well of total volume and incubated for overnight. Then, the cells were treated with equal volume of completed DMEM containing IC_{50} of H_2O_2.

3.9.2.2.2.2 RNA extraction and cDNA conversion

RNA extraction was performed after stress for an hour as described in step 3.9.1.4.2. High quality total RNA was kept at -80°C prior analysis. For the cDNA conversion, final concentration of total RNA was 1,680 ng. The reaction was performed using SuperScript®III First-Stranded synthesis kit as per the manufacturer's instruction. The cDNAs were kept at -20°C for further experiments.

3.9.2.2.2.3 Gene expression analysis

Four genes; *Nrf2, sod1, cat,* and *Hmox1* were amplified by PCR using specific primer pairs (Table 2 and Appendix 3). Gel electrophoresis was carried out using 1.2% agarose gel precasting 0.1 µL/mL of SYBR® safe DNA gel strain. Band intensities were analyzed by ImageJ. The housekeeping gene *β-actin* was used as an internal control gene.

3.10 Heterologous expression of M2G genes cluster in cyanobacterial model *Synechococcus elongatus* PCC 7942 under oxidative stress

3.10.1 Transformation of M2G biosynthetic gene cluster

3.10.1.1 Plasmid preparation and natural transformation

3.10.1.1.1 *E. coli* culture condition

Culture stock of *E. coli* DH5α harboring *Ap3858-3855*/pUC303 (Waditee-Sirisattha *et al.*, 2014) and the empty vector (pUC303) were grown in Luria-Bertani (LB) medium (Appendix 2) plus streptomycin (50 µg/mL) at 37°C for overnight. The cells growth was monitored via spectrophotometer (Shimadzu, Japan) at 620 nm.

3.10.1.1.2 Plasmid extraction

The growth cells were harvested by centrifugation at 13,000×g, 4°C for 5 minutes. Plasmids were extracted using HiYield™ Plasmid Mini Kit (RBC Bioscience, Taiwan) according to the manufacturer's protocol. The recombinant

plasmid was analyzed by restriction enzymes, BamHI and XhoI. The concentration and purity of plasmid was determined by using Nanodrop 200 (Thermo Scientific, USA).

3.10.1.1.3 Natural transformation

3.10.1.1.3.1 *S. elongatus* culture condition

Freshwater cyanobacterium *Synechococcus elongatus* was grown in BG11 medium under continuous light condition (28 μmol/m^2/s) at 30ºC. The cyanobacterial growth was monitored via spectrophotometry at 730 nm until the absorbance reached 1.0. The cells were harvested from 1 mL of culture by centrifugation at 8,000 rpm for 10 minutes at 25ºC and washed thrice with BG11 medium.

3.10.1.1.3.2 Transformation

The washed cells were mixed with 300 ng of each plasmid and incubated under the dark condition for overnight. The transformants was recovered in two sets. The first set, transformants were laid onto BG11 agar plates for 10 days and selected by adding streptomycin (50 μg/mL). For the second set, the transformants were cultured in BG11 medium in 12-well plates. After seven days, the transformants were transferred to BG11 agar plate plus streptomycin (50 μg/mL). The transformation was performed under the same condition as wild-type at 30ºC. The recovered transformants were verified by colony PCR analysis using specific primers for four biosynthetic genes *Ap3858*, *Ap3857*, *Ap3856*, and *Ap3855*, respectively.

3.10.2 Morphological and physiological investigations under oxidative stress

3.10.2.1 Culture and stress condition

The transformant cells was cultured in BG11 medium plus streptomycin (50 μg/mL) until the absorbance at 730 nm reached approximately 0.5. The cultures were transferred into 10 mL glass tubes and was stressed by adding H_2O_2 varying from 0-10 mM.

3.10.2.2 Morphological and physiological investigations

The stressed cells were observed their morphological changes under bright field microscope at 0, 24, and 48 hours. The transformant carrying empty vector pUC303 was used as a control. The cells were measured their absorbance at 730, 665, and 650 nm at 0, 24, and 48 hours. The absorbances were calculated to IC_{50} using Graphpad Prism 7. Chlorophyll and phycocyanin amounts were measured using the following formula (Colowick & Kaplan, 1988).

$$\text{Chlorophyll (µg/mL)} = A_{665} \times 13.8$$

$$\text{Phycocyanin (mg/mL)} = \frac{A_{620} - (0.7 \times A_{650})}{7.38}$$

3.10.2.3 Antioxidant gene expression analysis

3.10.2.3.1 Cell preparation

The transformant cells was cultured in BG11 medium plus streptomycin (50 µg/mL) until the absorbance at 730 nm reached approximately 0.5. Then, the cultures were transferred to BG11 medium plus streptomycin (50 µg/mL) supplemented by ½IC_{50}, IC_{50}, and IC_{50}+½IC_{50} concentrations of H_2O_2, respectively, and incubated under continuous light condition at 30°C. The cells were harvested at 6 hours by centrifugation at 8,500×g, 4°C for 15 minutes.

3.10.2.3.2 RNA extraction and cDNA conversion

Cell fresh weight (approximately 80-100 mg) were resuspended in cold TRIzol® reagent (Invitrogen, USA) on ice. Then, the suspension was transferred to chilled mortar and grinded. The mixture was collected in a microcentrifuge tube for RNA extraction and cDNA conversion, which was performed as the protocol as described in 3.9.1.4.2.

3.10.2.3.3 Gene expression analysis

Three candidate genes; *katG, sodB,* and *tpxA* were amplified by PCR using their specific primer pairs (Table 2 and Appendix 3) Gel electrophoresis was carried out using 1.2% agarose gel precasting with 0.1 µL/mL of SYBR® safe DNA gel strain. Band intensities were analyzed by ImageJ. The housekeeping gene *rnpB* was used as an internal control gene.

3.10 Statistical analysis

In this study, the calculated values were statistically analyzed within their datasets with student's t-test method by GraphPad Prism 7.

CHAPTER IV
RESULTS AND DISCUSSION

4.1 Extraction and purification of M2G

To obtain M2G, *Halothece* sp. PCC 7418 cells were extracted using methanol as described in Materials and Methods. The methanolic phase was obtained after high molecular weight compound filtrated by YM-3 membrane. The absorption measurement revealed that the impurity presented in the methanolic extract (shown as a high absorbance at < 280 nm in Figure 6 (A)). The extract was then further purified by using strong cation exchange and reverse phase columns, respectively. Two purification steps gave a high purity M2G fraction which exhibited a unique single absorbance peak with maxima absorption at 331 nm (Figure 6 (B)). This adsorption spectrum corresponds to maximal adsorption of M2G as previously described (Waditee-Sirisattha *et al.*, 2014). The purified compound was verified as M2G via TOF-MS and LC-MS/MS methods (kindly performed at Meijo University, Nagoya, Japan).

As for the priority of biotoxicity, the contaminated bacterial endotoxin could interfere the cell line experiments. Thus, the purified M2G sample was diluted with endotoxin-free ultrapure water to the highest biocompatible concentration at 10 μM (Cheewinthamrongrod *et al.*, 2016). Measurement of an endotoxin via LAL assay was performed (kindly performed at King Chulalongkorn Memorial Hospital). The result showed an endotoxin level of the purified M2G solution at 0.004 (EU/mL) (Table 3).

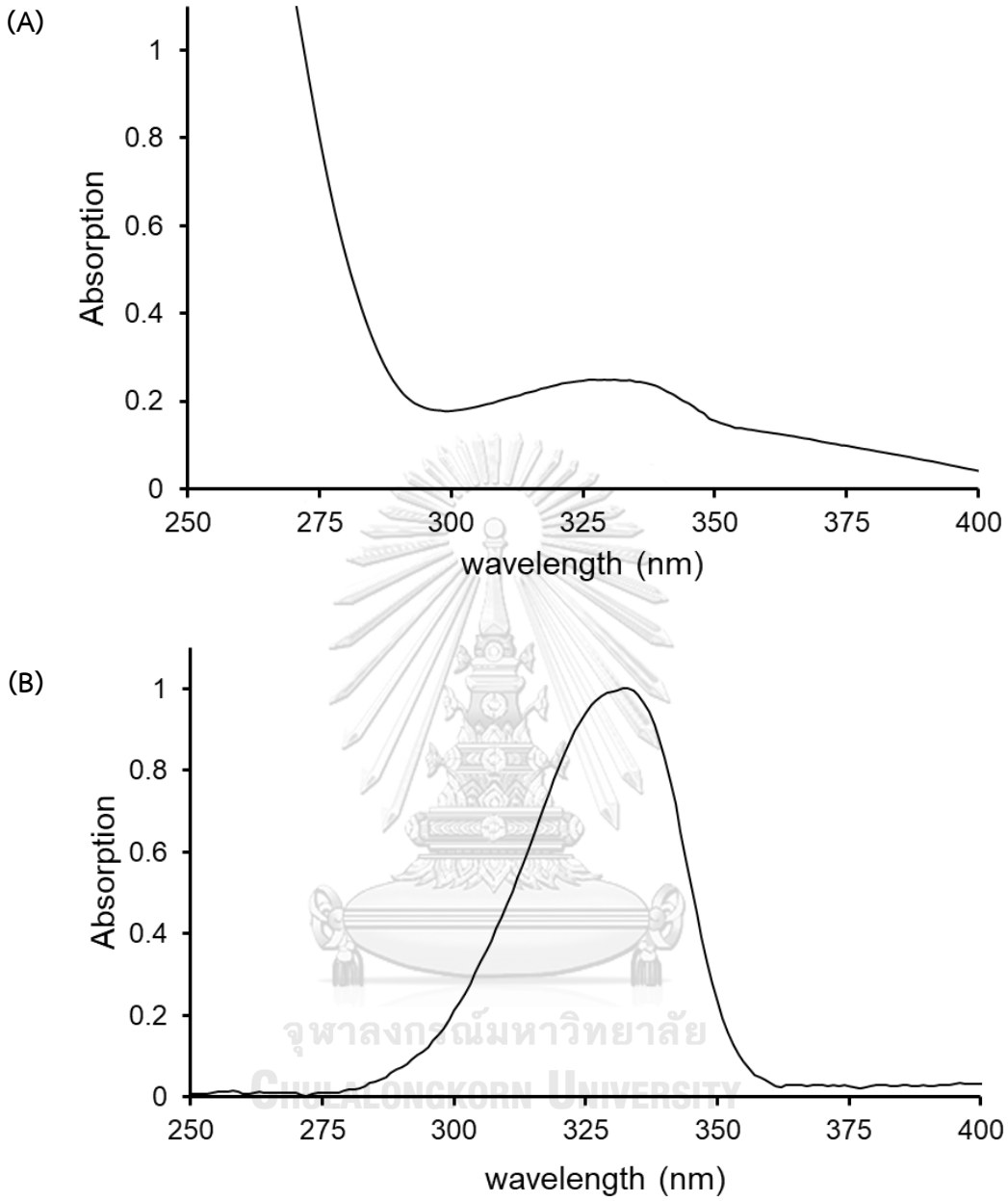

Figure 6: The absorption of fractions obtained from **(A)** methanolic phase and **(B)** purifications through strong cation exchange and reverse phase chromatographies using acetic acid (1% v/v) and 0.1 M ammonium acetate as diluents, respectively.

Table 3: Endotoxin level of purified M2G (10μM) and two references, the safety level of each water grade for medical and pharmaceutical approaches.

References	Samples	Endotoxin level (EU/mL)
This study	Purified M2G	0.004
European Pharmacopoeia	Regular water	< 0.25
	Ultrapure water	< 0.03
	Sterile water	< 0.03
AAMI 2012	Standard water	< 0.5
	Ultrapure water	<0.03

The results revealed the purified M2G obtained from the extraction and purification protocol described in this study, had high purity with a unique maxima absorbance for M2G at 331 nm and contained extremely low endotoxin level. This purified M2G met all standards for both medical and pharmaceutical approaches. These properties endorse the appropriateness of the purified M2G for further experiments and applications. This is the first report of a comprehensive protocol for purification of M2G with high purity and low endotoxin.

4.2 Determination of antioxidant activity of M2G under various pHs

In this study, antioxidant activity of M2G was determined under various pHs by DPPH method. M2G was resuspended with endotoxin-free water to 1 mM of concentration as a stock. pH adjusted buffers were used as diluents, reaching 5 μM of M2G solution in different pHs. DPPH testing solution was prepared at 0.1 mM by diluted with ethanol:water (1:1). Two hundred microliters of M2G solution was added to 800 μL of DPPH solution (0.1 mM). The mixture was incubated at dark for 30 minutes. After that, the absorbance at 517 nm was measured via spectrophotometer. The measured absorbances were calculated as % relative of scavenging activity.

As shown in Figure 7, M2G exhibited scavenging activities over a wide range of pHs; from 5-9. Thus, this is an advantage for utilizing in advance of applications.

Variations of the observed scavenging activities would be occurred from protons and electrons transfer capabilities of M2G under different proton concentration environments. This consequences to the majority of MAAs' electrons resonance capabilities, which is better in basic than in acidic surroundings (Wada *et al.*, 2013).

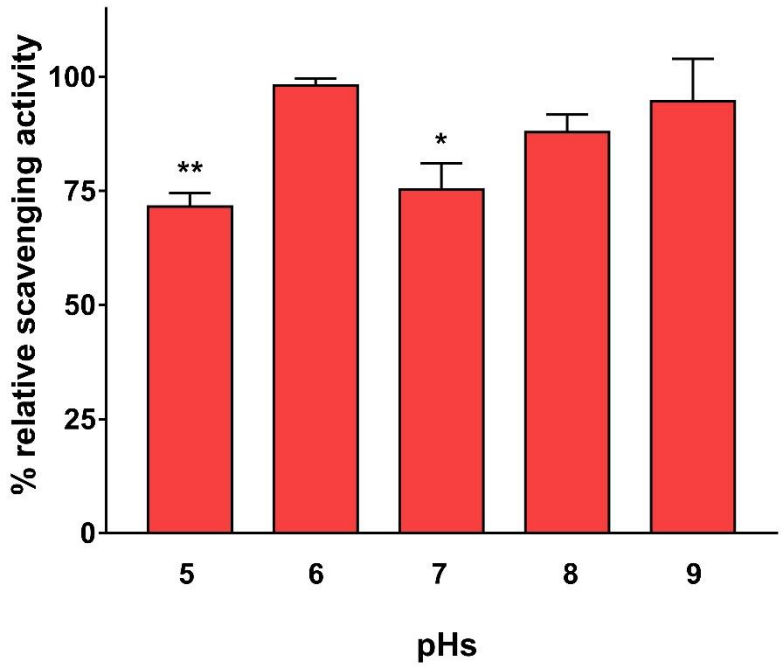

Figure 7: % relative of scavenging activity of M2G over a wide pHs. The experiment was conducted as a biological triplication, showed as mean ± standard deviation (SD). The highest observed value (at pH 6) was set at 100%. *, ** denoted significantly differences by student's t-test ($p<0.05$).

4.3 Determination of anti-inflammatory and antioxidative activities in cell lines

4.3.1 Anti-inflammatory activity in LPS-stimulated RAW 264.7 macrophage

4.3.1.1 Biocompatibility assay

In this study, RAW 264.7 murine macrophage (ATCC-TIB71) was used as a mammalian cell model for testing anti-inflammatory and antioxidative activities. For applications, the purified M2G must be biocompatible to the cells. Thus, the biocompatibility of M2G was examined via MTT assay. Concentrations of M2G used were in a range of 0.1 to 10 μM. As shown in Figure 8, the cell viabilities of all treated M2G concentrations were equal or slightly higher than the untreated cells. The untreated was set as 100% cell viability. These results indicated that M2G was biocompatible to RAW 264.7 murine macrophage in all concentrations tested from 0.1 to 10 μM (cells morphology was shown in Appendix 4). The result is consistent with the previous reports using M2G with normal human skin fibroblast (NHSF) (Cheewinthamrongrod *et al.*, 2016) and porphyra-334, an another common MAA which is found in many cyanobacteria and algae (Ryu *et al.*, 2014). Statistical analysis (student's t-test) showed significantly differences between untreated and M2G treated cells (5 μM and 10 μM), implied to cell proliferating promotion ability of M2G at these concentrations.

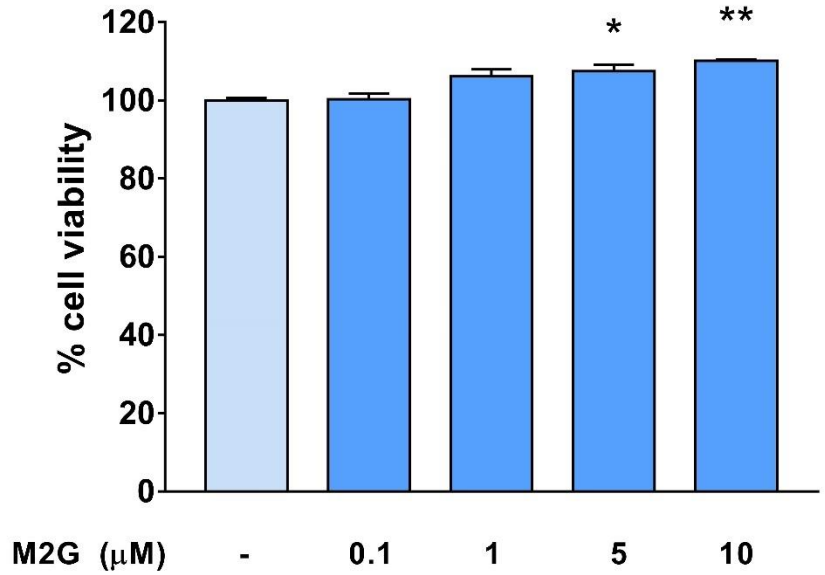

Figure 8: Biocompatibility assay. RAW 264.7 murine macrophage was used in this study. Cells were treated with M2G in concentrations of 0.1, 1, 5, and 10 μM for 24 hours. Cell viability of the untreated sample was set as 100% cell viability. The values were shown as mean ± standard error of mean (SEM). *, ** denoted significantly differences between the untreated and treated samples by student's t-test ($p<0.05$).

4.3.1.2 Measurement of nitric oxide as indicator of inflammation

Nitric oxide is one of the important proinflammatory cytokines, which is produced from the inflammatory-stimulated cells via NF-κB pathway (Chun *et al.*, 2004; Murakami & Ohigashi, 2007). An increasing nitric oxide level indicates the expression of *iNOS*, the important inflammatory gene (Massi *et al.*, 2001). To determine an anti-inflammatory activity of M2G, LPS from *Salmonella enterica* serovar Minnesota (100 ng/mL) was used as an inflammation inducer. The measured absorbances at 540 nm were compared with nitric oxide standard curve (Appendix 5) and calculated into nitric oxide content in form of a soluble nitrite concentration. The other four MAAs; shinorine+porphyra 334, mycosporine-glycine, and palythine were also used in this study.

The result showed a remarkable increase of the soluble nitrite to 27.53 ± 1.45 μM in the media harvested from LPS treated cells without M2G pretreatment, while the nitrite gradually decreased in the M2G pretreated cells. Interestingly, the trend of a detected nitrite concentration declined when the M2G concentration was increased. The lowest nitrite concentration was observed at 14.71 ± 1.02 μM from 10 μM M2G pretreated cells, counted as 46.57% (Figure 9 (A)) (cell morphology was shown in Appendix 4).

Figure 9 (B) showed the soluble nitrite concentration in non-pretreated and mycosporine-glycine pretreated macrophage media. The nitrite content was increased to 33.40 ± 2.12 μM in LPS treated cells without MG pretreatment. The soluble nitrite was detected in a smaller amount in mycosporine-glycine pretreated cells and the lowest amount was found to be 25.61 ± 1.21 μM (at the concentration of 0.1 μM), counted as 23.33%. Considering on pretreated cells, the soluble nitrite was increased by the MG concentration from 0.1 to 10 μM.

The combination of two MAAs which have been being used as an active ingredient in commercial sunscreens; shinorine and porphyra-334 (SHI+P334), was also tested in this study (Figure 9 (C)). The nitrite content was increased in LPS treated cells without SHI+P334 pretreatment and decreased slightly after pretreatment of 0.1 μM SHI+P334. The lowest nitrite concentration was found to be 25.61 ± 1.46 μM (at the

concentration of 1 μM), counted as 23.33%. Considering among pretreated cells, the nitrite levels were fluctuating by an increasing of the mixture concentration but lower than non-pretreated cells.

Figure 9 (D) showed the nitrite level of non-pretreated and palythine pretreated macrophage media. The content was increased to be 33.40 ± 2.12 μM in LPS treated cells without pretreatment, while oscillated in the pretreated-cells. The soluble nitrite was decreased to be 25.65 ± 0.60 μM (in 0.1 μM of palythine pretreated cells (23.21%)). When the concentration of palythine was boosted, the nitrite content was astonishingly increased. Then, it was dwindled again at higher concentrations.

From these results, M2G showed the strongest capability in reducing nitric oxide production among 5 MAAs tested. A significant reduction of the nitrite level is dose dependent. Thus, M2G may contribute as anti-inflammation for RAW 264.7 murine macrophage via NF-κB pathway.

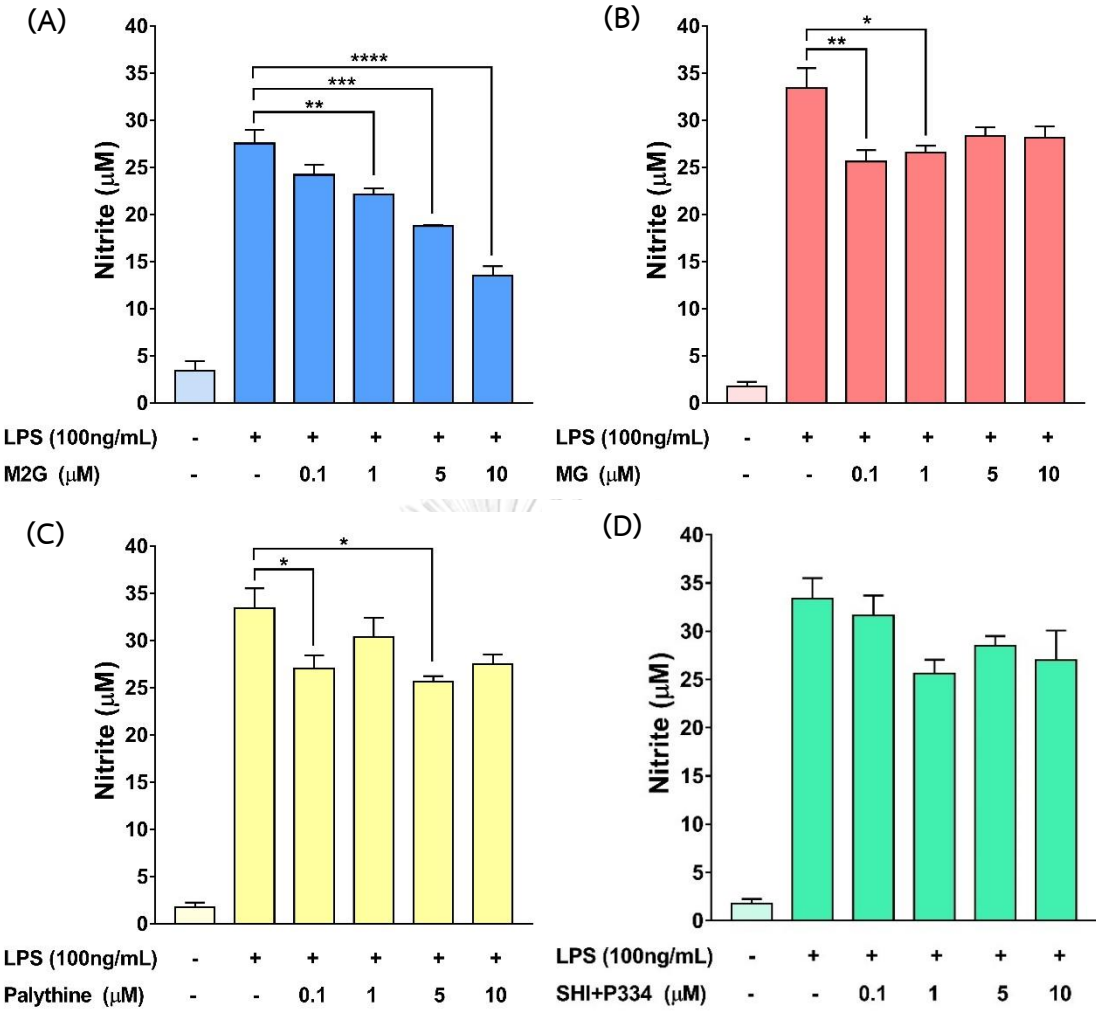

Figure 9: Nitric oxide assay. RAW 264.7 murine macrophage cells were pretreated with concentrations of five MAAs; mycosporine-2-glycine (M2G) **(A)**, mycosporine-glycine (MG) **(B)**, palythine **(C)**, and a mixture of shinorine and porphyra-334 (SHI+P334) **(D)** for an hour. For the inflammatory induction, Salmonella enterica serovar Minnesota LPS (100 ng/mL) was applied for 24 hours. The measured nitric oxide in form of soluble nitrite was shown as mean ± standard error of mean (SEM). **, ***, and **** denoted significantly differences between the untreated and MAAs treated inflammatory-induced samples by student's t-test ($p<0.05$).

4.3.1.3 Semiquantitative RT-PCR analysis

Semiquantitative RT-PCR analysis was performed to examine the anti-inflammatory effects of M2G at transcriptional level. Two marker genes *iNOS* and *COX-2* were monitored due to their importance as key regulator genes in inflammatory processes (Lee *et al.*, 2003b). In this study, RAW 264.7 murine macrophage was seeded 2×10^5 cells/well in 24-well plate and incubated for overnight. *Salmonella enterica* serovar Minnesota LPS was applied as an inflammation inducer. Concentrations of M2G were added into wells to pretreat the cells for an hour before the inflammatory stimulation. Total RNA was extracted from cells at interval times. The cDNA was prepared as described in Materials and Methods. PCR was performed by using the cDNA as a template with specific primer pairs (Appendix 3).

Figure 10 showed the expression of *iNOS* and *COX-2* under normal and inflammation-stimulated with or without M2G treatment macrophage. Quality and equality of total RNA concentrations used in this study were verified by 18s rRNA integrity and an internal control *β-actin* expression, respectively. Expression of *iNOS* was not detected in untreated macrophage. It was obviously; however, that *iNOS* expression was up-regulated in LPS-stimulated macrophage. Noteworthy, M2G treated-condition alleviated *iNOS* expression either 1 or 10 μM M2G. Bands quantitation revealed the dramatically decreased of *iNOS* gene expression by 50% using 1 μM M2G treatment. The highest efficiency of M2G in *iNOS* downregulation was 75% in the presence of 10 μM M2G (Figure 11 (A)).

The expression of *COX-2* was upregulated by the induction of LPS. M2G treatment at 1 μM resulted in the decreasing of gene expression (shown in Figure 10). Bands quantitation was performed and calculated to the relative intensity, shown in Figure 11 B). The transcriptional analysis revealed that M2G treatment could suppress the expression of *COX-2* gene by 65% at 3 hours at lower concentration (*i.e.* 1 μM), compared to an inflammatory-induced sample without any treatment. The expression; however, was increased after 6 hours of treatment. This result suggested that M2G efficiently suppressed *COX-2* expression at lower concentration (i.e. 1 μM) but not at high concentration.

Transcriptional analysis revealed an anti-inflammation capability of M2G. This compound is capable of downregulating *iNOS* gene expression. This is the first report to show MAA regulates iNOS at transcriptional level. Comparing to astaxanthin, the well-known strong antioxidant (Lee *et al.*, 2003a), M2G exhibited a better suppression using the same concentration. In case of *COX-2*, the downregulation of this gene was found when applied M2G at a low concentration (1 μM). *COX-2* transcriptional regulation of three MAAs; shinorine, porphyra-334, and mycosporine-glycine was previously reported using UV-A as an inflammatory-inducer (Suh *et al.*, 2014). Amongst these compounds, M2G exhibited the highest capability to suppress *COX-2* gene expression. That was, M2G could restrain the expression of *COX-2* at lower level while shinorine, porphyra-334 and mycosporine-glycine exhibited at higher levels (30, 150, and 300 μM, respectively).

From these results, M2G provided a strong anti-inflammation property in RAW 264.7 murine macrophage by suppression of *iNOS* and *COX-2* at lower concentrations.

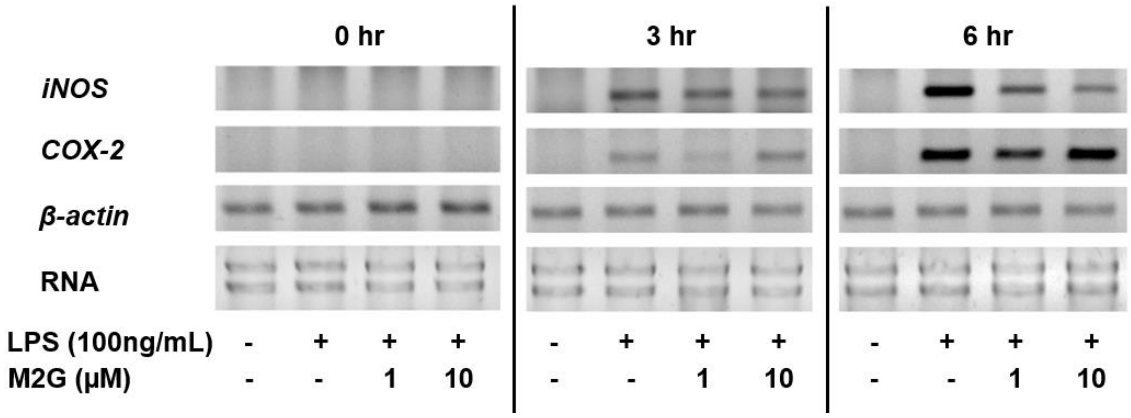

Figure 10: Semiquantitative RT-PCR analysis of two essential inflammatory genes; *iNOS* and *COX-2*. RAW 264.7 cells were pretreated with M2G for an hour before inflammatory stimulation by *Salmonella enterica* serovar Minnesota LPS (100 ng/mL). Quality and equality of total RNA concentrations were confirmed by 18s rRNA integrity and internal control *β-actin* expressions, respectively. PCR products were analyzed by 1.2% gel electrophoresis precasting with 0.1 μL/mL of SYBR® safe DNA gel stain.

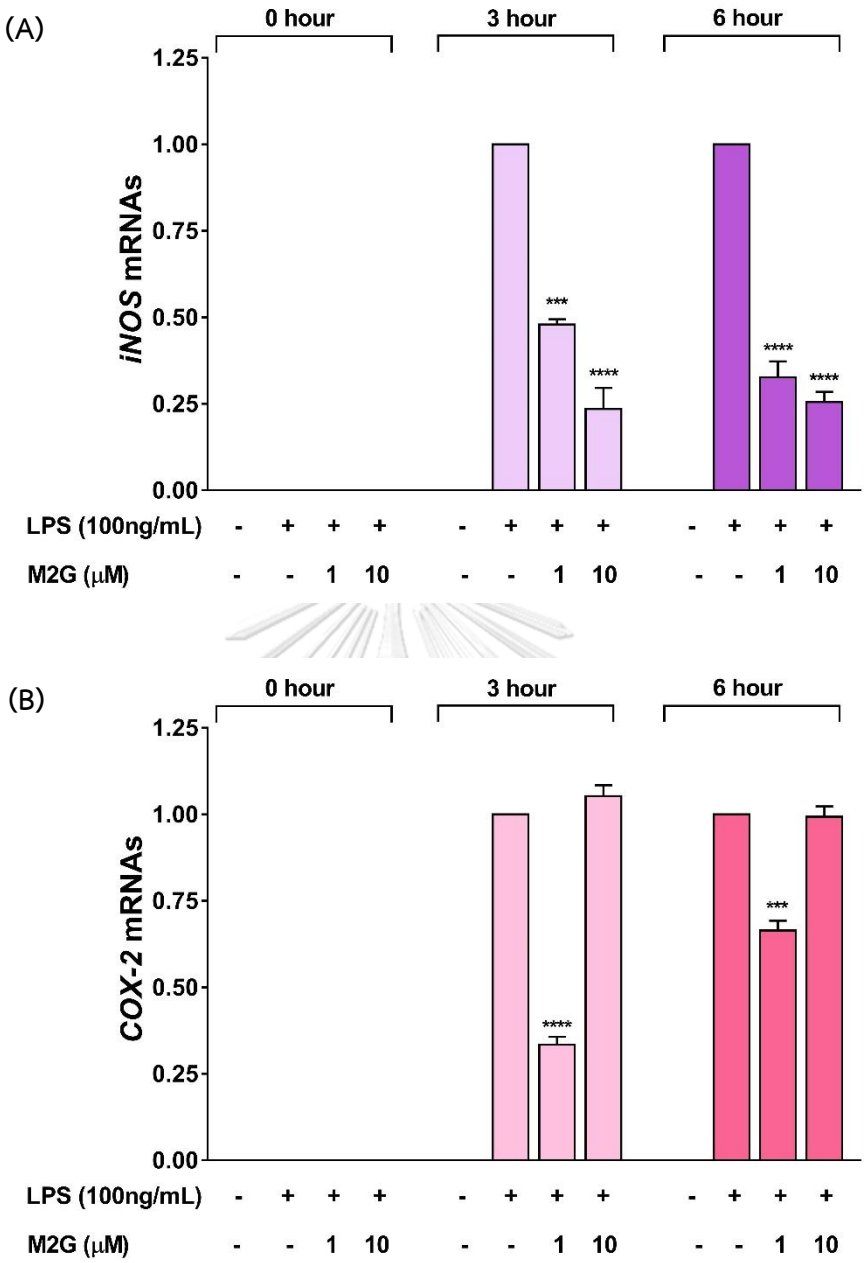

Figure 11: Relative bands intensity of two essential inflammatory genes; *iNOS* **(A)** and *COX-2* **(B)**. The intensity was obtained by band quantitation using ImageJ. The quantitated values were conducted by three individuals of RT-PCR and gel electrophoresis, shown as mean ± standard error of mean (SEM). *** and **** denoted significantly differences between the untreated and M2G treated inflammatory-induced samples by student's t-test ($p<0.05$).

4.3.2 Antioxidative property in RAW 264.7 macrophage

4.3.2.1 Cell viability assay

4.3.2.1.1 H_2O_2 toxicity

Hydrogen peroxide (H_2O_2) is known as a strong oxidizer in a group of ROS. It is widely used as an oxidant generator in *in vitro* analysis. The concentration used in each experiment is different, depending on cells durability. Thus, in this study, H_2O_2 toxicity to RAW 264.7 murine macrophage was firstly examined via MTT assay. The cells were seeded 2×10^4 cells/well for 24 hours. H_2O_2 was then added to the seeded cells, reaching final concentrations from 100 - 1,000 μM. As shown in Figure 12 (A), the macrophage could tolerate the concentrations of H_2O_2 up to 400 μM (calculated as 100% cell viability or above). At higher concentrations over 400 μM, the cell viability was progressively declined, caused an inverse sigmoidal trend line. The cells were completely devasted by 1,000 μM due to whether necrosis or apoptosis mechanisms by an induction of H_2O_2 (Lin *et al.*, 2007). IC_{50} for H_2O_2 was calculated by Graphpad Prism 7. It was 603.2 ± 5.73 μM (Figure 12 (B)).

According to above results, RAW 264.7 macrophage showed an ability to tolerate the toxicity of H_2O_2 in higher concentration when compared to other cell lines such as A375 melanoma or normal human skin fibroblast (NHSF) (Cheewinthamrongrod *et al.*, 2016). This is due to the development of series of antioxidant enzymes to reduce excess or redundant ROS naturally produced by itself (Tan *et al.*, 2016). IC_{50} of H_2O_2 for RAW 264.7 cells was previously reported, ranging from 400 to 1,000 μM (Lin *et al.*, 2007; Piao *et al.*, 2011; Wen *et al.*, 2013). Based on IC_{50} obtained in Figure 12 (B), thus, H_2O_2 in the concentration of 600 μM was used further.

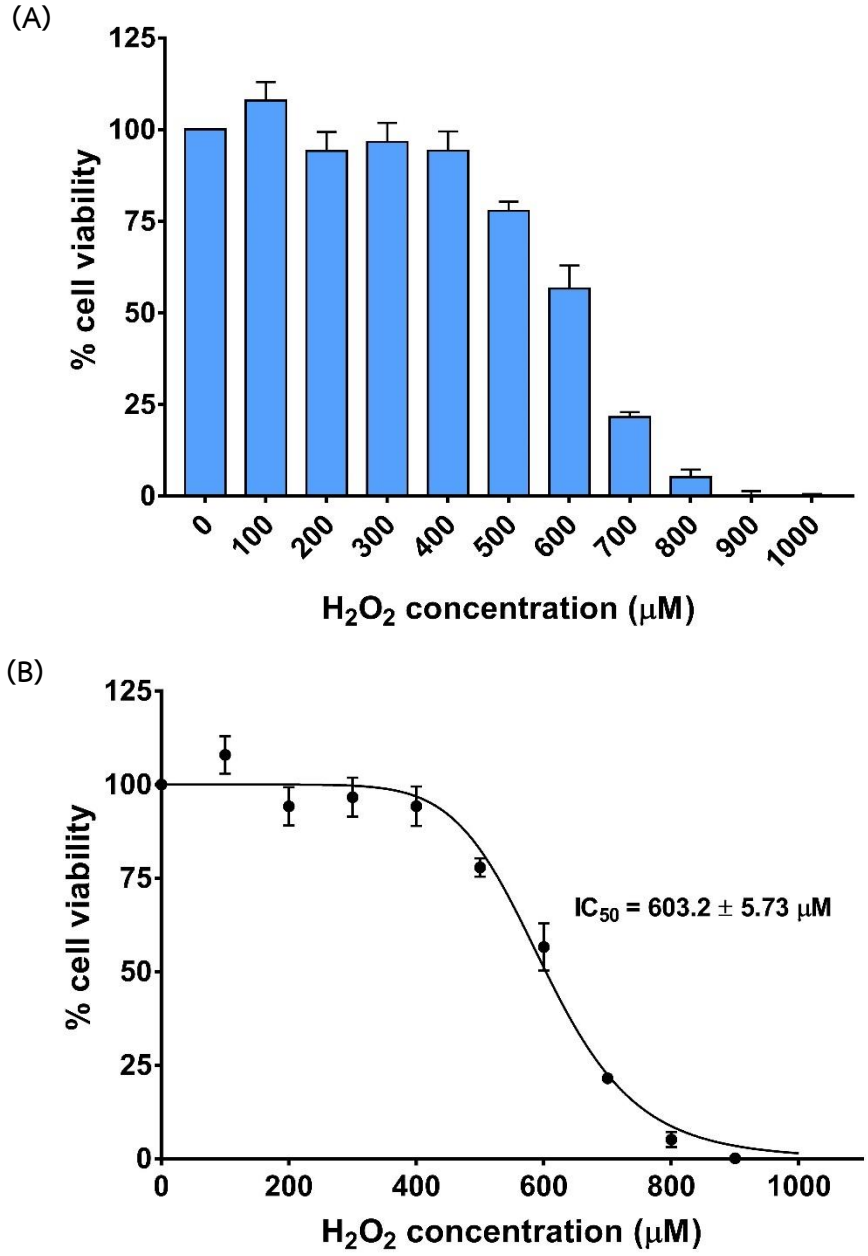

Figure 12: H_2O_2 toxicity assay **(A)** and its IC_{50} **(B)**. RAW 264.7 cells were oxidatively stressed by H_2O_2 ranging from 0 to 1,000 μM for 24 hours. Cell viability of the non-stressed condition was set at 100%. The cell viabilities were shown as mean ± standard error of mean (SEM). IC_{50} was calculated by Graphpad Prism 7 with 95% confidence (r^2 = 0.9841).

4.3.2.1.2 Antioxidative property of M2G via co-treatment

Due to the attribution as a rapid oxidizer of H_2O_2, stress condition and treatment protocol must be chosen conscientiously. Two treatment methods; pretreatment and co-treatment methods, were performed and measured via MTT assay for the purpose of achieving the proper approach. As for the co-treatment method, RAW 264.7 murine macrophage were seeded 2×10^4 cells/well and incubated for overnight. Cells were then co-treated by adding 600 μM H_2O_2 (IC_{50} value) together with concentrations of M2G varying from 0.1-10 μM. After 24 hours, cells were analyzed by MTT method. Figure 13 showed cells survival after 24 hours of co-treatment (as % cell viability). The untreated sample was set as 100% viability. According to Figure 13, cells survival rate was gradually increased by an escalation of M2G concentration. The highest recovery was retrieved from co-treatment with 10 μM M2G, count as 20% recovery or 70% cell viability, approximately (cell morphology was shown in Appendix 4).

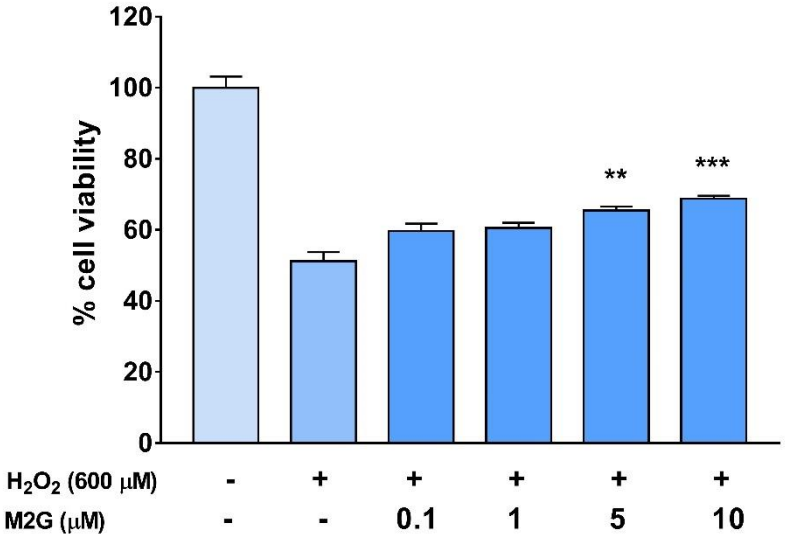

Figure 13: Cell viability assay via co-treatment method. RAW 264.7 murine macrophage were co-treated with 600 μM H_2O_2 together with concentrations of M2G for 24 hours. Cell viability of the non-stressed condition was set at 100%. The cell viabilities were shown as mean ± standard error of mean (SEM). **, *** denoted significantly differences between the stressed with untreated and treated samples by student's t-test ($p<0.05$).

4.3.2.1.3 Antioxidative property of M2G via pretreatment

Pretreatment method was conducted to compare with the co-treatment as described in 4.3.2.1.1. RAW 264.7 murine macrophage were seeded at the same concentration and incubated for overnight. Then, cells were pretreated by adding concentrations of M2G from 0.1 to 10 μM and incubated for an hour. After that, H_2O_2 was added into the wells to reach the final concentration at 600 μM (IC_{50} value). After 24 hours, treated cells were analyzed by MTT method. Figure 14 showed that the cells viability was decreased after M2G treatment. The lowest viability was observed at almost 35% from 1 μM of M2G, while more concentrations could recover the cells viability back to 40%, approximately.

Compared to co-treatment, this treatment method gave a poor cell recovery. This may occur from the time of reaction between M2G and H_2O_2. That is; in co-treatment, M2G reacts to the H_2O_2 instantly and reduces the radicals in the medium before the cells treatments. In pre-treatment; however, H_2O_2 in the medium was directly applied to the treated-cells. This may cause a radical-excessive condition to the cells before the reaction between M2G and H_2O_2.

From these results, M2G treatment by co-treatment is appropriate to recover cells from oxidative stress, induced by H_2O_2. To further observe transcriptional levels of related genes, co-treatment was performed.

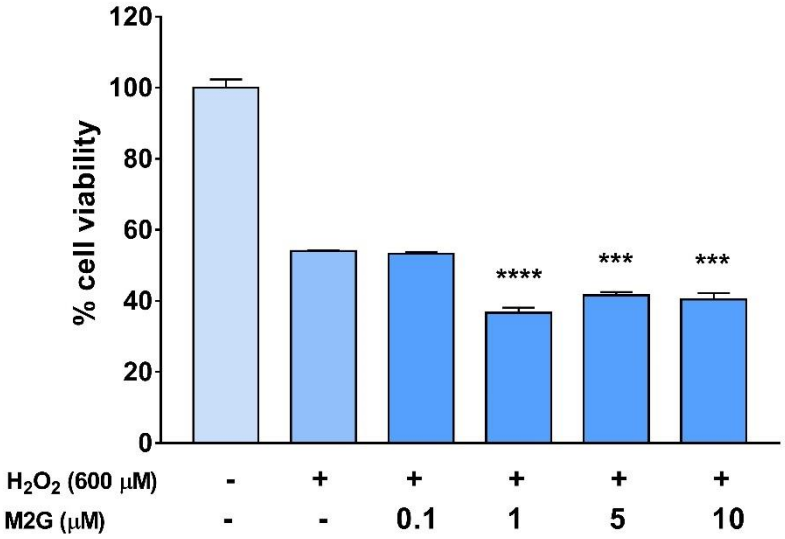

Figure 14: Cell viability assay via pretreatment method. RAW 264.7 murine macrophage were pretreated with concentrations of M2G from 0.1 to 10 μM for an hour, then treated with 600 μM for 24 hours. Cell viability of the non-stressed condition was set at 100%. The cell viabilities were shown as mean ± standard error of mean (SEM). ***, **** denoted significantly differences between untreated and treated stressed samples by student's t-test ($p<0.05$).

4.3.2.2 Semiquantitative RT-PCR analysis

4.3.2.2.1 Determination of time for H_2O_2 treatment

H_2O_2 is believed to be a chemical compound which freely diffuses through lipid bilayer of membranes (Bienert *et al.*, 2006). An excessive exposure of H_2O_2 would damage the biomolecule components in cells, such as DNA, proteins, and lipids rapidly (Watt *et al.*, 2004). This leads to expeditious responses by biosynthesizing series of antioxidant enzymes (Davies, 2000). Thus, contact time of the macrophages to H_2O_2 must be validated in transcriptional expression for further experiments.

Figure 15 revealed the semiquantitative expression of four antioxidative-related genes; *cat*, *Hmox1*, *sod1*, and *Nrf2* after oxidative stress by 600 μM of H_2O_2 at 0, 1, 3, and 6 hours, respectively. As shown in Figure 16, the expression of four genes was induced after 1 hour. Downregulation was clearly observed at 3 hours for *cat, Hmox1* and *Nrf2*, visibly remarkable by the signals declined in (A), (B), and (D), respectively. Signal upregulation was inspected in *cat*, and *Nrf2* at 6 hours, while *Hmox1* expression were slightly decreased. There was no significant change in *sod1* expression after 3 and 6 hours (C).

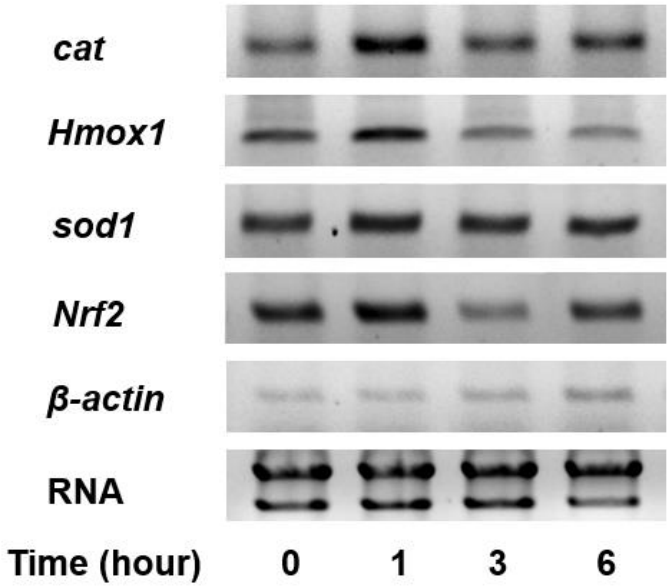

Figure 15: Semiquantitative RT-PCR analysis of four antioxidant-related genes; *cat*, *Hmox1*, *sod1*, and *Nrf2* in RAW 264.7 murine macrophage cell line. Quality and equality of total RNA concentrations were confirmed by 18s rRNA integrity and an internal control *β-actin* expression, respectively. PCR products were investigated by 1.2% gel electrophoresis precasting with 0.1 µL/mL of SYBR® safe DNA gel stain.

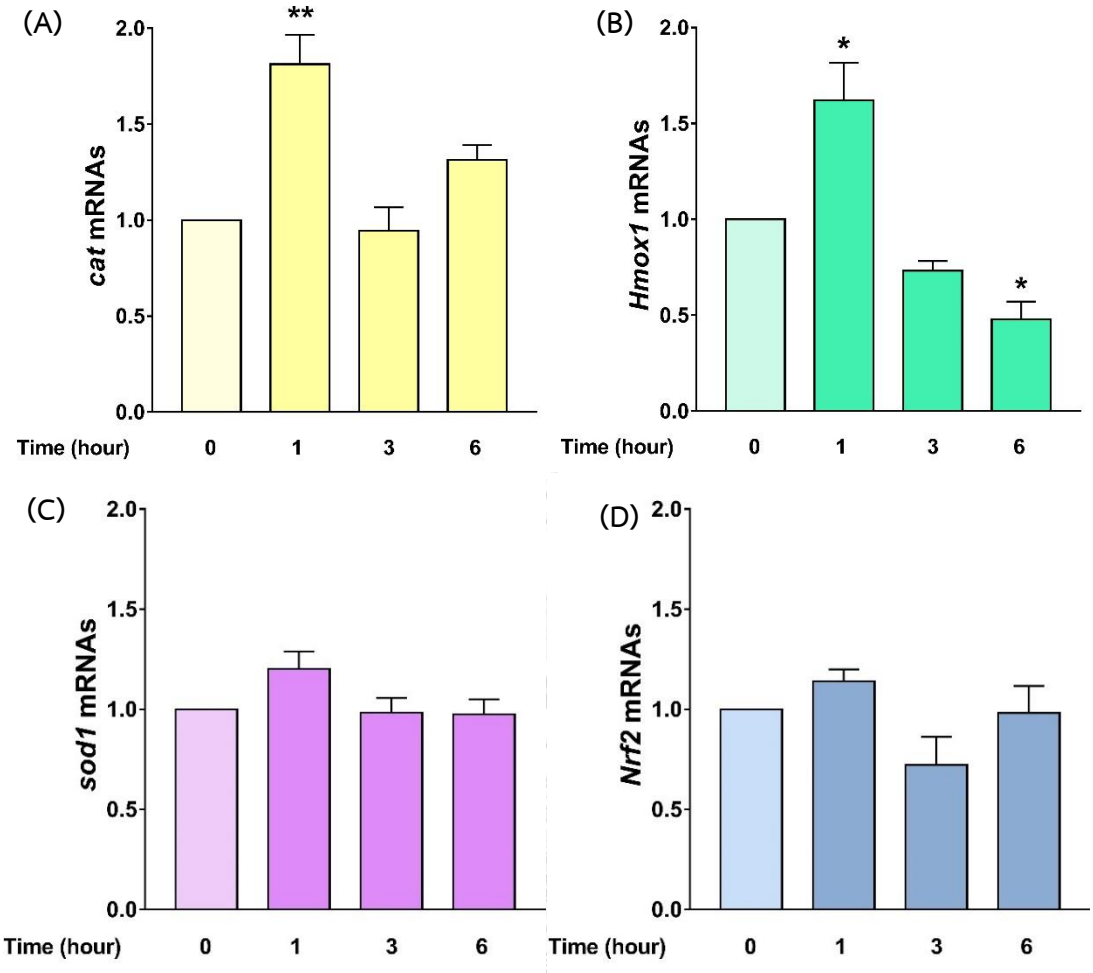

Figure 16: Relative bands intensity of four antioxidation-related genes; *cat* **(A)**, *Hmox1* **(B)**, *sod1* **(C)**, and *Nrf2* **(D)**. The intensity was obtained by ban quantitation using ImageJ. The quantitated values were conducted by three individuals of RT-PCR and gel electrophoresis, shown as mean ± standard error of mean (SEM). * and ** denoted significantly differences between the stressed samples by student's t-test ($p<0.05$).

According to these results, an hour of oxidative stress was found to be the most desirably eminent changes in all four genes inspected. This could be an advantageous for detection prospects in transcription level. Thus, H_2O_2 exposing for an hour was used for further experiments.

4.3.2.2.2 Semiquantitative RT-PCR analysis

To determine the antioxidative capability of M2G *in vitro* at transcriptional level, in this study, semiquantitative RT-PCR was performed on four essential antioxidant genes; *sod1*, *cat*, *Hmox1*, and *Nrf2*.

Figure 17 show the expression of four antioxidation-related genes; *sod1*, *cat*, *Hmox1*, and *Nrf2*, under normal and oxidative stress conditions with or without M2G co-treatment. Quality of total rRNA was verified by 18s rRNA integrity and internal control, *β-actin*, equality. The bands obtained from gel electrophoresis were then quantitated as relative intensity values, shown in Figure 18, to clarify the regulation of those four genes.

According to Figure 18 (A), the expression of *cat* was slightly increased in oxidative stressed cells. Bands quantitation revealed the dramatically upregulation in H_2O_2 plus 5 μM M2G co-treatment condition, counted as 2.2 folds, approximately, compared to the gene regulation in normal condition. The gene was found to be down-regulated in 10 μM M2G together with H_2O_2 treated cells. Interestingly, this suppression was resulted in lower *cat* expression than the mock.

Figure 18 (B) showed a high upregulation of *Hmox1* under oxidative stress condition, triggered by 600 μM of H_2O_2. The expression was highest in H_2O_2 plus 5 μM M2G co-treated cells, counted as 2.5 folds, approximately, to the normal condition. The signal was; however, declined after M2G concentration was increased to 10 μM.

Expression analysis revealed 2.2 folds, approximately, upregulation of *sod1* after oxidants exposure. Co-treatment of M2G and oxidants resulted in remarkably down-regulation of the gene. The highest M2G concentration tested showed an effective suppression of *sod1*, in adjacent to the untreated cells (Figure 18 (C).

The transcription factor gene *Nrf2* was monitored in this study. RT-PCR analysis exhibited an up-regulation of the gene by 1.4 folds, approximately, after oxidative stressing (Figure 18 (D). *Nrf2* transcription was highest increased in 5μM M2G plus H_2O_2 condition, counted as 1.7 folds, approximately, compared to the mock. The

expression was; however, suppressed to as the same level as the mock after co-treated with 10 μM M2G.

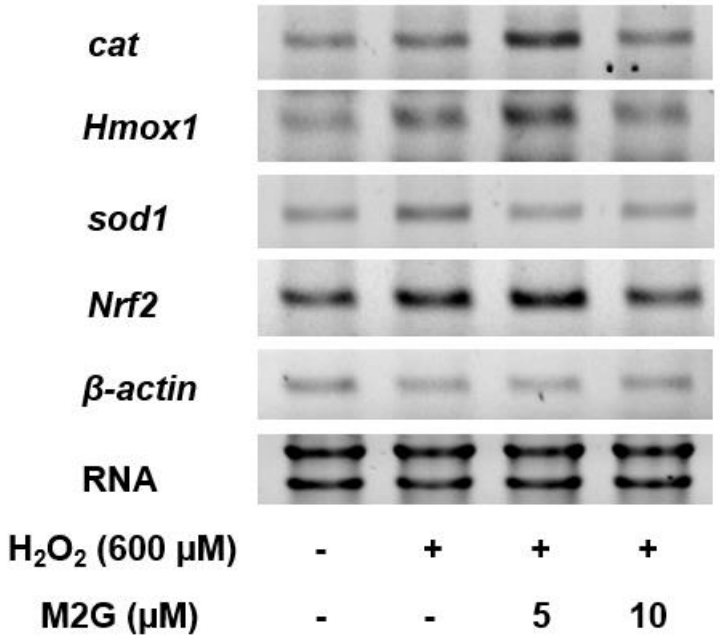

Figure 17: Semiquantitative RT-PCR analysis of four antioxidant-related genes; *cat*, *Hmox1*, *sod1*, and *Nrf2*, in RAW 264.7 murine macrophage under co-treatment of H_2O_2 and M2G for an hour. Quality and equality of total RNA concentrations were confirmed by 18s rRNA integrity and an internal control *β-actin* expression, respectively. PCR products were investigated by 1.2% gel electrophoresis precasting with 0.1 μL/mL of SYBR® safe DNA gel stain.

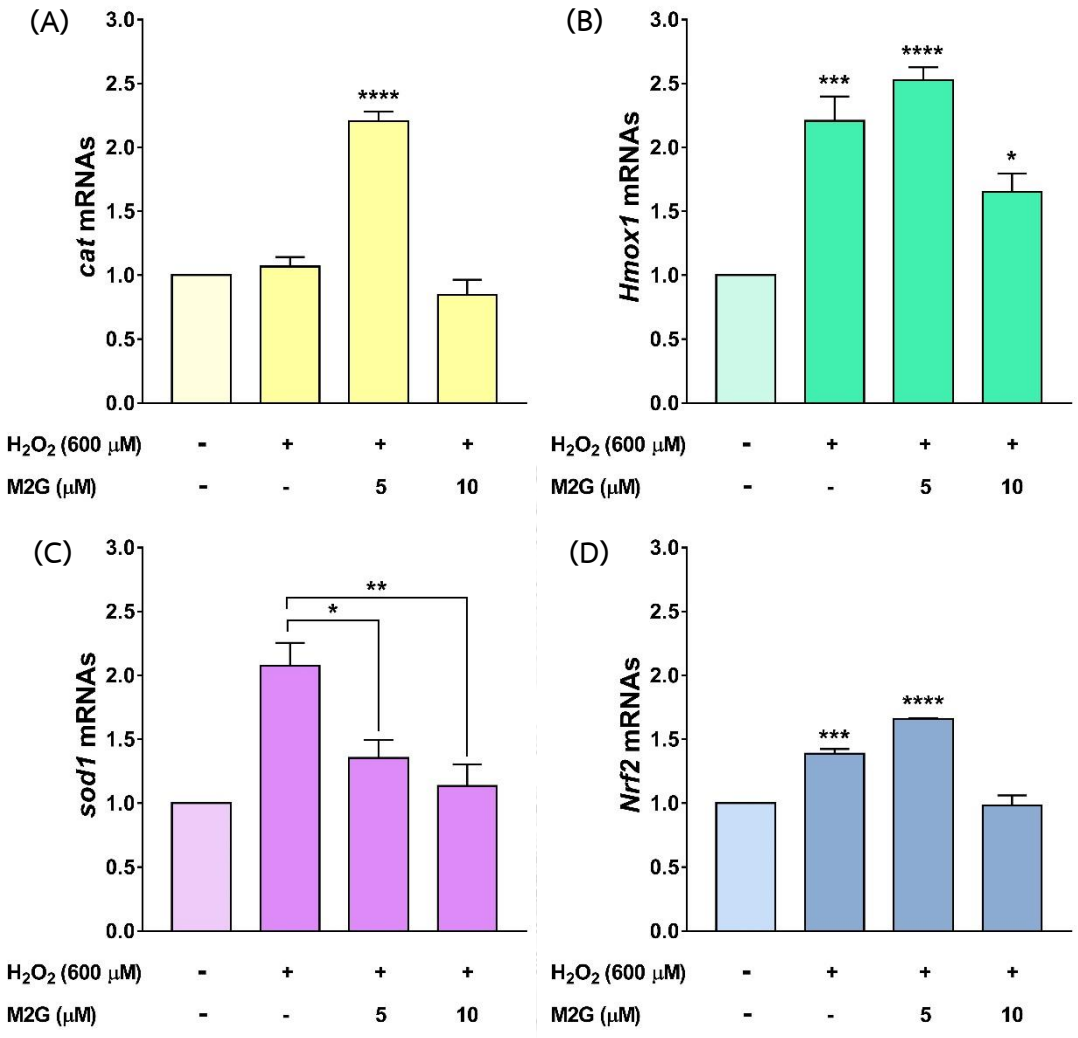

Figure 18: Relative bands intensity of four antioxidation-related genes; *cat* **(A)**, *Hmox1* **(B)**, *sod1* **(C)**, and *Nrf2* **(D)**. The intensity was obtained by band quantitation using ImageJ. The quantitated values were conducted by three individuals of RT-PCR and gel electrophoresis, shown as mean ± standard error of mean (SEM). *, **, *** and **** denoted significantly differences by student's t-test ($p<0.05$).

Transcriptional analysis revealed an effective antioxidative promotion of M2G in various manners. The compound at 5 μM concentration shows an up-regulation capability of three genes, *cat, Hmox1*, and *Nrf2*. In case of *cat,* this gene encodes an antioxidant enzyme catalase. The enzyme is capable to transform H_2O_2 into H_2O and O_2. The upregulation of *cat* would support the survival of cells under excess H_2O_2 condition. There is an evidence in resveratrol, a natural antioxidant in fruits, which increased the expression of *cat* in transcriptional level up to 40% in low concentration (1 nM) (Inglés *et al.*, 2014).

Hmox1 is an essential gene encoding heme-oxygenase 1, which eliminates an accumulated O_2 from intracellular metabolisms. The increase of *Hmox1* expression may promote the effectiveness of radical scavenging mechanisms in cells by prevent the cells from oxygen toxicity (Fernandez-Gonzalez *et al.*, 2012; Mihailovic-Stanojevic *et al.*, 2016).

Up-regulation of *Nrf2* is an impressive approach to boost an antioxidation mechanisms in cells. The increasing of *Nrf2* would result in overexpression of Nrf2, which is the transcription factor of antioxidative pathway. This leads to the production of downstream antioxidant enzymes. Thus, increasing of *Nrf2* expression could prevent cells from oxidative stress (Krajka-Kuzniak *et al.*, 2017; Soares *et al.*, 2017).

M2G also exhibits a scavenging activity *in vitro*, indicated by the down-regulation of *sod1*. Generally, *sod1* encodes the strong antioxidant enzyme Cu/Zn SOD. This enzyme was widely known as effective radical scavenger by its capability to attenuate the superoxide radical. Due to the same mechanism of action of M2G to eliminate the oxidants. Thus, down-regulation of *sod1* may consequence of the activity of M2G in radical scavenging. This was occurred in a well-known strong antioxidant compound *L*-ascorbic acid, which decreased mRNAs level of *sod1* as well as the activity of Cu/Zn SOD (Kao *et al.*, 2003).

4.4 Heterologous expression of M2G genes cluster in cyanobacterial model

4.4.1 Transformation of M2G biosynthetic gene cluster

To study the heterologous expression of M2G gene cluster, fresh water cyanobacterial transformant was constructed by natural transformation of the plasmid carrying the genes cluster. The fresh water cyanobacterial model *S. elongatus* PCC 7942 was grown in BG-11 medium until the absorbance at 730 nm reached 1.0. Then, cyanobacterial cells were harvested, mixed with 300 ng of expressing vector, and incubated at dark for overnight. The transformants were recovered for seven days in the medium, then selected by using BG-11 medium plus streptomycin (50 µg/mL). The selected transformants were verified via colony PCR using specific primer pairs for four biosynthetic genes; *Ap3858*, *Ap3857*, *Ap3856*, and *Ap3855*, respectively. The empty vector transformant was used as control.

Colony PCR analysis revealed the successful of natural transformation. Specific bands for the M2G biosynthetic genes were clearly observed, as shown in Figure 19.

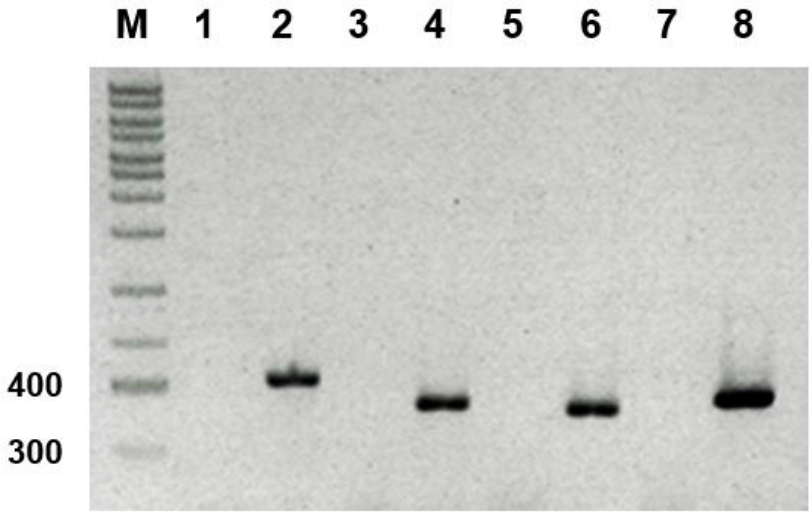

Figure 19: Colony PCR of *S. elongatus* PCC 7942 transformants. PCR products were analyzed by 1.2% gel electrophoresis precasting with 0.1 µL/mL of SYBR® safe DNA gel stain. Lane 1, 3, 5, and 7: cells harboring empty vector with specific primer pairs for *Ap3858*, *Ap3857*, *Ap3856*, and *Ap3855*, respectively; lane 2, 4, 6, and 8: candidate expressing cells harboring *Ap3858-3855* using specific primer pairs for *Ap3858*, *Ap3857*, *Ap3856*, and *Ap3855*, respectively, M: DNA marker.

4.4.2 Morphological and physiological investigations under oxidative stress

In cyanobacteria, oxidative stress effects directly to the photosystem and pigments. The radicals injure the photosystem and its component molecules such as D1 protein, chlorophyll, and phycobiliproteins (Nishiyama & Murata, 2014; Sae-Tang *et al.*, 2016). The Effect of oxidative stress, thus, can be easily observed by the difference of pigments in cells. In this study, the transformants were grown in BG-11 medium plus streptomycin (50 µg/mL) until the absorbance at 730 nm reached approximately 0.5. Then, H_2O_2 was then added into the cell suspension in concentrations from 0-10 mM. Stressed cells were observed under light microscope and measured their absorbance at 730, 665, and 650 nm at interval times. The measured absorbances were calculated to % cell viability, chlorophyll, and phycocyanin amounts by the formula described in Materials and Methods.

The microscopic observation did not show any difference in cells morphology in the investigated times (cell morphology was shown in Appendix 4). As for the physiological observation, the expressing cells exhibited the greater tolerance to the oxidative stress than the control after 48 hours. The inhibition concentration (IC_{50}) of H_2O_2 in the expressing cells was 2.293 ± 0.062 mM, while the control was 1.523 ± 0.049 (Figure 20 (A) and (B), respectively).

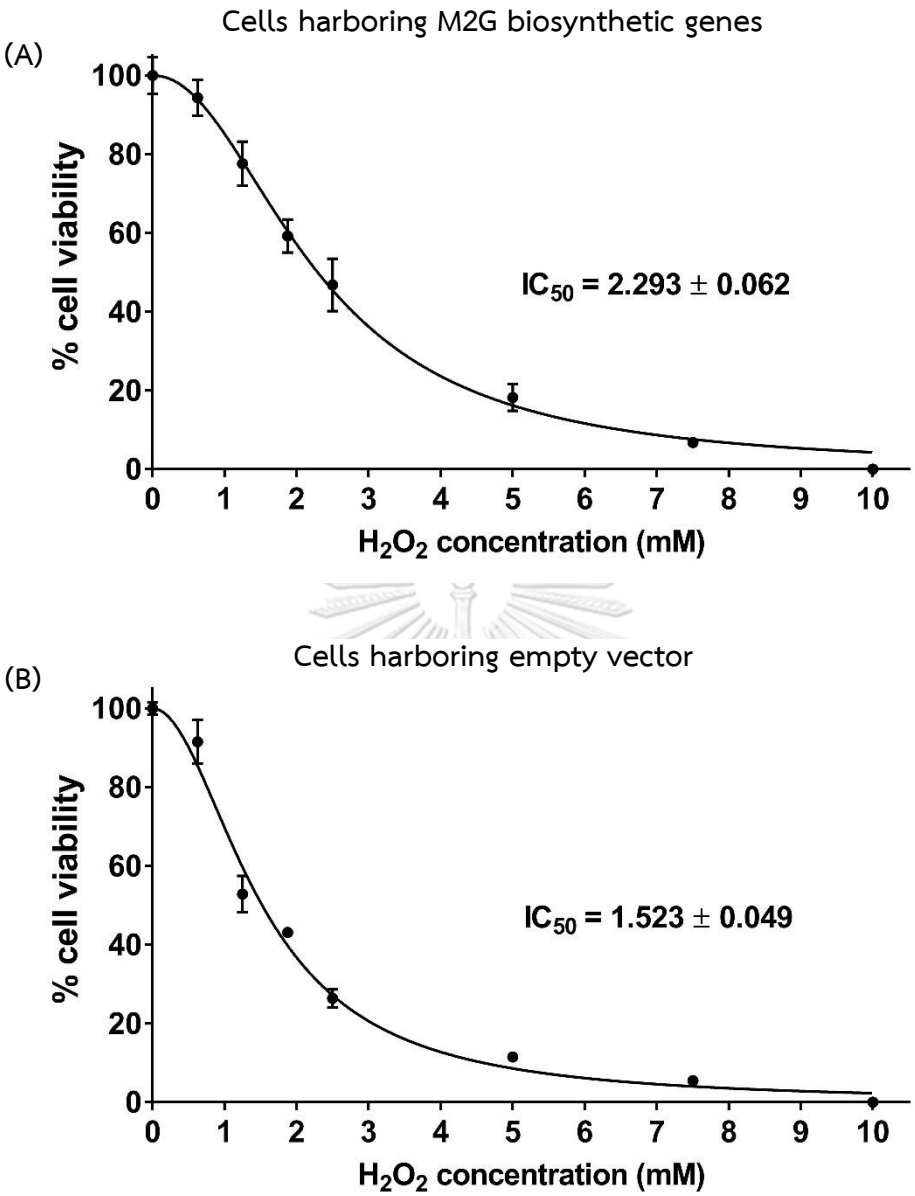

Figure 20: IC_{50} of H_2O_2 in transformant cells harboring M2G biosynthetic genes **(A)**, and empty vector cells **(B)**. *S. elongatus* PCC 7942 transformant and empty vector control cells were stressed with H_2O_2 with concentrations from 0-10 mM for 48 hours. Cell viability of the non-stressed condition was set at 100%. The cell viabilities were expressed as mean ± standard error of mean (SEM). IC_{50} were calculated by Graphpad Prism 7 with 95% confidence (r^2 = 0.9883 and 0.9849, respectively).

The observation showed chlorophyll contents in control and the transformant cells. As obviously shown in figure 21 (A), chlorophyll contents in transformants remained the similar level up from 0-2.5 mM H_2O_2 tested concentrations. However, empty vector became sensitive to H_2O_2. Its tolerancy was limited at 0.625 mM H_2O_2 (Figure 21 (B)).

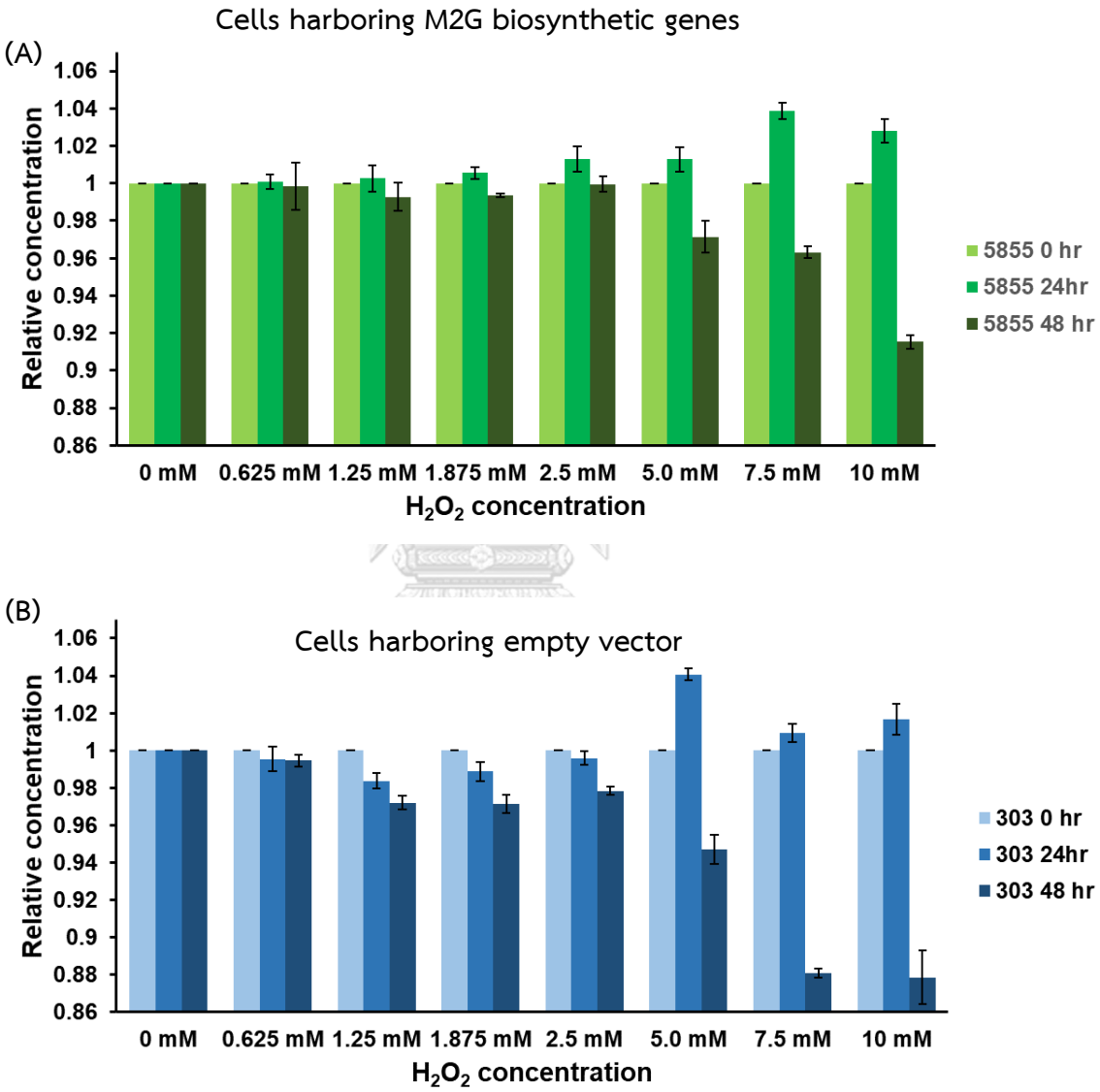

Figure 21: Relative concentration of chlorophyll in transformant cells harboring M2G biosynthetic genes **(A)**, and empty vector cells **(B)**. A_{665} was measured from the cell suspensions and calculated to chlorophyll concentration using the formula described in Materials and Methods. The experiment was conducted as a biological triplication, showed as mean ± standard deviation (SD).

Phycocyanin concentration was also calculated from the measured absorbances, resulted in Figure 22. The observation found that the expressing cells possessed a capability to maintain phycocyanin level in cells under the oxidative stress by H_2O_2 from 0-2.5 mM. While H_2O_2 in higher concentrations (more than 2.50 mM) caused a change in phycocyanin content (Figure 22 (A)). In empty vector control (Figure 22 (B)), the pigment control was provided from 0-0.625 mM of H_2O_2. The increase of oxidative stress leaded to a dramatically fluctuation of phycocyanin concentration.

According to above results, compared to the empty vector control cells, the expressing cells are more endurable to the oxidative stress generated from H_2O_2. Thus, heterologous expression of M2G biosynthetic genes contributes oxidative stress tolerance and the maintaining of photosystem pigments in *S. elongatus* PCC 7942.

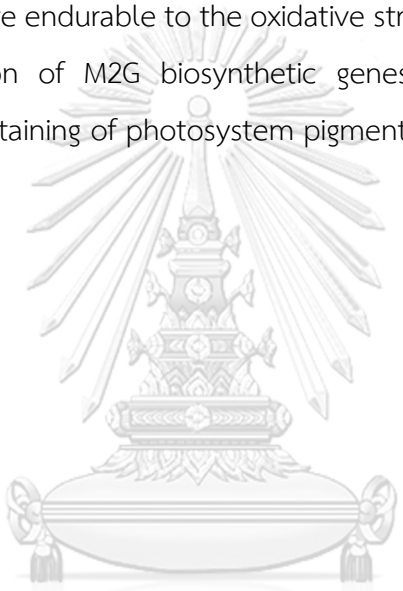

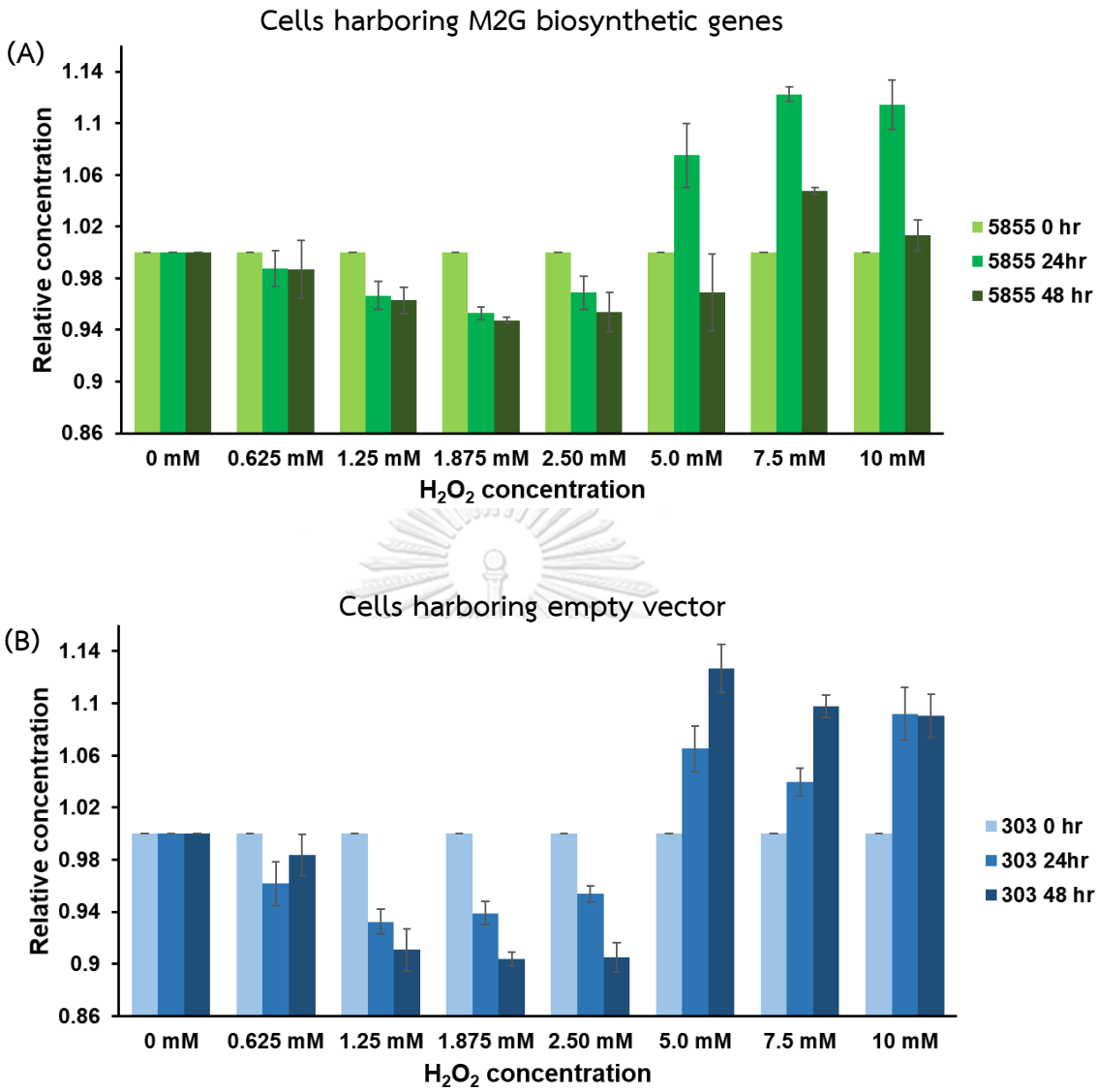

Figure 22: Relative concentration of phycocyanin in transformant cells harboring M2G biosynthetic genes **(A)**, and empty vector cells **(B)**. A_{665} and A_{650} were measured from the cell suspensions and calculated to chlorophyll concentration using the formula described in Materials and Methods. The experiment was conducted as a biological triplication, showed as mean ± standard deviation (SD).

4.3.1 Semiquantitative RT-PCR analysis

Antioxidant genes were analyzed at transcriptional level to observe effects of M2G biosynthetic genes to the heterologous expression. Expression analysis revealed that M2G biosynthetic genes modulated antioxidant genes tested in this study. As showed in Figure 23, at IC_{50} and IC_{50}+½IC_{50} H_2O_2 stress conditions, all three genes (*cat*, *sodB*, and *tpxA*) were significantly up-regulated. According to the bands intensity shown in Figure 24, *cat* was upregulated approximately 4.5±0.4 folds at IC_{50}. The expression was slightly decreased in IC_{50}+½IC_{50} condition. While there was about 1.5±0.4 folds of *cat* in the control at the same conditions, as shown in Figure 24 (A1).

For *sodB*, the expression level increased to 3±0.3 folds after stress using IC_{50}-+½IC_{50} H_2O_2. This was 2 folds higher than the stressed control cells, as shown in Figure 24 (B1 and B2).

Up-regulation of *tpxA* was found to be the highest among the tested antioxidant genes, by up to 6±0.2 folds, approximately. The increasing of *tpxA* expression was found in much lower level in the control cells, shown in Figure 24 (C1 and C2).

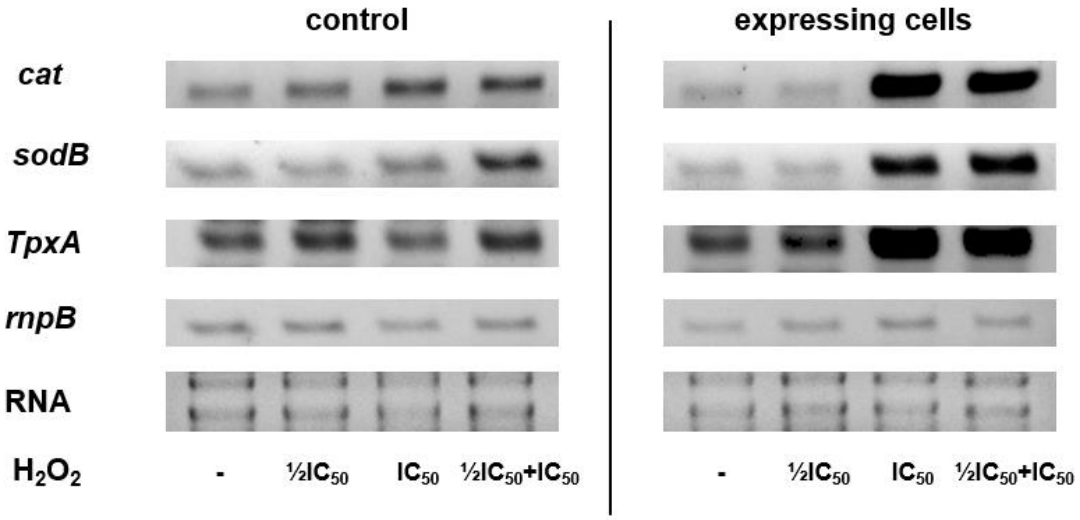

Figure 23: Semiquantitative RT-PCR analysis of three antioxidant-related genes; *cat*, *sodB*, and *tpxA*, in *S. elongatus* PCC 7942 transformant harboring M2G biosynthetic gene cluster (and the empty vector carrier as a control) under H_2O_2-induced oxidative stress condition for 6 hours. Quality and equality of total RNA concentrations were confirmed by 16s rRNA integrity and an internal control *rnpB* expression, respectively. PCR products were investigated by 1.2% gel electrophoresis precasting with 0.1 µL/mL of SYBR® safe DNA gel stain.

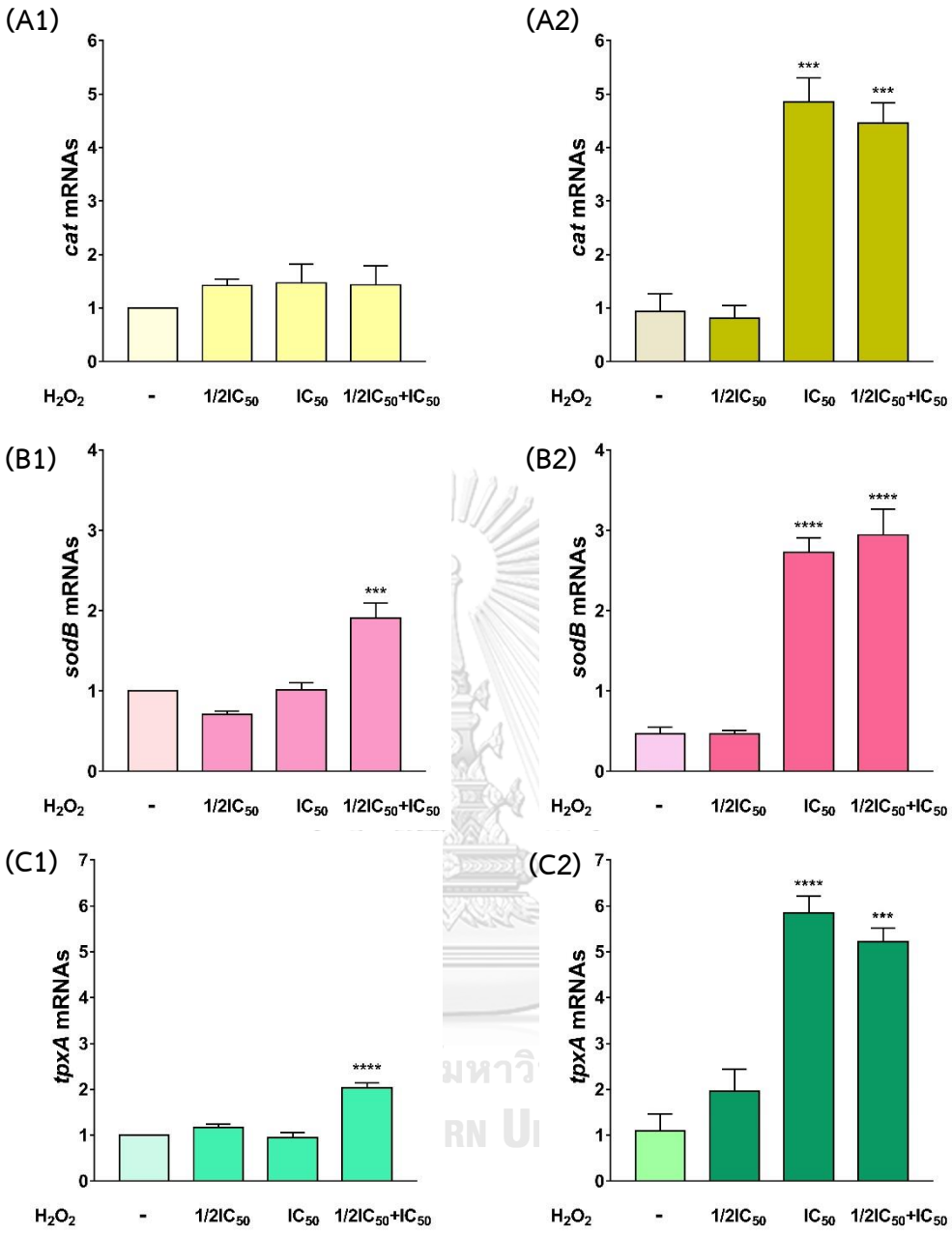

Figure 24: Relative bands intensity of three antioxidation-related genes; *cat* **(A)**, *sodB* **(B)**, and *tpxA* **(C)** in empty vector **(1)** and transformant harboring M2G biosynthetic genes cluster **(2)**. The quantitated values were analyzed using three independent experiments of RT-PCR and gel electrophoresis, data shown as mean ± standard error of mean (SEM). *** and **** denoted significantly differences by student's t-test ($p<0.05$).

From these results, introduction of M2G biosynthetic gene cluster in *S. elongatus* PCC 7942 up-regulated the antioxidant genes. This was the first report which indicated the modulation property of MAA biosynthetic genes to the antioxidative-related genes under heterologous expression. To verified this ability, *Ap3858-3555* (encoding for the enzymes in M2G biosynthetic pathway) were observed their expression levels by semiquantitative RT-PCR.

Transcriptional analysis of M2G biosynthetic genes revealed that all four genes was up-regulated by the oxidative stress for 6 hours, as shown in Figures 25-26. The expression of *Ap3858* in the transformant, exposed with IC_{50} and IC_{50}+½IC_{50} H_2O_2, shown in Figure 26 (A), was upregulated by 7 folds from the normal conditions, as well as the *Ap3857*. This was increased by 4 times (Figure 26 (B). *Ap3856* exhibited a very high expression, up to 12 folds, after stressed by H_2O_2 at the same concentrations (Figure 26 (C). The most upregulated gene observed in this study was *Ap3855*, as shown in Figure 26 (D), with 14 times higher than control condition.

According to above results, this can be concluded that heterologous expression of M2G biosynthetic genes cluster highly induces antioxidant genes; *cat, sodB,* and *tpxA*, under moderate to high oxidative stress conditions, but not at low oxidative stress condition. Furthermore, the M2G-biosythetic genes in expressing cells are also exhibited massive expressions under these stress conditions.

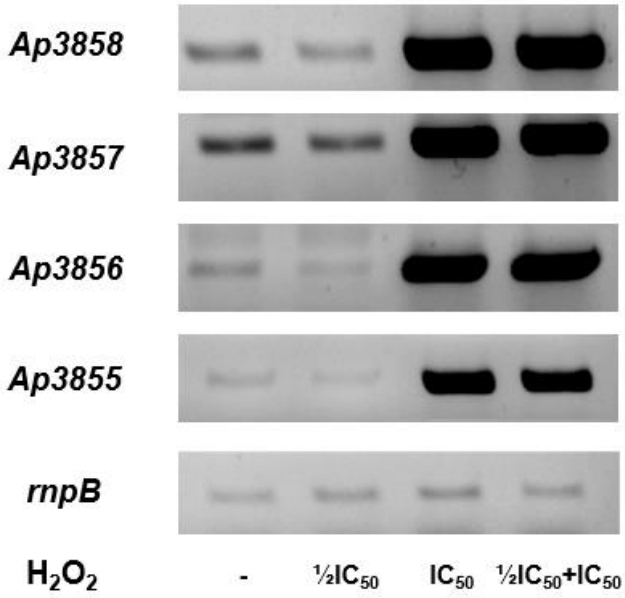

Figure 25: Semiquantitative RT-PCR analysis of M2G biosynthetic genes; *Ap3858* to *Ap3855* in *S. elongatus* PCC 7942 transformant, carrying M2G biosynthetic gene cluster, under H_2O_2-induced oxidative stress condition for 6 hours. Quality and equality of total RNA concentrations were confirmed by 16s rRNA integrity and an internal control *rnpB* expression, respectively. PCR products were investigated by 1.2% gel electrophoresis precasting with 0.1 µL/mL of SYBR® safe DNA gel stain.

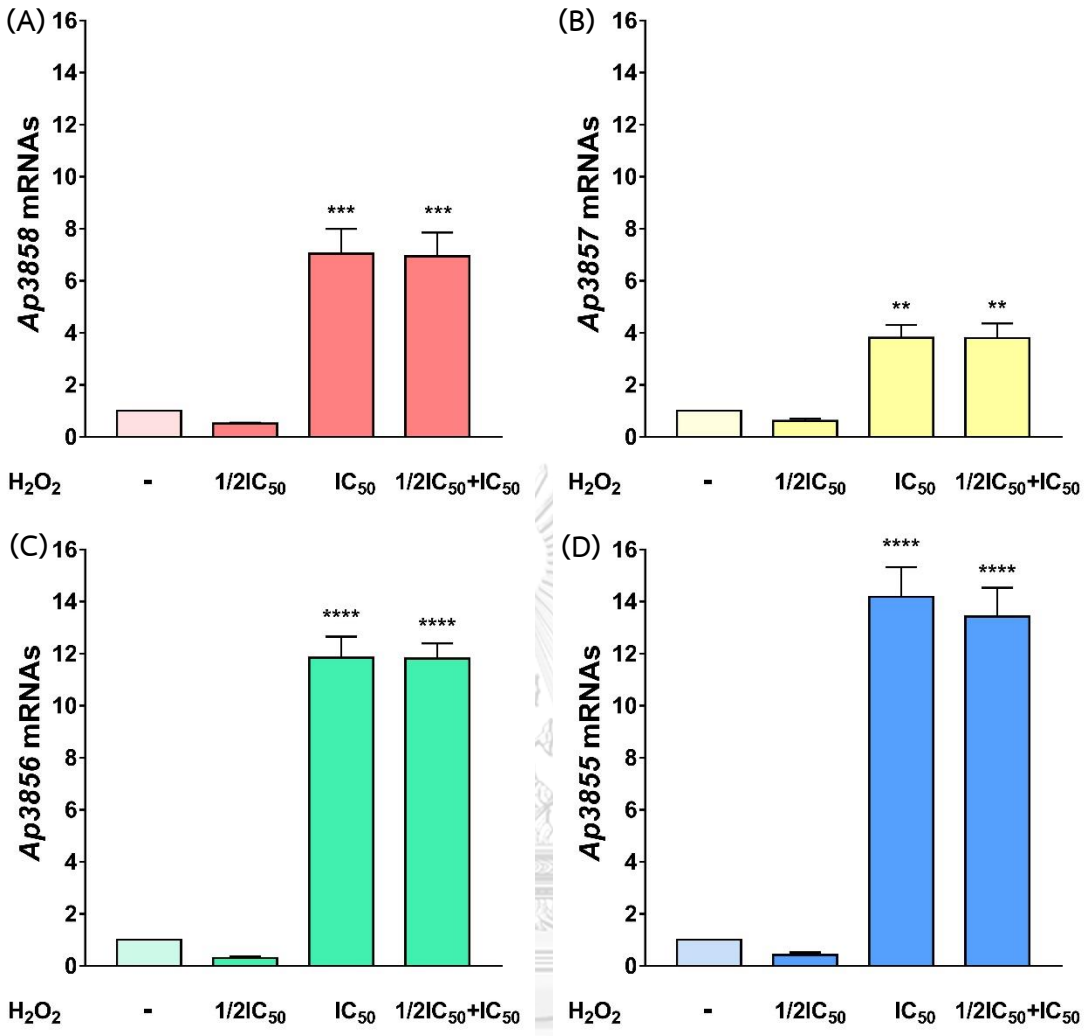

Figure 26: Relative bands intensity of M2G biosynthetic genes; *Ap3858* **(A)**, *Ap3857* **(B)**, *Ap3856* **(C)**, and *Ap3855* **(D)** in *S. elongatus* PCC 7942 transformant after exposed oxidative stress by 6 hours. The quantitated values were conducted by three individuals of RT-PCR and gel electrophoresis, shown as mean ± standard error of mean (SEM). **, ***, and **** denoted significantly differences by student's t-test ($p<0.05$).

CHAPTER V
CONCLUSIONS

I) High purity M2G was successfully extracted and purified by using three steps of purification; strong cation exchange chromatography and reverse phase chromatographies with acetic acid (1%) and ammonium acetate (0.1M) as mobile phases, respectively.

II) The purified M2G was biocompatible and met all standards for medical and pharmaceutical approaches.

III) Radical scavenging activity of M2G exhibited in a wide range of pHs, with the highest activity at pH 6.

IV) Strong inflammation activity was provided in RAW 264.7 murine macrophage by low concentration of M2G, via suppressing *iNOS* and *COX-2* transcription.

V) Antioxidative activity of RAW 264.7 murine macrophage was endorsed by 5 μM M2G, via suppression of *sod1* and upregulation of *cat*, *Hmox1*, and *Nrf2* transcriptions under oxidative stress.

VI) Heterologous expression of M2G biosynthetic genes cluster enhanced oxidative stress tolerance of *S. elongatus* PCC 7942 by upregulation of antioxidant genes (*sodB*, *tpxA,* and *cat*).

VII) M2G biosynthetic genes (*Ap3858*, *Ap3857*, *Ap3856*, and *Ap3855*) were highly expressed in the transformant under oxidative stress.

REFERENCES

Ahmed, S. M., Luo, L., Namani, A. *et al.* **(2017)**. Nrf2 signaling pathway: Pivotal roles in inflammation. *Biochimica et Biophysica Acta,* 1863, 585-597.

Alexander, J. W., & Supp, D. M. **(2014)**. Role of arginine and omega-3 fatty acids in wound healing and infection. *Advances in Wound Care,* 3, 682-690.

Allen, M. M. **(1968)**. Simple conditions for growth of unicellular blue-green algae on plates (1, 2). *Journal of Phycology,* 4, 1-4.

Bienert, G. P., Schjoerring, J. K., & Jahn, T. P. **(2006)**. Membrane transport of hydrogen peroxide. *Biochimica et Biophysica Acta (BBA) - Biomembranes,* 1758, 994-1003.

Carreto, J. I., & Carignan, M. O. **(2011)**. Mycosporine-like amino acids: relevant secondary metabolites. Chemical and ecological aspects. *Marine Drugs,* 9, 387-446.

Cheewinthamrongrod, V., Kageyama, H., Palaga, T. *et al.* **(2016)**. DNA damage protecting and free radical scavenging properties of mycosporine-2-glycine from the Dead Sea cyanobacterium in A375 human melanoma cell lines. *Journal of Photochemistry and Photobiology B: Biology,* 164, 289-295.

Choi, Y. H., Yang, D. J., Kulkarni, A. *et al.* **(2015)**. Mycosporine-like amino acids promote wound healing through focal adhesion kinase (FAK) and mitogen-activated protein kinases (MAP Kinases) signaling pathway in keratinocytes. *Marine Drugs,* 13, 7055-7066.

Chun, K. S., Cha, H. H., Shin, J. W. *et al.* **(2004)**. Nitric oxide induces expression of cyclooxygenase-2 in mouse skin through activation of NF-kappaB. *Carcinogenesis,* 25, 445-454.

Colowick, S. P., & Kaplan, N. O. **(1988)**. *Cyanobacteria* (1st ed. Vol. 167). San Diego, California 92101: Academic Press, inc.

D'Agostino, P. M., Javalkote, V. S., Mazmouz, R. *et al.* **(2016)**. Comparative profiling and discovery of novel glycosylated mycosporine-like amino acids in two strains of

the cyanobacterium *Scytonema* cf. crispum. *Applied and Environmental Microbiology,* 82, 5951-5959.

Davies, K. J. **(2000)**. Oxidative stress, antioxidant defenses, and damage removal, repair, and replacement systems. *IUBMB Life,* 50, 279-289.

Fernandez-Gonzalez, A., Alex Mitsialis, S., Liu, X. *et al.* **(2012)**. Vasculoprotective effects of heme oxygenase-1 in a murine model of hyperoxia-induced bronchopulmonary dysplasia. *American Journal of Physiology - Lung Cellular and Molecular Physiology,* 302, L775-L784.

Garcia-Pichel, F., Wingard, C. E., & Castenholz, R. W. **(1993)**. Evidence regarding the UV sunscreen role of a mycosporine-Like compound in the cyanobacterium *Gloeocapsa* sp. *Applied and Environmental icrobiology,* 59, 170-176.

Infantino, V., Convertini, P., Cucci, L. *et al.* **(2011)**. The mitochondrial citrate carrier: a new player in inflammation. *Biochemical Journal,* 438, 433-436.

Inglés, M., Gambini, J., Miguel, M. *et al.* **(2014)**. PTEN mediates the antioxidant effect of resveratrol at nutritionally relevant concentrations. *BioMed Research International,* 2014, 1-6.

Ishihara, K., Watanabe, R., Uchida, H. *et al.* **(2017)**. Novel glycosylated mycosporine-like amino acid, 13-O-(β-galactosyl)-porphyra-334, from the edible cyanobacterium *Nostoc sphaericum*-protective activity on human keratinocytes from UV light. *Journal of Photochemistry and Photobiology B: Biology,* 172, 102-108.

Kao, P. F., Lee, W. S., Liu, J. C. *et al.* **(2003)**. Downregulation of Superoxide Dismutase Activity and Gene Expression in Cultured Rat Brain Astrocytes after Incubation with Vitamin C. *Pharmacology,* 69, 1-6.

Kedar, L., Kashman, Y., & Oren, A. **(2002)**. Mycosporine-2-glycine is the major mycosporine-like amino acid in a unicellular cyanobacterium (*Euhalothece* sp.) isolated from a gypsum crust in a hypersaline saltern pond. *FEMS Microbiology Letters,* 208, 233-237.

Krajka-Kuzniak, V., Paluszczak, J., & Baer-Dubowska, W. **(2017)**. The Nrf2-ARE signaling pathway: An update on its regulation and possible role in cancer prevention and treatment. *Pharmacological Reports,* 69, 393-402.

Lee, S. J., Bai, S. K., Lee, K. S. *et al.* **(2003a)**. Astaxanthin inhibits nitric oxide production and inflammatory gene expression by suppressing I(kappa)B kinase-dependent NF-kappaB activation. *Molecules and Cells,* 16, 97-105.

Lee, S. J., Lee, I. S., & Mar, W. **(2003b)**. Inhibition of inducible nitric oxide synthase and cyclooxygenase-2 activity by 1,2,3,4,6-penta-O-galloyl-beta-D-glucose in murine macrophage cells. *Archives of Pharmacal Research,* 26, 832-839.

Lin, H.-Y., Shen, S.-C., Lin, C.-W. *et al.* **(2007)**. Baicalein inhibition of hydrogen peroxide-induced apoptosis via ROS-dependent heme oxygenase 1 gene expression. *Biochimica et Biophysica Acta (BBA) - Molecular Cell Research,* 1773, 1073-1086.

Ma, Q. **(2013)**. Role of Nrf2 in oxidative stress and toxicity. *Annual Review of Pharmacology and Toxicology,* 53, 401-426.

Massi, D., Franchi, A., Sardi, I. *et al.* **(2001)**. Inducible nitric oxide synthase expression in benign and malignant cutaneous melanocytic lesions. *The Journal of Pathology,* 194, 194-200.

Matsui, K., Nazifi, E., Kunita, S. *et al.* **(2011)**. Novel glycosylated mycosporine-like amino acids with radical scavenging activity from the cyanobacterium *Nostoc commune*. *Journal of Photochemistry and Photobiology B: Biology,* 105, 81-89.

Matsuyama, K., Matsumoto, J., Yamamoto, S. *et al.* **(2015)**. pH-Independent charge resonance mechanism for UV protective functions of shinorine and related mycosporine-like amino acids. *The Journal of Physical Chemistry A,* 119, 12722-12729.

Mihailovic-Stanojevic, N., Miloradovic, Z., Ivanov, M. *et al.* **(2016)**. Upregulation of heme oxygenase-1 in response to wild thyme treatment protects against hypertension and oxidative Stress. *Oxidative Medicine and Cellular Longevity,* 2016, 1458793.

Mitchell, S., Vargas, J., & Hoffmann, A. **(2016)**. Signaling via the NF**K**B system. *Wiley Interdisciplinary Reviews: Systems Biology and Medicine,* 8, 227-241.

Murakami, A., & Ohigashi, H. **(2007)**. Targeting NOX, INOS and COX-2 in inflammatory cells: chemoprevention using food phytochemicals. *International Journal of Cancer,* 121, 2357-2363.

Napetschnig, J., & Wu, H. **(2013)**. Molecular Basis of NF-**K**B Signaling. *Annual Review of Biophysics,* 42, 443-468.

Nazifi, E., Wada, N., Yamaba, M. *et al.* **(2013)**. Glycosylated porphyra-334 and palythine-threonine from the terrestrial cyanobacterium *Nostoc commune*. *Marine Drugs,* 11, 3124-3154.

Newton, K., & Dixit, V. M. **(2012)**. Signaling in innate immunity and inflammation. *Cold Spring Harbor Perspectives in Biology,* 4.

Nishiyama, Y., & Murata, N. **(2014)**. Revised scheme for the mechanism of photoinhibition and its application to enhance the abiotic stress tolerance of the photosynthetic machinery. *Applied Microbiology and Biotechnology,* 98, 8777-8796.

Oyamada, C., Kaneniwa, M., Ebitani, K. *et al.* **(2008)**. Mycosporine-like amino acids extracted from scallop (*Patinopecten yessoensis*) ovaries: UV protection and growth stimulation activities on human cells. *Marine Biotechnology,* 10, 141-150.

Piao, S., Cha, Y. N., & Kim, C. **(2011)**. Taurine chloramine protects RAW 264.7 macrophages against hydrogen peroxide-induced apoptosis by increasing antioxidants. *Journal of Clinical Biochemistry and Nutrition,* 49, 50-56.

Pope, M. A., Spence, E., Seralvo, V. *et al.* **(2015)**. O-Methyltransferase is shared between the pentose phosphate and shikimate pathways and is essential for mycosporine-like amino acid biosynthesis in *Anabaena variabilis* ATCC 29413. *Chembiochem,* 16, 320-327.

Rastogi, R., Sonani, R., Madamwar, D. *et al.* **(2015)**. *The potential of Mycosporine-like amino acids as UV-sunscreens* (S. H. Sharp Ed.): Nova Science Publishers, Inc.

Rosic, N. N., & Dove, S. **(2011)**. Mycosporine-like amino acids from coral dinoflagellates. *Applied and Environmental Microbiology,* 77, 8478-8486.

Ryu, J., Park, S. J., Kim, I. H. *et al.* **(2014)**. Protective effect of porphyra-334 on UVA-induced photoaging in human skin fibroblasts. *International Journal of Molecular Medicine,* 34, 796-803.

Sae-Tang, P., Hihara, Y., Yumoto, I. *et al.* **(2016)**. Overexpressed superoxide dismutase and catalase act synergistically to protect the repair of PSII during

photoinhibition in *Synechococcus elongatus* PCC 7942. *Plant and Cell Physiology,* 57, 1899-1907.

Shang, J. L., Zhang, Z. C., Yin, X. Y. *et al.* **(2018)**. UV-B induced biosynthesis of a novel sunscreen compound in solar radiation and desiccation tolerant cyanobacteria. *Environmental Microbiology,* 20, 200-213.

Shick, J. M., Dunlap, W. C., Pearse, J. S. *et al.* **(2002)**. Mycosporine-like amino acid content in four species of sea anemones in the genus Anthopleura reflects phylogenetic but not environmental or symbiotic relationships. *The Biological Bulletin,* 203, 315-330.

Singh, S. P., Kumari, S., Rastogi, R. P. *et al.* **(2008)**. Mycosporine-like amino acids (MAAs): chemical structure, biosynthesis and significance as UV-absorbing/screening compounds. *Indian Journal of Experimental Biology,* 46, 7-17.

Siomek, A. **(2012)**. NF-kappaB signaling pathway and free radical impact. *Acta Biochimica Polonica,* 59, 323-331.

Soares, E. R., Monteiro, E. B., de Bem, G. F. *et al.* **(2017)**. Up-regulation of Nrf2-antioxidant signaling by Açaí (*Euterpe oleracea* Mart.) extract prevents oxidative stress in human endothelial cells. *Journal of Functional Foods,* 37, 107-115.

Sommaruga, R., Whitehead, K., Shick, J. M. *et al.* **(2006)**. Mycosporine-like amino acids in the zooxanthella-ciliate symbiosis *Maristentor dinoferus*. *Protist,* 157, 185-191.

Stochaj, W. R., Dunlap, W. C., & Shick, J. M. **(1994)**. Two new UV-absorbing mycosporine-like amino acids from the sea anemone *Anthopleura elegantissima* and the effects of zooxanthellae and spectral irradiance on chemical composition and content. *Marine Biology,* 118, 149-156.

Suh, S. S., Hwang, J., Park, M. *et al.* **(2014)**. Anti-inflammation activities of mycosporine-like amino acids (MAAs) in response to UV radiation suggest potential anti-skin aging activity. *Marine Drugs,* 12, 5174-5187.

Tan, H. Y., Wang, N., Li, S. *et al.* **(2016)**. The reactive oxygen species in macrophage polarization: reflecting Its dual role in progression and treatment of human diseases. *Oxidative Medicine and Cellular Longevity,* 2016.

Wada, N., Sakamoto, T., & Matsugo, S. **(2013)**. Multiple roles of photosynthetic and sunscreen pigments in cyanobacteria focusing on the oxidative stress. *Metabolites,* 3, 463-483.

Wada, N., Sakamoto, T., & Matsugo, S. **(2015)**. Mycosporine-like amino acids and their derivatives as natural antioxidants. *Antioxidants,* 4.

Waditee-Sirisattha, R., Kageyama, H., Sopun, W. *et al.* **(2014)**. Identification and upregulation of biosynthetic genes required for accumulation of Mycosporine-2-glycine under salt stress conditions in the halotolerant cyanobacterium *Aphanothece halophytica*. *Applied and Environmental Microbiology,* 80, 1763-1769.

Waditee, R., Hibino, T., Tanaka, Y. *et al.* **(2001)**. Halotolerant cyanobacterium *Aphanothece halophytica* contains an Na(+)/H(+) antiporter, homologous to eukaryotic ones, with novel ion specificity affected by C-terminal tail. *The Journal of Biological Chemistry,* 276, 36931-36938.

Watt, B. E., Proudfoot, A. T., & Vale, J. A. **(2004)**. Hydrogen peroxide poisoning. *Toxicological Reviews,* 23, 51-57.

Wen, Z. S., Liu, L. J., Qu, Y. L. *et al.* **(2013)**. Chitosan nanoparticles attenuate hydrogen peroxide-induced stress injury in mouse macrophage RAW264.7 cells. *Marine Drugs,* 11, 3582-3600.

Wendum, D., Svrcek, M., Rigau, V. *et al.* **(2003)**. COX-2, inflammatory secreted PLA2, and cytoplasmic PLA2 protein expression in small bowel adenocarcinomas compared with colorectal adenocarcinomas. *Modern Pathology,* 16, 130-136.

Zhang, H., Davies, K. J. A., & Forman, H. J. **(2015)**. Oxidative stress response and Nrf2 signaling in aging. *Free Radical Biology and Medicine,* 88, 314-336.

APPENDICES

Appendix 1

BG 11 medium (Allen, 1968)

BG 11 solution

$NaNO_3$	1.5	g
K_2HPO_4	40	mg
$MgSO_4 \cdot 7H_2O$	75	mg
$CaCl_2 \cdot H_2O$	36	mg
Na_2CO_3	20	mg
EDTA 2Na	1	mg
Citric acid	6	mg
Ferric ammonium nitrate	6	mg
Trace element solution	1	mL

Dissolve all compositions with distilled water to 1 liter, sterilize by autoclaving at 121 °C, 15 lb/in^2 pressurized for 15 minutes. Add 15 g/L of Bacto® agar for solidified media.

Trace element solution

H_3BO_3	2.8	g
$MnCl_2 \cdot 4H_2O$	1.81	g
$ZnSO_4 \cdot 7H_2O$	0.22	g
$CuSO_4 \cdot 5H_2O$	0.079	g
$Co(NO_3)_2 \cdot 6H_2O$	0.049	g

Dissolve all compositions with distilled water to 1 liter, sterilize by autoclaving at 121 °C, 15 lb/in^2 pressurized for 15 minutes.

Turk island salts solution

NaCl	28.17	g
KCl	0.67	g
$MgSO_4 \cdot 7H_2O$	6.92	g
$MgCl_2 \cdot 6H_2O$	5.50	g
$CaCl_2 \cdot H_2O$	1.47	g

Dissolve all compositions with distilled water to 1 liter, sterilize by autoclaving at 121 °C, 15 lb/in^2 pressurized for 15 minutes.

Appendix 2

LB medium

Composition per 1 liter

Bacto® Tryptone	10	g
Yeast extract	5	g
NaCl	10	g

Dissolve all compositions with distilled water to 1 liter, adjust the pH to 7.0 with 6 M NaOH. Sterilize by autoclaving at 121 °C, 15 lb/in^2 pressurized for 15 minutes. Add 15 g/L of Bacto® agar for solidified media.

Appendix 3

Nucleotide sequence, primer design, and gene organization

RAW 264.7 murine macrophage (*Mus musculus*)

β-actin (mRNA 1,935 bps (from genomic DNA 3,640 bps)) Accession number: NM_007393.5

Highlighted texts are nucleotide sequences for forward and reverse primers.

TATAAAACCCGGCGGCGCAACGCGCAGCCACTGTCGAGTCGCGTCCACCCGCGAGCACAGCTT
CTTTGCAGCTCCTTCGTTGCCGGTCCACACCCGCCACCAGTTCGCCATGGATGACGATATCGCT
GCGCTGGTCGTCGACAACGGCTCCGGCATGTGCAAAGCCGGCTTCGCGGGCGACGATGCTCCC
CGGGCTGTATTCCCCTCCATCGTGGGCCGCCCTAGGCACCAGGGTGTGATGGTGGGAATGGGT
CAGAAGGACTCCTATGTGGGTGACGAGGCCCAGAGCAAGAGAGGTATCCTGACCCTGAAGTAC
CCCATTGAACATGGCATTGTTACCAACTGGGACGACATGGAGAAGATCTGGCACCACACCTTCT
ACAATGAGCTGCGTGTGGCCCCTGAGGAGCACCCTGTGCTGCTCACCGAGGCCCCCCTGAACC
CTAAGGCCAACCGTGAAAAGATGACCCAGATCATGTTTGAGACCTTCAACACCCCAGCCATGTA
CGTAGCCATCCAGGCTGTGCTGTCCCTGTATGCCTCTGGTCGTACCACAGGCATTGTGATGGAC
TCCGGAGACGGGGTCACCCACACTGTGCCCATCTACGAGGGCTATGCTCTCCCTCACGCCATCC
TGCGTCTGGACCTGGCTGGCCGGGACCTGACAGACTACCTCATGAAGATCCTGACCGAGCGTG
GCTACAGCTTCACCACCACAGCTGAGAGGGAAATCGTGCGTGACATCAAAGAGAAGCTGTGCTA
TGTTGCTCTAGACTTCGAGCAGGAGATGGCCACTGCCGCATCCTCTTCCTCCCTGGAGAAGAGC
TATGAGCTGCCTGACGGCCAGGTCATCACTATTGGCAACGAGCGGTTCCGATGCCCTGAGGCTC
TTTTCCAGCCTTCCTTCTTGGGTATGGAATCCTGTGGCATCCATGAAACTACATTCAATTCCATC
ATGAAGTGTGACGTTGACATCCGTAAAGACCTCTATGCCAACACAGTGCTGTCTGGTGGTACCA
CCATGTACCCAGGCATTGCTGACAGGATGCAGAAGGAGATTACTGCTCTGGCTCCTAGCACCAT
GAAGATCAAGATCATTGCTCCTCCTGAGCGCAAGTACTCTGTGTGGATCGGTGGCTCCATCCTG
GCCTCACTGTCCACCTTCCAGCAGATGTGGATCAGCAAGCAGGAGTACGATGAGTCCGGCCCCT
CCATCGTGCACCGCAAGTGCTTCTAGGCGGACTGTTACTGAGCTGCGTTTTACACCCTTTCTTT
GACAAAACCTAACTTGCGCAGAAAAAAAAAAAATAAGAGACAACATTGGCATGGCTTTGTTTTT
TTAAATTTTTTTTAAAGTTTTTTTTTTTTTTTTTTTTTTTTTTTTAAGTTTTTTTGTTTTGTTTTG
GCGCTTTTGACTCAGGATTTAAAAACTGGAACGGTGAAGGCGACAGCAGTTGGTTGGAGCAAAC
ATCCCCCAAAGTTCTACAAATGTGGCTGAGGACTTTGTACATTGTTTTGTTTTTTTTTTTTTTG

GTTTTGTCTTTTTTTAATAGTCATTCCAAGTATCCATGAAATAAGTGGTTACAGGAAGTCCCTCA
CCCTCCCAAAAGCCACCCCCACTCCTAAGAGGAGGATGGTCGCGTCCATGCCCTGAGTCCACCC
CGGGGAAGGTGACAGCATTGCTTCTGTGTAAATTATGTACTGCAAAAATTTTTTTAAATCTTCCG
CCTTAATACTTCATTTTTGTTTTTAATTTCTGAATGGCCCAGGTCTGAGGCCTCCCTTTTTTTTG
TCCCCCCAACTTGATGTATGAAGGCTTTGGTCTCCCTGGGAGGGGGTTGAGGTGTTGAGGCAGC
CAGGGCTGGCCTGTACACTGACTTGAGACCAATAAAAGTGCACACCTTACCTTACACAAACAAA
AAAAAAAAAAAAA

Forward primer	Pos	Len	Tm	Reverse primer	Pos	Len	Tm	Amp	dG
5′-ATGGTGGGAATGGGTC-3′	238	16	55.23	5′-CATACAGGGACAGCAC-3′	538	16	53.66	300	0

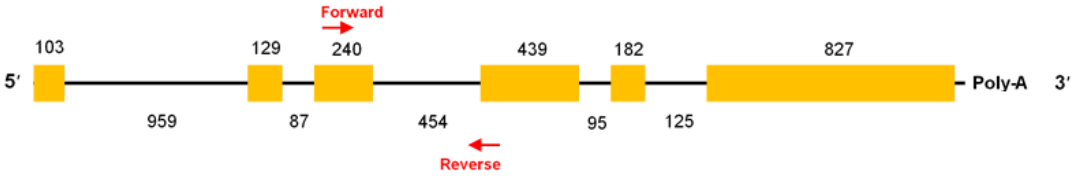

Cat (Catalase) (mRNA 2,551 bps (from genomic DNA 31,250 bps)) Accession number: NM_009804.2

Highlighted texts are nucleotide sequences for forward and reverse primers.

GAAGTCACCACTCCAGCGGGCCTGGCCAACAAGATTGCCTTCTCCGGGTGGAGACCGCTGCGT
CCGTCCCTGCTGTCTCACGTTCCGCAGCTCTGCAGCTCCGCAATCCTACACCATGTCGGACAGT
CGGGACCCAGCCAGCGACCAGATGAAGCAGTGGAAGGAGCAGCGGGCCTCGCAGAGACCTGAT
GTCCTGACCACCGGAGGCGGGAACCCAATAGGAGATAAACTTAATATCATGACCGCGGGGTCCC
GAGGGCCCCTCCTCGTTCAGGATGTGGTTTTCACTGACGAGATGGCACACTTTGACAGAGAGCG
GATTCCTGAGAGAGTGGTACACGCAAAAGGAGCAGGTGCTTTTGGATACTTTGAGGTCACCCAC
GATATCACCAGATACTCCAAGGCAAAGGTGTTTGAGCATATTGGAAAGAGGACCCCTATTGCCG
TTCGATTCTCCACAGTCACTGGAGAGTCAGGCTCAGCTGACACAGTTCGTGACCCTCGGGGGTT
TGCAGTGAAATTTTACACTGAAGATGGTAACTGGGATCTTGTGGGAAACAACACCCCTATTTTC
TTCATCAGGGATGCCATATTGTTTCCATCCTTTATCCATAGCCAGAAGAGAAACCCACAGACTC
ACCTGAAGGATCCTGACATGGTCTGGGACTTCTGGAGTCTTCGTCCCGAGTCTCTCCATCAGGT
TTCTTTCTTGTTCAGTGACCGAGGGATTCCCGATGGTCACCGGCACATGAATGGCTATGGATCA
CACACCTTCAAGTTGGTTAATGCAGATGGAGAGGCAGTCTATTGCAAGTTCCATTACAAGACCG
ACCAGGGCATCAAAAATTGCCTGTTGGAGAGGCAGGAAGGCTTGCTCAGGAAGATCCGGATTAT
GGCCTCCGAGATCTTTTCAATGCCATCGCCAATGGCAATTACCCGTCCTGGACGTTTTACATCC
AGGTCATGACTTTTAAGGAGGCAGAAACTTTCCCATTTAATCCATTTGATCTGACCAAGGTTTG
GCCTCACAAGGACTACCCTCTTATACCAGTTGGCAAACTGGTTTTAAACAAAAATCCAGTTAATT
ACTTTGCTGAAGTTGAACAGATGGCTTTTGACCCAAGCAATATGCCCCCTGGCATCGAGCCCAG
CCCTGACAAAATGCTTCAGGGCCGCCTTTTTGCCTACCCGGACACTCACCGCCACCGCCTGGGA
CCCAACTATCTGCAGATACCTGTGAACTGTCCCTACCGCGCTCGAGTGGCCAACTACCAGCGTG
ATGGCCCCATGTGCATGCATGACAACCAGGGTGGTGCCCCCAACTATTACCCCAACAGCTTCAG
CGCACCAGAGCAGCAGCGCTCAGCCCTGGAGCACAGCGTCCAGTGCGCTGTAGATGTGAAACG
CTTCAACAGTGCTAATGAAGACAATGTCACTCAGGTGCGGACATTCTACACAAAGGTGTTGAAC
GAGGAGGAGAGGAAACGCCTGTGTGAGAACATTGCCGGCCACCTGAAGGACGCTCAGCTTTTC
ATTCAGAAGAAAGCGGTCAAGAATTTCACTGACGTCCACCCTGACTATGGGGCCCGCATCCAGG
CTCTTCTGGACAAGTACAACGCTGAGAAGCCTAAGAACGCAATTCACACCTACACGCAGGCCGG
CTCTCACATGGCTGCGAAGGGAAAAGCTAACCTGTAACTCCGGTGCTCAGCCTCCGCTGAGGAG
ACCTCTCGTGAAGCCGAGCCTGAGGATCACCTGTAATCAACGCTGGATGGATTCTCCCACTCCG

GAGCGCAGACTCACGCTGATGACTTTAAAACGATAATCCGGGCTTCTAGAGTGAATGATAACCA
TGCTTTTGATGCCGTTTCCTGAAGGGAAATGAAAGGTTAGGGCTTAGCAATCATTTAACAGAAA
CATGGATCTAATAGGACTTCTGTTTGGATTATTCATTTAAATGACTACATTTAAAATGATTACAA
GAAAGGTGTTCTAGCCAGAAACATGACTTGATTAGACAAGATAAAAATCTTGGCGAGAATAGTG
TATTCTCCTATTACCTCATGGTCTGGTATATATACAATACAACACACATACCACACACACACACA
CATGCAATACACACACTACACACACATACACACACTCACACACACTCATACACACACATGAAGA
GATGATAAAGATGGCCCACTCAGAATTTTTTTTTTTATTTTTCTAAGGTCCTTATAAGCAAAACC
ATACTTGCATCATGTCTTCCAAAAGTAACTTTAGCACTGTTGAAACTTAATGTTTATTCCTGTGC
TGTGCGGTGCTGTGCTGTGCTGTGCTGTGCAGCTAATCAGATTCTTGTTTTTTCCCACTTGGAT
TATGTTGATGTTAATACGCAGTGATTTCACATAGGATGATTTGTACTTGCTTACATTTTTACAAT
AAAATGATCTACATGGAAGGACCGTGTTTGGTTGCTTTCAGCTCTGTATAATGTGGAATGTGAA
GTAGAGATTACCAGCTCTCTCTGCAGTAACAATAAAAGCGCCAGCGGCCAGA

Forward primer	Pos	Len	Tm	Reverse primer	Pos	Len	Tm	Amp	dG
5′-GGGATTCCCGATGGT-3′	724	15	54.19	5′-GCCAAACCTTGGTCAG-3′	1024	16	54.99	300	0

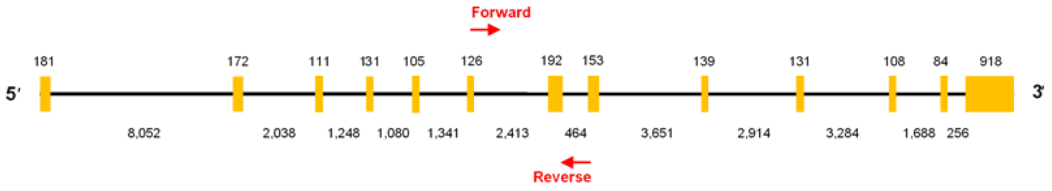

COX-2 (Cyclooxygenase-2) [also known as *Ptgs2*] (mRNA 4,460 bps (from genomic DNA 8,204 bps)) Accession number: NM_011198.4

Highlighted texts are nucleotide sequences for forward and reverse primers.

AGAGTCACCACTACGTCACGTGGAGTCCGCTTTACAGACTTAAAAGCAAGGTTCTCCCCATTAG
CAGCCAGTTGTCAAACTGCGAGCTAAGAGCTTCAGGAGTCAGTCAGGACTCTGCTCACGAAGGA
ACTCAGCACTGCATCCTGCCAGCTCCACCGCCACCACTACTGCCACCTCCGCTGCCACCTCTGC
GATGCTCTTCCGAGCTGTGCTGCTCTGCGCTGCCCTGGGGCTCAGCCAGGCAGCAAATCCTTGC
TGTTCCAATCCATGTCAAAACCGTGGGGAATGTATGAGCACAGGATTTGACCAGTATAAGTGTG
ACTGTACCCGGACTGGATTCTATGGTGAAAACTGTACTACACCTGAATTTCTGACAAGAATCAA
ATTACTGCTGAAGCCCACCCCAAACACAGTGCACTACATCCTGACCCACTTCAAGGGAGTCTGG
AACATTGTGAACAACATCCCCTTCCTGCGAAGTTTAATCATGAAATATGTGCTGACATCCAGAT
CATATTTGATTGACAGTCCACCTACTTACAATGTGCACTATGGTTACAAAAGCTGGGAAGCCTT
CTCCAACCTCTCCTACTACACCAGGGCCCTTCCTCCCGTAGCAGATGACTGCCCAACTCCCATG
GGTGTGAAGGGAAATAAGGAGCTTCCTGATTCAAAAGAAGTGCTGGAAAAGGTTCTTCTACGGA
GAGAGTTCATCCCTGACCCCCAAGGCTCAAATATGATGTTTGCATTCTTTGCCCAGCACTTCAC
CCATCAGTTTTTCAAGACAGATCATAAGCGAGGACCTGGGTTCACCCGAGGACTGGGCCATGGA
GTGGACTTAAATCACATTTATGGTGAAACTCTGGACAGACAACATAAACTGCGCCTTTTCAAGG
ATGGAAAATTGAAATATCAGGTCATTGGTGGAGAGGTGTATCCCCCCACAGTCAAAGACACTCA
GGTAGAGATGATCTACCCTCCTCACATCCCTGAGAACCTGCAGTTTGCTGTGGGGCAGGAAGTC
TTTGGTCTGGTGCCTGGTCTGATGATGTATGCCACCATCTGGCTTCGGGAGCACAACAGAGTGT
GCGACATACTCAAGCAGGAGCATCCTGAGTGGGGTGATGAGCAACTATTCCAAACCAGCAGACT
CATACTCATAGGAGAGACTATCAAGATAGTGATCGAAGATACGTGCAACACCTGAGCGGTTACC
ACTTCAAACTCAAGTTTGACCCAGAGCTCCTTTTCAACCAGCAGTTCCAGTATCAGAACCGCAT
TGCCTCTGAATTCAACACACTCTATCACTGGCACCCCCTGCTGCCCGACACCTTCAACATTGAA
GACCAGGAGTACAGCTTCAAACAGTTTCTCTACAACAACTCCATCCTCCTGGAACATGGACTCA
CTCAGTTTGTTGAGTCATTCACCAGACAGATTGCTGGCCGGGTTGCTGGGGGAAGAAATGTGCC
AATTGCTGTACAAGCAGTGGCAAAGGCCTCCATTGACCAGAGCAGAGAGATGAAATACCAGTCT
CTCAATGAGTACCGCAAACGCTTCTCCCTGAAGCCGTACACATCATTTGAAGAACTTACAGGAG
AGAAGGAAATGGCTGCAGAATTGAAAGCCCTCTACAGTGACATCGATGTCATGGAACTGTACCC
TGCCCTGCTGGTGGAAAAACCTCGTCCAGATGCTATCTTTGGGGAGACCATGGTAGAGCTTGGA
GCACCATTCTCCTTGAAAGGACTTATGGGAAATCCCATCTGTTCTCCTCAATACTGGAAGCCGA

GCACCTTTGGAGGCGAAGTGGGTTTTAAGATCATCAATACTGCCTCAATTCAGTCTCTCATCTG
CAATAATGTGAAGGGGTGTCCCTTCACTTCTTTCAATGTGCAAGATCCACAGCCTACCAAAACA
GCCACCATCAATGCAAGTGCCTCCCACTCCAGACTAGATGACATTAACCCTACAGTACTAATCA
AAAGGCGTTCAACTGAGCTGTAAAAGTCTACTGACCATATTTATTTATTTATGTGAAGAATTTAA
TTTAATTATTTAATATTTATACTGAATTTTTTTTCATGTAACATCTTCCATAACAGAAGGCAATG
TTCTTGAACAATGTTACATTTGTGAAGATTCCCTCCGGTGTTTGTCCTTTAAATATGTGTTACCT
GAAACTGAAAGGAAATCAGCATTCATTCCTCTACATAAGCCAGTGAGAAGGGAAATGAATTTTG
ATATCTTTATACTTGAATTTCAGATCATGATTAGCTTAACAAGAACCAAGGAAAAATGTATGAAT
ATGTGAGTGTTGTTACAAGATGAAAAATGCTGCAGGTATCAACACTGTTGGTTACAACTGTGTC
TTCTTTACTATGATAGGAGCATGTAATGTGGAATTCTTCTTAAATCTTGCATATCTTTATCTCAT
CAAACAAAGGGGTCCAAGTTCAGTTTTAAATAAGCATTTAAGGCAGATACTGACAACAATCTCA
TTTTTTAAAATGTTGTCTTGAGACAAATAATTTGAAATTTCTAAATTGGGAGTTTGAATCACTTT
TGAAAGCTCTTACTTTCTTAAGCTGTCAGGTTTGTACCGACATGGAGTAAACAGCTATCATAAAC
GTAAATCTCCAAAACTAGTAGAAATTATGTCATGATTGATGGTTAAGATACCATGTCAGGGATT
GTCTTTTCTTAGAAGTAGTGAAAGCTACTTACTATGACAATCAGACCTTCCTTGTATGTCAAAAT
GCTGGTGTGGAAGGTGGTGGAGCCCGTGCTGCTCTGTCTTAACTATGAGTGTGAGCTTTAAAGC
TCGTTGATGAGTGGTAGCCAGCAAAGCCTAGAGCAACAAAAGCTTCTACAAAGGAACTAACCAA
GAACAAAGAAGGGTTCCCAATTAAAGATCACATTCAGGGTTAAACTTCCAAAGGAGACATCCTG
ATCCTGGTTTTGTGCTGGCCTGGTACTCAGTAGGTTTTTGCTGTGAGGTTAAAGACTTGCCAGG
CTGAACTTCGAAACAGTTTTTCTGTTGCACAGTATGATGTAACAGTCCATCTCTCAATGCAATAG
GTATCAGTGGCCTCGTGAGCTTCTTCACAATATTGATATGTCTTCCAGCCCATTGAACCTGGAC
TGCAGAAGGCCCCATGTCATGTGTGAGCTCAGCCTGGATGCCAGCATTGCTGCTCCTCTTAGTT
CCGTTTCTCGTGGTCACTTTACTACGAGAAACGCTGATTGGGTTTTCGTAGCTGTGTTCCAGGT
TTTTAGTATCAGAACTATTCTTTCTTTAACCTCTATTCATATTTTCTCTACTTGAAGTTTTACATT
CAGGAAAACCTCAGCTCAGGACTACTATGTACCTCCCCTTTGGAGGGAAAAATTATTTTAGGTA
AAAGGCAAAAATTTTTTAAAAATATTTTTATTTATAATTATATGGAAGGGCCCTACCAAGATGCT
AGAAATATAGGGAGTTCCTGACAAGAAATTTCCATTCTTATTCTGAAGAATTGCTTTCTTACTTA
AAAACAAAGACAGTTTGTGAGTAGTTCTGGGCAATAGGGATAAATATAAAACAATAATGATGAT
CATTTTCTACATCTCATTATCAGCTGAGGTACTGTATATTACTGAATTTATTGAAGATAGTTATG
TCTTTTAGACATTGTTGTTATAAACTATGTTTAAGCCTACTACAAGTGTTTCTTTTTGCATTATG
TTGGAATTGATGTACCTTTTTTATGATTACCTCTCTGAACTATGGTGTGAACAATCAAACAAAAT

GATGAGATTAACGTTCATGGATAAATTCTAAGAAAACTAGTGTATTTTTTTGAAAAGTTTGAAGT
TAGAACTTAGGCTGTTGGAATTTACGCATAAAGCAGACTGCATAGATCCAATATTGACTGACCC
AAGCATGTTATAAAGACTGACATTTTAGACATTTTGAAGGCCCTGTAAGTGTTTATTAATTAGTT
AGAACTTAATTGATTAAAAAATATATCCAAAGCACTATAGGCATTAGAATTCGTGCATCAAGAAA
TGATGACAAATAATACTGTTATTTATATAAATAACTAAAAAGGGTGTCTAATGAAGAAATATATT
TTATTACAAAGAAATTATAAAACATTTTGAAGATTATATGCTTTAAAAGTTTAAGATGAAAAAAT
AATCAACCTTAGAAAAAATGTATAAAAATATATAAATTGTTAATGTCATTGATTAAAAAAAAAAA
AAACTAGCCAACATGATTTTTGTGAATATCAACCTGCTGATTGAACCTGGGAATTCAGGTTAAG
TATGTGACTGCTACAGTGCCTCAGAGAAATTTGTATTTAAATTAACTTATGTAAAAAATAAATCT
TAGAGCAAATGCTTGTTTATTTTTATACTTATTTAAGAATTGAAAACTTCTGAAAATAAAGTTTG
ATTGTTTCTTTATATCATG

Forward primer	Pos	Len	Tm	Reverse primer	Pos	Len	Tm	Amp	dG
5′-ACAGATTGCTGGCCG-3′	1434	15	56.37	5′-TGGTGCTCCAAGCTC-3′	1734	15	55.37	300	-0.01

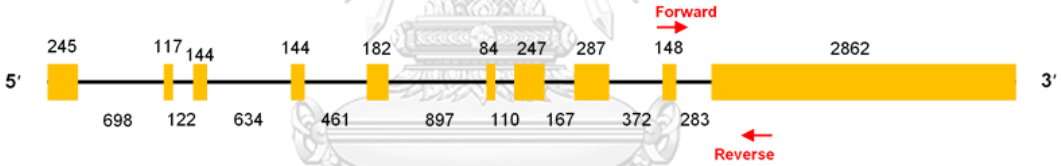

Hmox1 (Heme oxygenase-1) (mRNA 1,634 bps (from genomic DNA 6,976 bps))
Accession number: NM_010442.2

Highlighted texts are nucleotide sequences for forward and reverse primers.

GCTCACGGTCTCCAGTCGCCTCCAGAGTTTCCGCATACAACCAGTGAGTGGAGCCTGCCCGCGC
AGAGCCGTCTCGAGCATAGCCCGGAGCCTGAATCGAGCAGAACCAGCCTGAACTAGCCCAGTC
CGGTGATGGAGCGTCCACAGCCCGACAGCATGCCCCAGGATTTGTCTGAGGCCTTGAAGGAGG
CCACCAAGGAGGTACACATCCAAGCCGAGAATGCTGAGTTCATGAAGAACTTTCAGAAGGGTCA
GGTGTCCAGAGAAGGCTTTAAGCTGGTGATGGCTTCCTTGTACCATATCTACACGGCCCTGGAA
GAGGAGATAGAGCGCAACAAGCAGAACCCAGTCTATGCCCCACTCTACTTCCCTGAGGAGCTGC
ACCGAAGGGCTGCCCTGGAGCAGGACATGGCCTTCTGGTATGGGCCTCACTGGCAGGAAATCA
TCCCTTGCACGCCAGCCACACAGCACTATGTAAAGCGTCTCCACGAGGTGGGGCGCACTCACCC
TGAGCTGCTGGTGGCCCACGCATATACCCGCTACCTGGGTGACCTCTCAGGGGGTCAGGTCCTG
AAGAAGATTGCACAGAAGGCCATGGCCTTGCCCAGCTCTGGGGAGGGCCTGGCTTTTTTTACCT
TCCCGAACATCGACAGCCCCACCAAGTTCAAACAGCTCTATCGTGCTCGAATGAACACTCTGGA
GATGACACCTGAGGTCAAGCACAGGGTGACAGAAGAGGCTAAGACCGCCTTCCTGCTCAACATT
GAGCTGTTTGAGGAGCTGCAGGTGATGCTGACAGAGGAACACAAAGACCAGAGTCCCTCACAG
ATGGCGTCACTTCGTCAGAGGCCTGCTAGCCTGGTGCAAGATACTGCCCCTGCAGAGACACCCC
GAGGGAAACCCCAGATCAGCACTAGCTCATCCCAGACACCGCTCCTCCAGTGGGTCCTCACTCT
CAGCTTCCTGTTGGCAACAGTGGCAGTGGGAATTTATGCCATGTAAATGCAATACTGGCCCCCA
GGGGCTGTGAACTCTGTCCAATGTGGCCTTCTCTCTGTAAGGGAGAATCTTGCCTGGCTCTCTT
CTCTTGGGCCTCTAAGAAAGCTTTTGGGGTCCCTAGCCCACTCCCTGTGTTTCCTTTCTCTCTG
GAATGGAGGGAGATACCTGACACAGTTCCCTCACCAAAAGCACATCCAGCCAGTGGCCTGAACT
TTGAAACCAGCAGCCCCAAATCCTGCAGCAGAGCCCCAAAACTGGCCTGTAAAAGCAGCTGTTC
TGAGCCCAGTGCCCATGGTTGTAAGCATCCATGTTGACTGACCACGACTGCTGTCCCCCAGTGC
CATGGCCACTTTGATATCCGTTTCCAGACATTTCTGTCTCGTATTTCTGTCTTGTTTTTTATTAT
TTCCCCAGTTCTACCAGAGTAATGGTATTTTGTTGTTTTGTTTTGTCTTGTTTTTCCTAACAAAG
TGGGGCTATCTTTTGAGGGGTGGGTGGGAAAGAATTATTTAATAGTTGTAACCTTGGTCTCTAA
CTTCTGTGTGAAATAATAAATGGCATTATCTAACAGTCACTAAAAAAAAAAAAAAAAAAAAAAAA
AAAAAAAAAAAAAAAAAAAAAAAAAAAAAAAAA

Forward primer	Pos	Len	Tm	Reverse primer	Pos	Len	Tm	Amp	dG
5′-CTGGGTGACCTCTCAG-3′	543	16	55.01	5′-GACGAAGTGACGCCA-3′	843	15	55.99	300	0

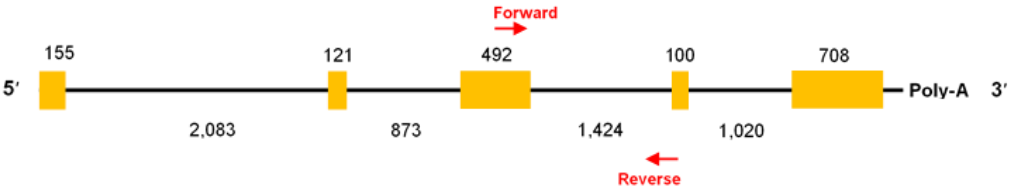

iNOS (inducible nitric oxide synthase) [also known as *Nos2*] (mRNA 4,164 bps (from genomic DNA 39,446 bps)) Accession number: NM_010927.4

Highlighted texts are nucleotide sequences for forward and reverse primers.

CTGGAGGGGTATAAATACCTGATGGCTGCTGCCAGGGTCACAACTTTACAGGGAGTTGAAGACT
GAGACTCTGGCCCCACGGACACAGTGTCACTGGTTTGAAACTTCTCAGCCACCTTGGTGAAGGG
ACTGAGCTGTTAGAGACACTTCTGAGGCTCCTCACGCTTGGGTCTTGTTCACTCCACGGAGTAG
CCTAGTCAACTGCAAGAGAACGGAGAACGTTGGATTTGGAGCAGAAGTGCAAAGTCTCAGACAT
GGCTTGCCCCTGGAAGTTTCTCTTCAAAGTCAAATCCTACCAAAGTGACCTGAAAGAGGAAAAG
GACATTAACAACAACGTGAAGAAAACCCCTTGTGCTGTTCTCAGCCCAACAATACAAGATGACC
CTAAGAGTCACCAAAATGGCTCCCCGCAGCTCCTCACTGGGACAGCACAGAATGTTCCAGAATC
CCTGGACAAGCTGCATGTGACATCGACCCGTCCACAGTATGTGAGGATCAAAAACTGGGGCAGT
GGAGAGATTTTGCATGACACTCTTCACCACAAGGCCACATCGGATTTCACTTGCAAGTCCAAGT
CTTGCTTGGGGTCCATCATGAACCCCAAGAGTTTGACCAGAGGACCCAGAGACAAGCCTACCCC
TCTGGAGGAGCTCCTGCCTCATGCCATTGAGTTCATCAACCAGTATTATGGCTCCTTTAAAGAG
GCAAAAATAGAGGAACATCTGGCCAGGCTGGAAGCTGTAACAAAGGAAATAGAAACAACAGGAA
CCTACCAGCTCACTCTGGATGAGCTCATCTTTGCCACCAAGATGGCCTGGAGGAATGCCCCTCG
CTGCATCGGCAGGATCCAGTGGTCCAACCTGCAGGTCTTTGACGCTCGGAACTGTAGCACAGCA
CAGGAAATGTTTCAGCACATCTGCAGACACATACTTTATGCCACCAACAATGGCAACATCAGGT
CGGCCATCACTGTGTTCCCCCAGCGGAGTGACGGCAAACATGACTTCAGGCTCTGGAATTCACA
GCTCATCCGGTACGCTGGCTACCAGATGCCCGATGGCACCATCAGAGGGGATGCTGCCACCTTG
GAGTTCACCCAGTTGTGCATCGACCTAGGCTGGAAGCCCCGCTATGGCCGCTTTGATGTGCTGC
CTCTGGTCTTGCAAGCTGATGGTCAAGATCCAGAGGTCTTTGAAATCCCTCCTGATCTTGTGTT
GGAGGTGACCATGGAGCATCCCAAGTACGAGTGGTTCCAGGAGCTCGGGTTGAAGTGGTATGC
ACTGCCTGCCGTGGCCAACATGCTACTGGAGGTGGGTGGCCTCGAATTCCCAGCCTGCCCCTTC
AATGGTTGGTACATGGGCACCGAGATTGGAGTTCGAGACTTCTGTGACACACAGCGCTACAACA
TCCTGGAGGAAGTGGGCCGAAGGATGGGCCTGGAGACCCACACACTGGCCTCCCTCTGGAAAG
ACCGGGCTGTCACGGAGATCAATGTGGCTGTGCTCCATAGTTTCCAGAAGCAGAATGTGACCAT
CATGGACCACCACACAGCCTCAGAGTCCTTCATGAAGCACATGCAGAATGAGTACCGGGCCCGT
GGAGGCTGCCCGGCAGACTGGATTTGGCTGGTCCCTCCAGTGTCTGGGAGCATCACCCCTGTGT
TCCACCAGGAGATGTTGAACTATGTCCTATCTCCATTCTACTACTACCAGATCGAGCCCTGGAA
GACCCACATCTGGCAGAATGAGAAGCTGAGGCCCAGGAGGAGAGAGATCCGATTTAGAGTCTT

GGTGAAAGTGGTGTTCTTTGCTTCCATGCTAATGCGAAAGGTCATGGCTTCACGGGTCAGAGCC
ACAGTCCTCTTTGCTACTGAGACAGGGAAGTCTGAAGCACTAGCCAGGGACCTGGCCACCTTGT
TCAGCTACGCCTTCAACACCAAGGTTGTCTGCATGGACCAGTATAAGGCAAGCACCTTGGAAGA
GGAGCAACTACTGCTGGTGGTGACAAGCACATTTGGGAATGGAGACTGTCCCAGCAATGGGCA
GACTCTGAAGAAATCTCTGTTCATGCTTAGAGAACTCAACCACACCTTCAGGTATGCTGTGTTT
GGCCTTGGCTCCAGCATGTACCCTCAGTTCTGCGCCTTTGCTCATGACATCGACCAGAAGCTGT
CCCACCTGGGAGCCTCTCAGCTTGCCCCAACAGGAGAAGGGGACGAACTCAGTGGGCAGGAGG
ATGCCTTCCGCAGCTGGGCTGTACAAACCTTCCGGGCAGCCTGTGAGACCTTTGATGTCCGAAG
CAAACATCACATTCAGATCCCGAAACGCTTCACTTCCAATGCAACATGGGAGCCACAGCAATAT
AGGCTCATCCAGAGCCCGGAGCCTTTAGACCTCAACAGAGCCCTCAGCAGCATCCATGCAAAGA
ACGTGTTTACCATGAGGCTGAAATCCCAGCAGAATCTGCAGAGTGAAAAGTCCAGCCGCACCAC
CCTCCTCGTTCAGCTCACCTTCGAGGGCAGCCGAGGGCCCAGCTACCTGCCTGGGGAACACCT
GGGGATCTTCCCAGGCAACCAGACCGCCCTGGTGCAGGGAATCTTGGAGCGAGTTGTGGATTG
TCCTACACCACACCAAACTGTGTGCCTGGAGGTTCTGGATGAGAGCGGCAGCTACTGGGTCAAA
GACAAGAGGCTGCCCCCCTGCTCACTCAGCCAAGCCCTCACCTACTTCCTGGACATTACGACCC
CTCCCACCCAGCTGCAGCTCCACAAGCTGGCTCGCTTTGCCACGGACGAGACGGATAGGCAGA
GATTGGAGGCCTTGTGTCAGCCCTCAGAGTACAATGACTGGAAGTTCAGCAACAACCCCACGTT
CCTGGAGGTGCTTGAAGAGTTCCCTTCCTTGCATGTGCCCGCTGCCTTCCTGCTGTCGCAGCTC
CCTATCTTGAAGCCCCGCTACTACTCCATCAGCTCCTCCCAGGACCACACCCCCTCGGAGGTTC
ACCTCACTGTGGCCGTGGTCACCTACCGCACCCGAGATGGTCAGGGTCCCCTGCACCATGGTGT
CTGCAGCACTTGGATCAGGAACCTGAAGCCCCAGGACCCAGTGCCCTGCTTTGTGCGAAGTGTC
AGTGGCTTCCAGCTCCCTGAGGACCCCTCCCAGCCTTGCATCCTCATTGGGCCTGGTACGGGCA
TTGCTCCCTTCCGAAGTTTCTGGCAGCAGCGGCTCCATGACTCCCAGCACAAAGGGCTCAAAGG
AGGCCGCATGAGCTTGGTGTTTGGGTGCCGGCACCCGGAGGAGGACCACCTCTATCAGGAAGA
AATGCAGGAGATGGTCCGCAAGAGAGTGCTGTTCCAGGTGCACACAGGCTACTCCCGGCTGCC
CGGCAAACCCAAGGTCTACGTTCAGGACATCCTGCAAAAGCAGCTGGCCAATGAGGTACTCAGC
GTGCTCCACGGGGAGCAGGGCCACCTCTACATTTGCGGAGATGTGCGCATGGCTCGGGATGTG
GCTACCACATTGAAGAAGCTGGTGGCCACCAAGCTGAACTTGAGCGAGGAGCAGGTGGAAGAC
TATTTCTTCCAGCTCAAGAGCCAGAAACGTTATCATGAAGATATCTTCGGTGCAGTCTTTTCCTA
TGGGGCAAAAAAGGGCAGCGCCTTGGAGGAGCCCAAAGCCACGAGGCTCTGACAGCCCAGAGT
TCCAGCTTCTGGCACTGAGTAAAGATAATGGTGAGGGGCTTGGGGAGACAGCGAAATGCAATCC

CCCCCAAGCCCCTCATGTCATTCCCCCCTCCTCCACCCTACCAAGTAGTATTGTACTATTGTGG
ACTACTAAATCTCTCTCCTCTCCTCCCTCCCCTCTCTCCCTTTCCTCCCTTCTTCTCCACTCCCC
AGCTCCCTCCTTCTCCTTCTCCTCCTTTGCCTCTCACTCTTCCTTGGAGCTGAGAGCAGAGAAA
AACTCAACCTCCTGACTGAAGCACTTTGGGTGACCACCAGGAGGCACCATGCCGCCGCTCTAAT
ACTTAGCTGCACTATGTACAGATATTTATACTTCATATTTAAGAAAACAGATACTTTTGTCTACT
CCCAATGATGGCTTGGGCCTTTCCTGTATAATTCCTTGATGAAAAATATTTATATAAAATACATT
TTATTTTAATCA

Forward primer	Pos	Len	Tm	Reverse primer	Pos	Len	Tm	Amp	dG
5′-AGATCGAGCCCTGGA-3′	1711	15	55.33	5′-GTGCTTGTCACCACC-3′	2011	15	54.27	300	0

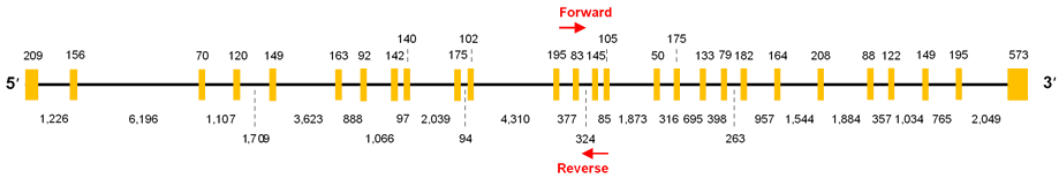

Nrf2 (Nuclear factor, erythroid derived 2, like 2 (Nfe2l2*)*) (mRNA 2,497 bps (from genomic DNA 29,151 bps) Accession number: NM_010902.4

Highlighted texts are nucleotide sequences for forward and reverse primers.

CTCCATGCCCTTGTCCTGCCTCTGGCCCTTGCCTCTTGCCCTAGCCTTTTCTCCGCCTCTAAGTT
CTTGTCCCGTCCCTAGGTCCTTGTTCCGCCCCCAGGGGGCGGGGGCGGGGCGGACTAAGGCTG
GCCTGCCACTCCAGCGAGCAGGCTATCTCCTAGTTCTCCGCTGCTCGGACTAGCCATTGCCGCC
GCCTCACCTCTGCTGCAAGTAGCCTCGCCGTCGGGGAGCCCTACCACAGCGTCCGCCCTCAGCA
TGATGGACTTGGAGTTGCCACCGCCAGGACTACAGTCCCAGCAGGACATGGATTTGATTGACAT
CCTTTGGAGGCAAGACATAGATCTTGGAGTAAGTCGAGAAGTGTTTGACTTTAGTCAGCGACAG
AAGGACTATGAGCTGGAAAAACAGAAAAAACTCGAAAAGGAAAGACAAGAGCAACTCCAGAAGG
AACAGGAGAAGGCCTTTTTTGCTCAGTTTCAACTGGATGAAGAAACAGGAGAATTCCTCCCAAT
TCAGCCGGCCCAGCACATCCAGACAGACACCAGTGGATCCGCCAGCTACTCCCAGGTTGCCCAC
ATTCCCAAACAAGATGCCTTGTACTTTGAAGACTGTATGCAGCTTTTGGCAGAGACATTCCCAT
TTGTAGATGACCATGAGTCGCTTGCCCTGGATATCCCCAGCCACGCTGAAAGTTCAGTCTTCAC
TGCCCCTCATCAGGCCCAGTCCCTCAATAGCTCTCTGGAGGCAGCCATGACTGATTTAAGCAGC
ATAGAGCAGGACATGGAGCAAGTTTGGCAGGAGCTATTTTCCATTCCCGAATTACAGTGTCTTA
ATACCGAAAACAAGCAGCTGGCTGATACTACCGCTGTTCCCAGCCCAGAAGCCACACTGACAGA
AATGGACAGCAATTACCATTTTTACTCATCGATCTCCTCGCTGGAAAAAGAAGTGGGCAACTGT
GGTCCACATTTCCTTCATGGTTTTGAGGATTCTTTCAGCAGCATCCTCTCCACTGATGATGCCA
GCCAGCTGACCTCCTTAGACTCAAATCCCACCTTAAACACAGATTTTGGCGATGAATTTTATTCT
GCTTTCATAGCAGAGCCCAGTGACGGTGGCAGCATGCCTTCCTCCGCTGCCATCAGTCAGTCAC
TCTCTGAACTCCTGGACGGGACTATTGAAGGCTGTGACCTGTCACTGTGTAAAGCTTTCAACCC
GAAGCACGCTGAAGGCACAATGGAATTCAATGACTCTGACTCTGGCATTTCACTGAACACGAGT
CCCAGCCGAGCGTCCCCAGAGCACTCCGTGGAGTCTTCCATTTACGGAGACCCACCGCCTGGGT
TCAGTGACTCGGAAATGGAGGAGCTAGATAGTGCCCCTGGAAGTGTCAAACAGAACGGCCCTAA
AGCACAGCCAGCACATTCTCCTGGAGACACAGTACAGCCTCTGTCACCAGCTCAAGGGCACAGT
GCTCCTATGCGTGAATCCCAATGTGAAAATACAACAAAAAAAGAAGTTCCCGTGAGTCCTGGTC
ATCAAAAAGCCCCATTCACAAAAGACAAACATTCAAGCCGCTTAGAGGCTCATCTCACACGAGA
TGAGCTTAGGGCAAAAGCTCTCCATATTCCATTCCCTGTCGAAAAAATCATTAACCTCCCTGTTG
ATGACTTCAATGAAATGATGTCCAAGGAGCAATTCAATGAAGCTCAGCTCGCATTGATCCGAGA
TATACGCAGGAGAGGTAAGAATAAAGTCGCCGCCCAGAACTGTAGGAAAAGGAAGCTGGAGAA

CATTGTCGAGCTGGAGCAAGACTTGGGCCACTTAAAAGACGAGAGAGAAAAACTACTCAGAGAA
AAGGGAGAAAACGACAGAAACCTCCATCTACTGAAAAGGCGGCTCAGCACCTTGTATCTTGAAG
TCTTCAGCATGTTACGTGATGAGGATGGAAAGCCTTACTCTCCCAGTGAATACTCTCTGCAGCA
AACCAGAGATGGCAATGTGTTCCTTGTTCCCAAAAGCAAGAAGCCAGATACAAAGAAAAACTAG
GTTCGGGAGGATGGAGCCTTTTCTGAGCTAGTGTTTGTTTTGTACTGCTAAAACTTCCTACTGT
GATGTGAAATGCAGAAACACTTTATAAGTAACTATGCAGAATTATAGCCAAAGCTAGTATAGCA
ATAATATGAAACTTTACAAAGCATTAAAGTCTCAATGTTGAATCAGTTTCATTTTAACTCTCAAG
TTAATTTCTTAGGCACCATTTGGGAGAGTTTCTGTTTAAGTGTAAATACTACAGAACTTATTTAT
ACTGTTCTCACTTGTTACAGTCATAGACTTATATGACATCTGGCTAAAAGCAAACTATTGAAAAC
TAACCAGACCACTATACTTTTTTATATACTGTATGAACAGGAAATGACATTTTTATATTAAATTG
TTTAGCTCATAAAAATTAAAAGGAGCTAGCACTAATAAAAGAATATCATGACTTAAACTA

Forward primer	Pos	Len	Tm	Reverse primer	Pos	Len	Tm	Amp	dG
5′-GCCCAGAACTGTAGGA-3′	1761	16	54.49	5′-CATCCTCCCGAACCT-3′	2061	15	53.74	300	0

sod1 (Cu/Zn-superoxide dismutase) (mRNA 661 bps (from genomic DNA 5,583 bps))

Accession number: NM_011434.1

Highlighted texts are nucleotide sequences for forward and reverse primers.

GCCAGGGCCTCGTTTTTTTGCGCGGTCCTTTCCTGCGGCGCCTTCCGTCCGTCGGCTTCTCGTC
TTGCTCTCTCTGGTCCCTCCGGAGGAGGCCGCCGCGCGTCTCCCGGGGAAGCATGGCGATGAA
AGCGGTGTGCGTGCTGAAGGGCGACGGTCCGGTGCAGGGAACCATCCACTTCGAGCAGAAGGC
AAGCGGTGAACCAGTTGTGTTGTCAGGACAAATTACAGGATTAACTGAAGGCCAGCATGGGTTC
CACGTCCATCAGTATGGGGACAATACACAAGGCTGTACCAGTGCAGGACCTCATTTTAATCCTC
ACTCTAAGAAACATGGTGGCCCGGCGGATGAAGAGAGGCATGTTGGAGACCTGGGCAATGTGA
CTGCTGGAAAGGACGGTGTGGCCAATGTGTCCATTGAAGATCGTGTGATCTCACTCTCAGGAGA
GCATTCCATCATTGGCCGTACAATGGTGGTCCATGAGAAACAAGATGACTTGGGCAAAGGTGGA
AATGAAGAAAGTACAAAGACTGGAAATGCTGGGAGCCGCTTGGCCTGTGGAGTGATTGGGATTG
CGCAGTAAACATTCCCTGTGTGGTCTGAGTCTCAGACTCATCTGCTACCCTCAAACCATTAAAC
TGTAATCTGAAAAAAAAAAAAAAA

Forward primer	Pos	Len	Tm	Reverse primer	Pos	Len	Tm	Amp	dG
5′-GGAACCATCCACTTCG-3′	164	16	54.04	5′-TACGGCCAATGATGGA-3′	476	16	54.55	300	-0.01

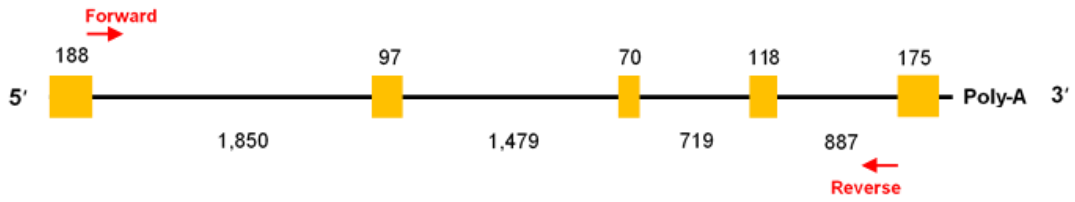

***Synechococcus elongatus* PCC 7942**

KatG (Catalase/peroxidase) (mRNA 2163 bps) KEGG accession number: Synpcc7942_1656

Highlighted texts are nucleotide sequences for forward and reverse primers.

ATGACAGCAACTCAGGGTAAATGTCCGGTCATGCACGGCGGAGCAACAACCGTTAATATTTCGA
CTCTGAGTGGTGGCCAAAGGCACTCAACCTGGATATTTTGAGCCAGCACGATCGCAAGACCAAC
CCAATGGGGCCAGACTTCAACTATCAGGAAGAAGTCAAGAAACTGGATGTCGCTGCGCTCAAGC
AAGATTTACAGGCGCTGATGACCGATAGCCAAGACTGGTGGCCGGCAGACTGGGGTCACTACG
GCGGTCTGATGATTCGCCTCACTTGGCACGCGGCGGGCACCTACCGAATTGCCGATGGTCGCG
GTGGTGCAGGCACGGGGAACCAGCGCTTTGCTCCCCTCAATTCTTGGCCAGACAACACAAATTT
AGACAAAGCGCGTCGCTTGCTTTGGCCGATCAAGCAAAAGTACGGCAACAAGTTGAGTTGGGCA
GATTTAATTGCCTATGCCGGCACGATCGCCTACGAATCGATGGGGCTTAAAACCTTTGGTTTTG
CCTTTGGACGAGAAGATATTTGGCATCCTGAGAAAGATATCTACTGGGGGCCTGAGAAGGAATG
GGTTCCCCCAAGCACCAATCCCAACAGTCGCTATACGGGCGATCGCGAACTTGAAAATCCGCTA
GCAGCCGTGACAATGGGGCTGATTTACGTCAACCCCGAAGGCGTGGATGGCAATCCTGATCCGC
TCAAAACCGCCCATGACGTGCGCGTCACCTTTGCGCGGATGGCGATGAACGATGAGGAAACGG
TGGCGCTAACTGCTGGTGGACACACCGTTGGCAAATGTCATGGCAATGGCAATGCTGCTTTGCT
AGGACCCGAACCGGAAGGGGCGGATGTGGAAGATCAAGGCTTGGGCTGGATCAATAAAACCCA
GAGCGGTATTGGTCGCAACGCTGTCACCAGTGGGCTGGAAGGGGCTTGGACACCCCACCCGAC
TCAATGGGACAACGGCTATTTCCGTATGCTCCTGAACTATGACTGGGAACTGAAGAAAAGCCCT
GCAGGCGCATGGCAGTGGGAACCGATTAATCCCCGAGAAGAAGATCTACCGGTCGATGTCGAA
GATCCATCGATTCGCCGCAACTTGGTGATGACCGACGCCGACATGGCCATGAAGATGGACCCAG
AGTATCGGAAAATCTCGGAGCGCTTCTACCAAGATCCGGCCTACTTTGCGGATGTGTTTGCACG
GGCTTGGTTCAAGTTAACCCACCGCGATATGGGGCCGAAAGCCCGTTACATTGGCCCGGATGTG
CCACAGGAAGACCTGATTTGGCAGGATCCAATTCCGGCGGGCAACCGCAACTATGACGTGCAAG
CGGTGAAAGATCGGATTGCTGCCAGTGGACTAAGTATCAGTGAGCTAGTCAGCACAGCTTGGGA
TAGCGCCCGTACTTATCGAAATTCGGATAAGCGGGGCGGGGCGAATGGGGCACGGATTCGGTT

AGCACCCCAGAAAGATTGGGAAGGGAATGAACCCGATCGCTTGGCGAAAGTGCTGGCTGTGCT
GGAAGGAATTGCTGCCGCTACTGGGGCGAGCGTTGCCGACGTCATTGTTCTGGCTGGCAATGTT
GGGGTGGAGCAAGCAGCCAGGGCTGCCGGTGTTGAAATTGTGCTTCCCTTTGCGCCGGGTCGT
GGCGATGCAACGGCTGAGCAAACGGATACGGAATCCTTTGCAGTGCTGGAGCCGATTCACGAT
GGCTATCGCAACTGGCTCAAGCAGGACTATGCGGCAACGCCTGAAGAATTGCTGCTTGATCGCA
CGCAACTGTTGGGTCTGACGGCTCCAGAGATGACGGTGTTGATTGGTGGCCTGCGTGTCTTGGG
AACCAACCATGGCGGTACGAAGCACGGTGTCTTCACCGATCGCGAAGGGGTGTTAACGAATGAC
TTTTTCGTGAATCTGACCGACATGAATTATCTGTGGAAACCGGCTGGAAAAAACCTGTATGAAA
TCTGCGATCGCAAGACGAATCAGGTGAAGTGGACGGCAACGCGAGTCGATTTGGTCTTTGGATC
AAATTCGATTCTGCGAGCCTACTCAGAGCTCTATGCACAAGACGACAACAAAGAGAAGTTTGTG
CGAGACTTTGTCGCTGCCTGGACGAAGGTGATGAATGCCGATCGCTTTGATCTGGACTAA

Forward primer	Pos	Len	Tm	Reverse primer	Pos	Len	Tm	Amp	dG
5′-CTACCGAATTGCCGA-3′	295	15	52.46	5′-GGGATTGGTGCTTGG-3′	595	15	53.86	300	0

rnpB (RNA component of RNaseP) (mRNA 312 bp) KEGG accession number: Synpcc7942_R0036

Highlighted texts are nucleotide sequences for forward and reverse primers.

GAGGAAAGTCCGGGCTCCCAAAAGACCAGACTTGCTGGGTAACGCCCAGTGCGGGTGACCGTG
AGGAGAGTGCCACAGAAACATACCGCCGATGGCCTGCTTGCAGGCACAGGTAAGGGTGCAAGG
GTGCGGTAAGAGCGCACCAGCAACATCGAGAGGTGTTGGCTCGGTAAACCCCGGTTGGGAGCA
AGGTGGAGGGACAACGGTTGGTCTTTTACCTGTTCCGTTTATGGACCGCTAGAGGTGGCTAGTA
ATAGCCATCCCAGAGAGATAACTGCCCTCTGTCTTCGACAGAGAACAGAACCCGGCTTA

Forward primer	Pos	Len	Tm	Reverse primer	Pos	Len	Tm	Amp	dG
5′-GAGGAAAGTCCGGGCTCCC-3′	1	19	64.80	5′-TAAGCCGGGTTCTGTTCTC-3′	294	19	59.49	312	0

sodB (Fe/Mn-superoxide dismutase) (mRNA 690 bp) KEGG accession number: Synpcc7942_0801

Highlighted texts are nucleotide sequences for forward and reverse primers.

GTGCTGCAGGAGACGCTCAGACGAGGGAAGCGTCCGGTTTTTATTAATCTAGGTAAAGACAACC
TGCTCAAGAGAACACACTGCATGTCCTACGAATTGCCAGCATTGCCCTTTGACTACACGGCACT
GGCGCCTTACATCACCAAGGAAACGCTGGAGTTCCACCACGATAAGCACCACGCGGCCTACGTC
AATAACTACAACAACGCCGTCAAAGACACCGACCTCGATGGCCAGCCGATCGAAGCCGTGATCA
AAGCGATCGCGGGTGACGCTAGCAAAGCCGGTCTGTTCAACAATGCGGCTCAAGCTTGGAACCA
CAGCTTTTACTGGAACTCGATCAAGCCCAATGGCGGTGGCGCTCCCACCGGCGCGTTGGCCGAC
AAAATCGCCGCTGACTTCGGCAGTTTCGAGAACTTCGTGACCGAGTTCAAACAAGCCGCAGCAA
CCCAGTTCGGCAGCGGCTGGGCTTGGTTGGTGCTGGACAATGGCACCCTCAAAATCACCAAAAC
CGGCAACGCCGACACCCCGATTGCCCATGGTCAAACCCCGCTACTGACCATCGATGTCTGGGAA
CACGCTTACTACCTCGACTACCAAAACCGTCGTCCCGACTACATCAGCACCTTCGTTGAGAAGC
TGGCGAACTGGGACTTCGCCTCTGCCAACTACGCAGCTGCGATCGCTTAG

Forward primer	Pos	Len	Tm	Reverse primer	Pos	Len	Tm	Amp	dG
5′-ACCAAGGAAACGCTG-3′	141	15	53.34	5′-CGGCTTGTTTGAACTC-3′	441	16	52.94	300	0

tpxA (Thioredoxin peroxidase) (mRNA 597 bps) KEGG Accession number: Synpcc7942_2309

Highlighted texts are nucleotide sequences for forward and reverse primers.

ATGACCGAAGGAGCCCTGCGCGTCGGCCAATTGGCCCCCGATTTTGAAGCGACTGCAGTCGTTG
ATCAGGAATTCCAGACGATCAAGCTATCCAATTACCGGGGCAAATACGTCGTTCTGTTCTTCTA
TCCCCTCGACTTCACCTTTGTTTGCCCGACCGAAATTACTGCTTTTAGCGATCGCTATGCAGAC
TTTTCAGCCCTGAACACCGAAATCTTGGGTGTCTCGGTCGATAGCCAATTCAGCCACTTGGCTT
GGATTCAAACCAGCCGTAAAGAAGGTGGTTTGGGTGACTTGGCTTACCCGCTGGTTGCTGACCT
CAAGAAAGAAATCAGCACTGCCTACAACGTGCTTGATCCGGCTGAAGGCATTGCCCTGCGCGGT
CTGTTCATCATCGACAAAGAAGGTGTGATCCAGCACGCCACCATCAACAACCTGGCGTTTGGCC
GCAGCGTTGATGAAACCCTGCGGGTGCTGCAAGCCATTCAGTACGTCCAAAGTCACCCCGATGA
AGTTTGCCCCGCCAATTGGCAACCGGGTGCAGCGACGATGAACCCCGACCCTGTTAAGTCGAAA
GAGTTCTTCGCTGCAGTCTAG

Forward primer	Pos	Len	Tm	Reverse primer	Pos	Len	Tm	Amp	dG
5′-CCGTAAAGAAGGTGGT-3′	269	16	52.56	5′-CTTAACAGGGTCGGG-3′	569	15	52.28	300	0

Appendix 4

Cell morphology

RAW 264.7 cells in M2G biocompatibility assay

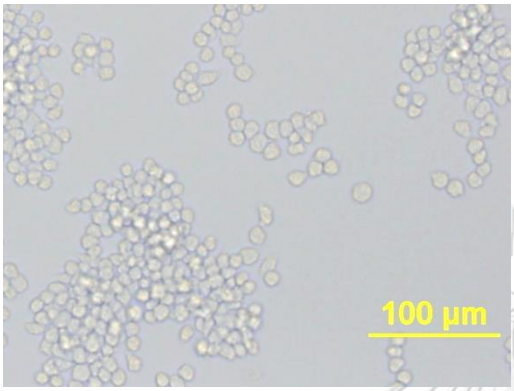

control

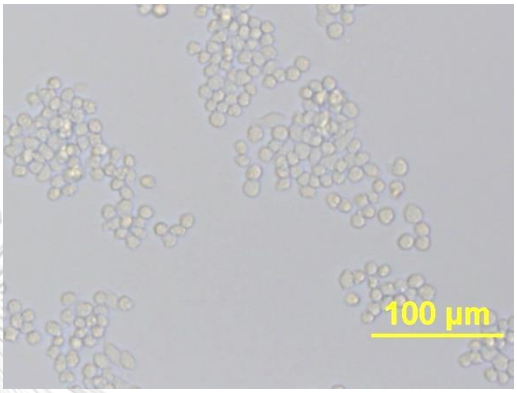

0.1 µM M2G

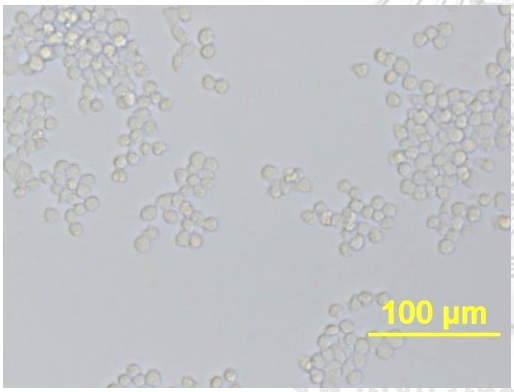

1 µM M2G

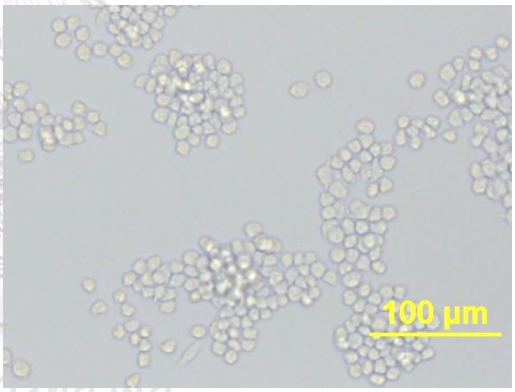

5 µM M2G

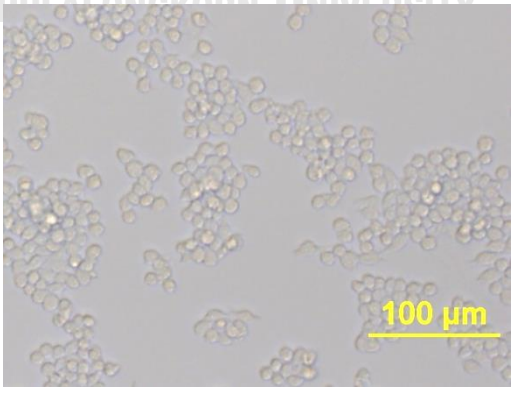

10 µM M2G

RAW 264.7 cells in M2G Nitric oxide assay

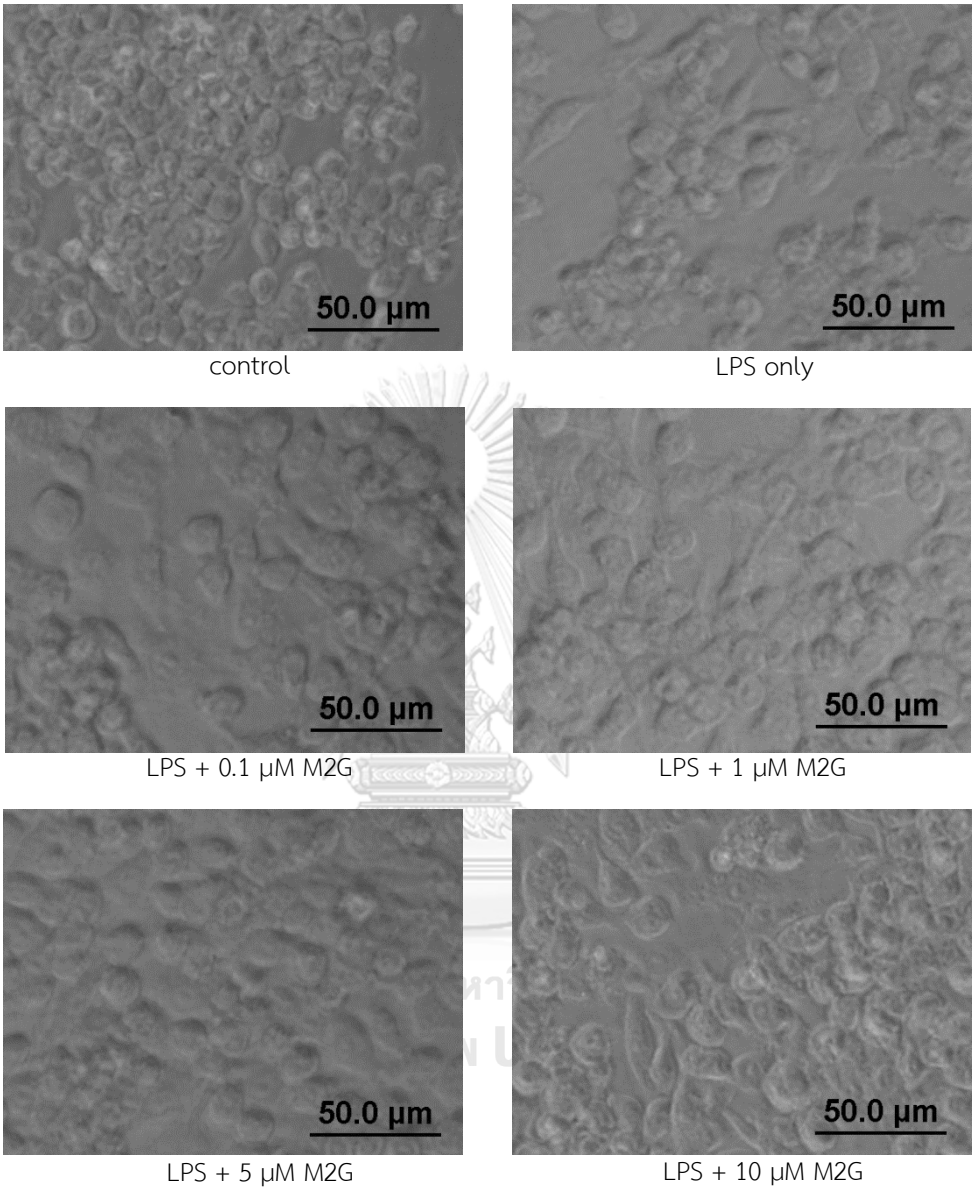

control

LPS only

LPS + 0.1 µM M2G

LPS + 1 µM M2G

LPS + 5 µM M2G

LPS + 10 µM M2G

RAW 264.7 cells in antioxidative property of M2G via co-treatment

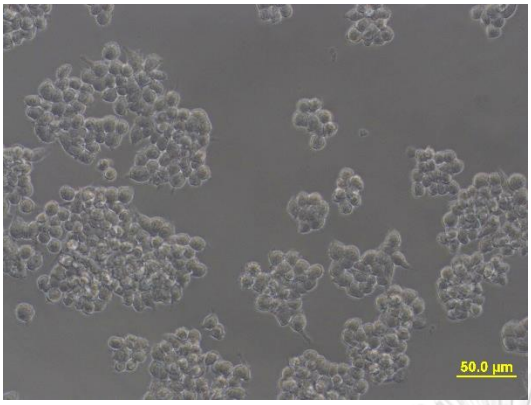

control

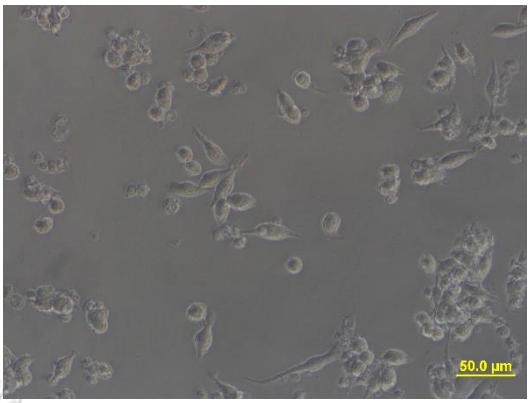

600 µM H_2O_2

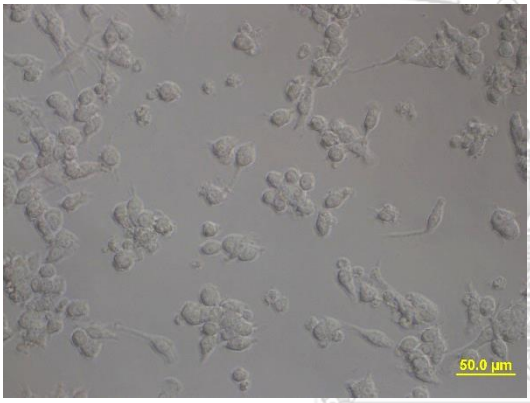

600 µM H_2O_2 + 0.1 µM M2G

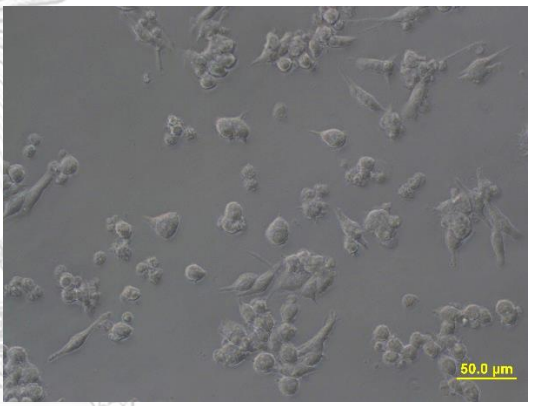

600 µM H_2O_2 + 1 µM M2G

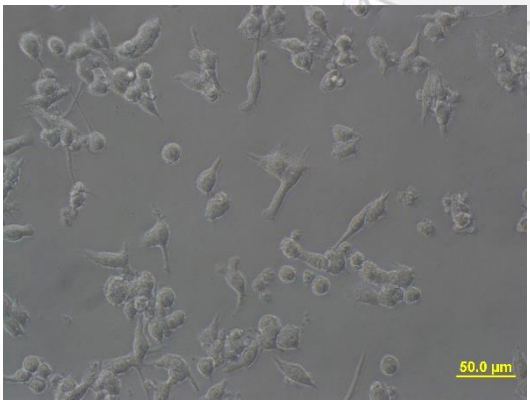

600 µM H_2O_2 + 5 µM M2G

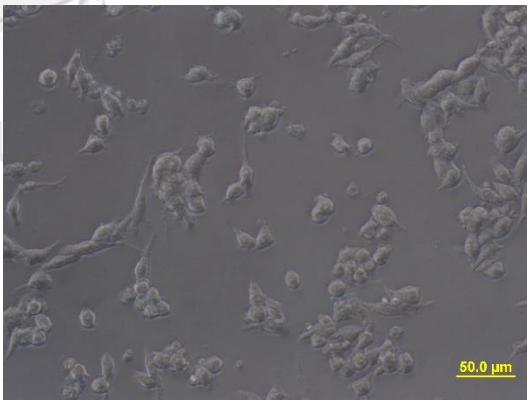

600 µM H_2O_2 + 10 µM M2G

S. elongatus PCC 7942 carrying pUC303 under oxidative stress induced by H_2O_2

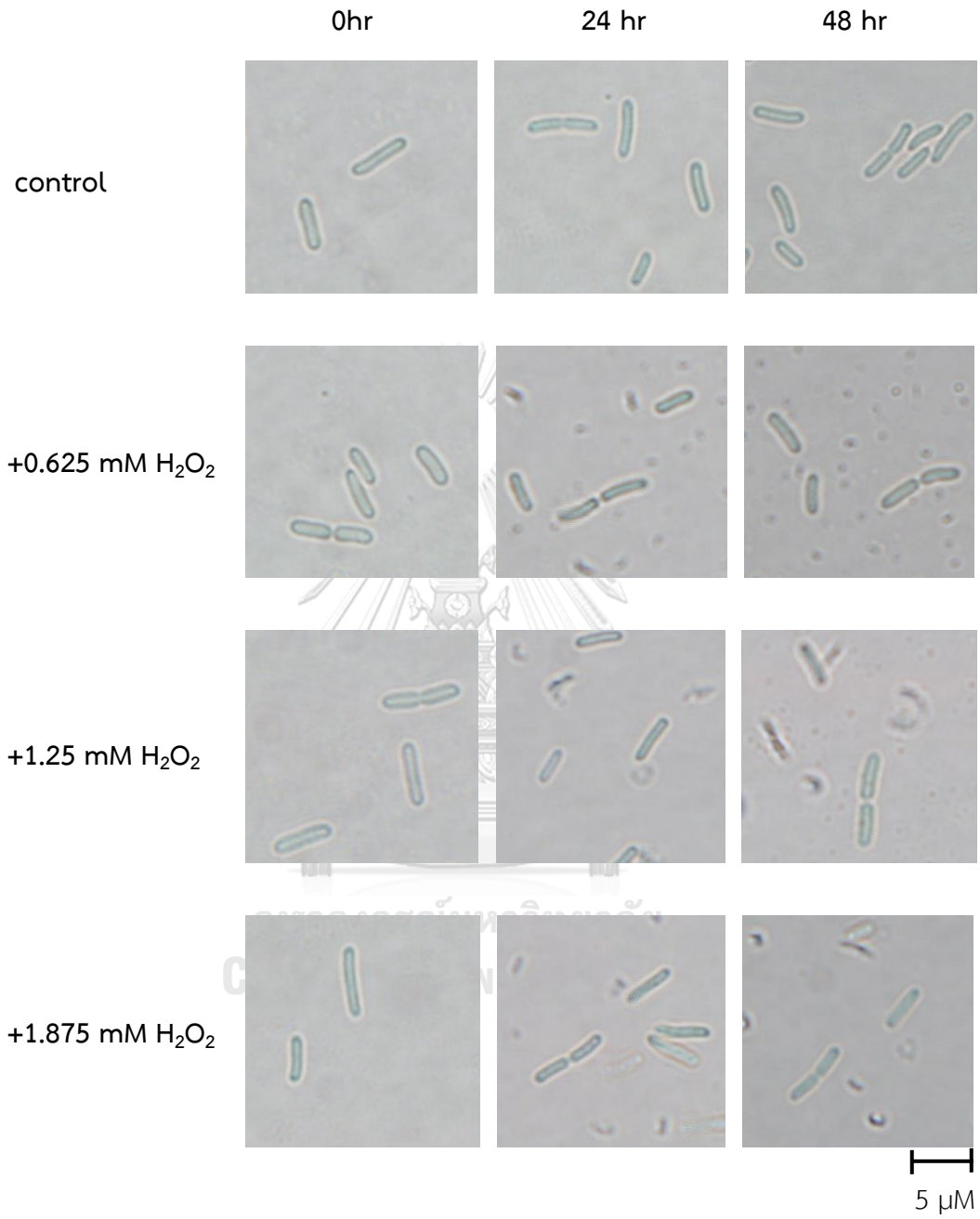

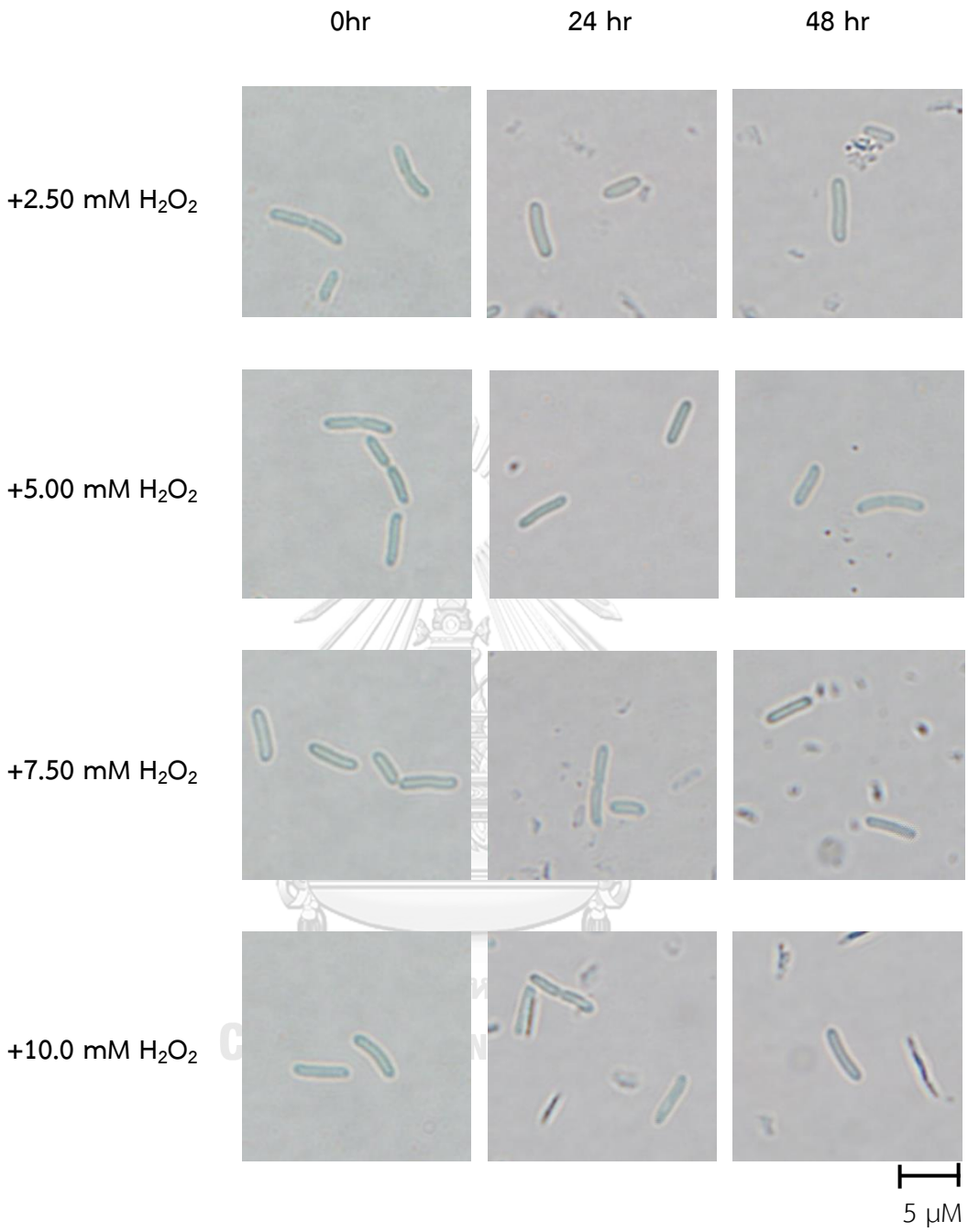
0hr
24 hr
48 hr
+2.50 mM H_2O_2
+5.00 mM H_2O_2
+7.50 mM H_2O_2
+10.0 mM H_2O_2
5 µM

S. elongatus PCC 7942 carrying *Ap3858-3855*/pUC303 under oxidative stress induced by H_2O_2

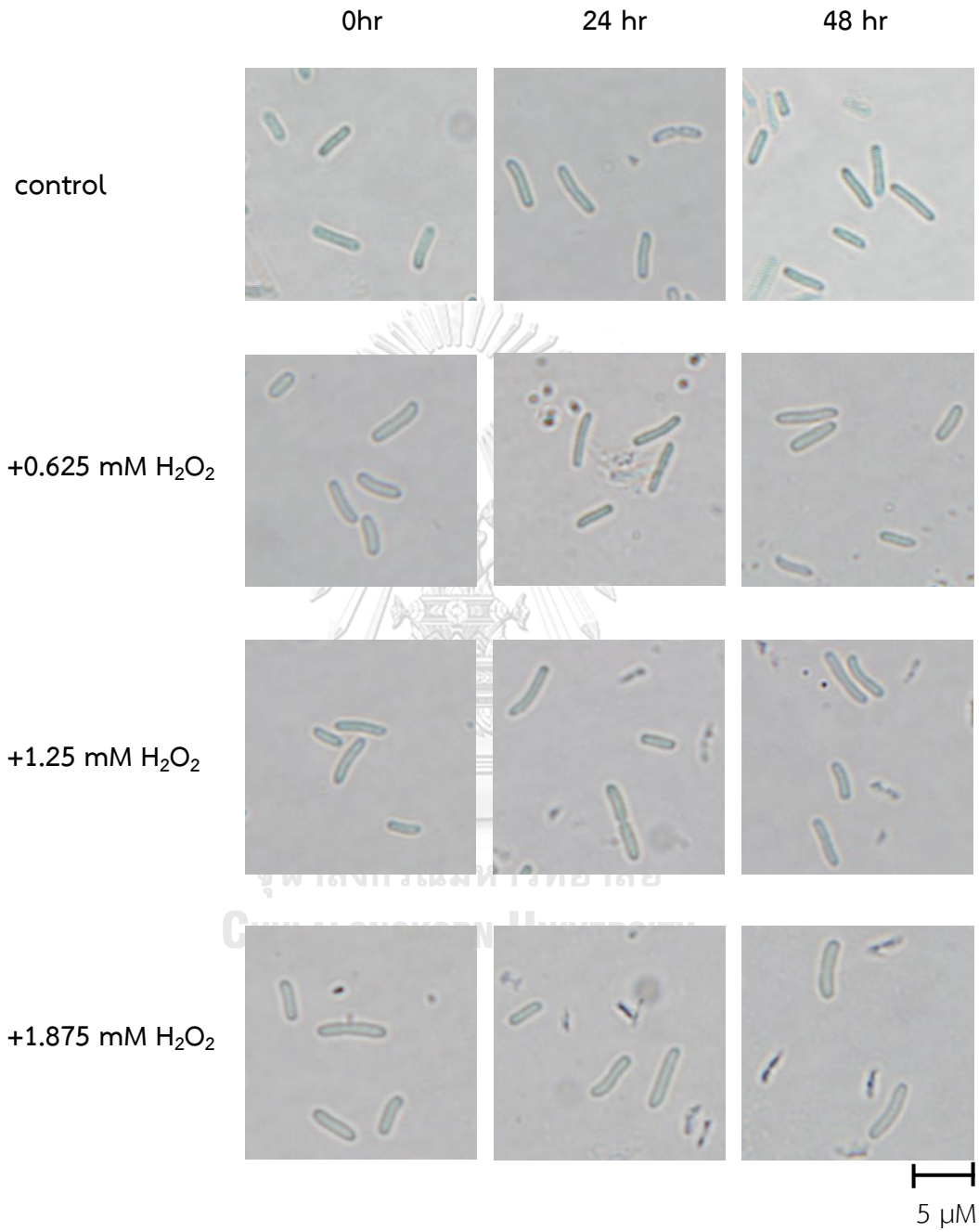

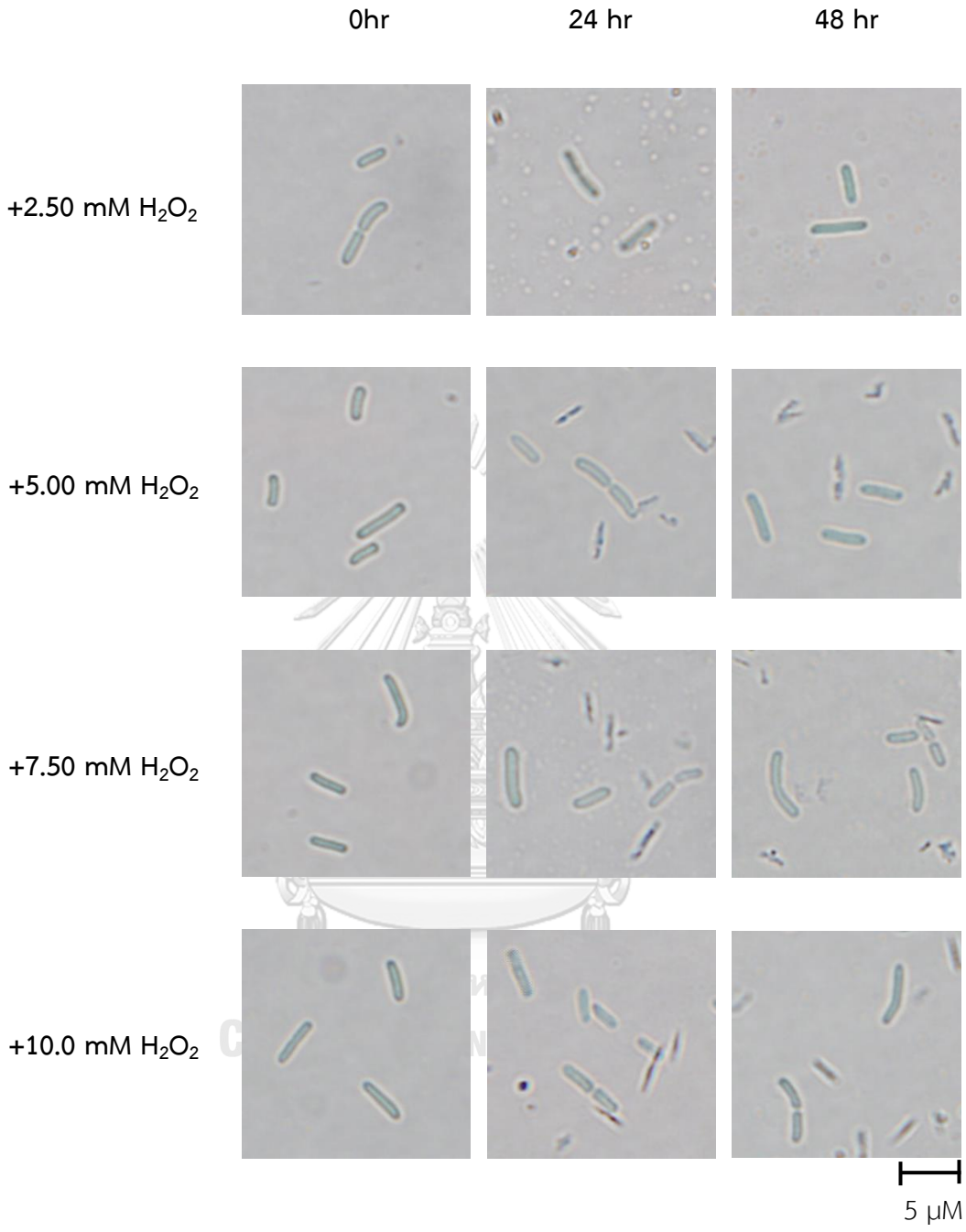
0hr
24 hr
48 hr
+2.50 mM H_2O_2
+5.00 mM H_2O_2
+7.50 mM H_2O_2
+10.0 mM H_2O_2
5 μM

Appendix 5

Nitric oxide standard

Standard nitric oxide for nitric oxide assay under M2G plus LPS treatment

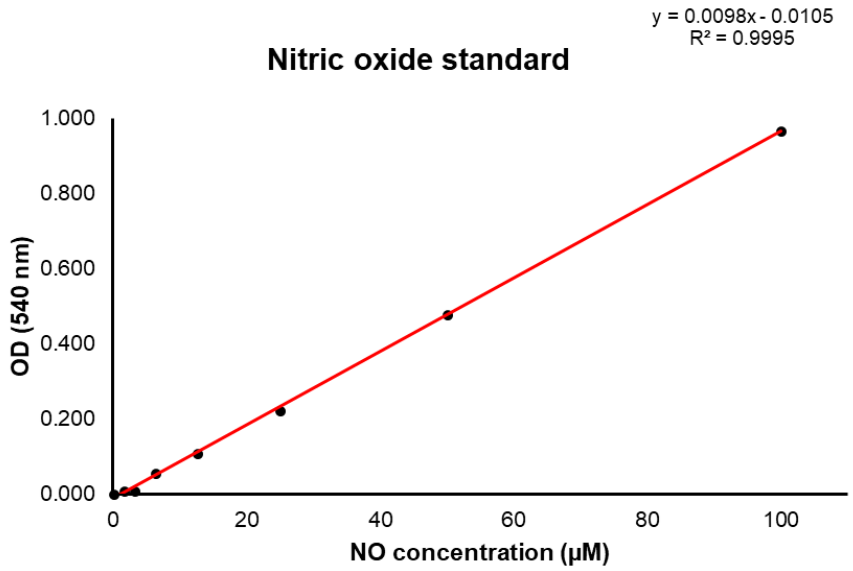

Standard nitric oxide for nitric oxide assay under other MAAs plus LPS treatment

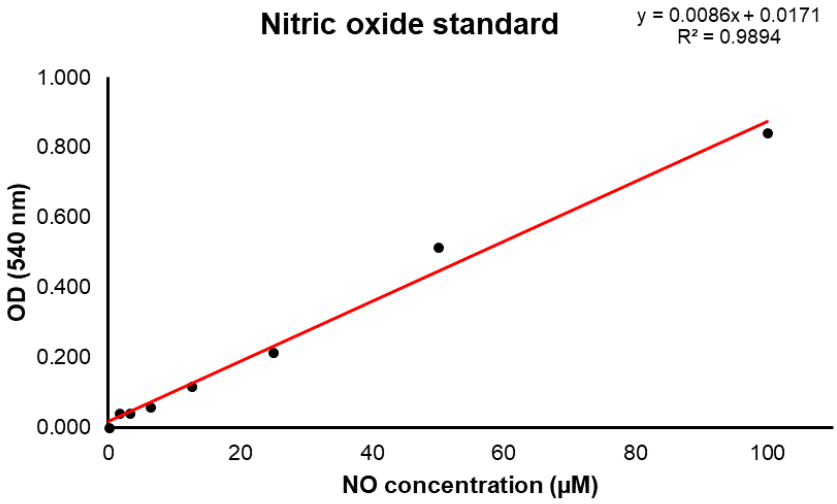

VITA

Mister Supamate Tarasuntisuk was born on February 18, 1994 in Bangkok, Thailand. He graduated from Department of Microbiology, Faculty of Science, Chulalongkorn University in 2015 with a Bachelor degree of Science (Microbiology). During his graduated study in Microbiology and Microbial Technology, he published some parts of this work in the 29th Annual Meeting of Thai Society for Biotechnology and International Conference. The topic was Natural Sunscreen Compound from Marine Extremophile: Production, Purification, and Radical Scavenging Activity.